MOLECULAR MECHANISMS OF THE DNA DAMAGE RESPONSE INDUCED DURING PARVOVIRUS INFECTION

BY

Yong Luo

Submitted to the graduate degree program in Microbiology, Molecular Genetics and Immunology and the Graduate Faculty of the University of Kansas in partial fulfillment of the requirements for the degree of Doctor of Philosophy.

Dissertation Committee:

_____
Jianming Qiu, Ph.D., Chairperson

_____
Nikki Cheng, Ph.D.

_____
Mohammad Ayoub Mir, Ph.D.

_____
Joe Lutkenhaus, Ph.D.

_____
Edward Stephens, Ph.D.

_____
Charlotte Vines, Ph.D.

Date defended: November 14th 2012

The Dissertation Committee for Yong Luo

certifies that this is the approved version of the following dissertation:

MOLECULAR MECHANISMS OF THE DNA DAMAGE RESPONSE INDUCED DURING PARVOVIRUS INFECTION

_____

Jianming Qiu, Ph.D, Chairperson.

Date approved: December 4th, 2012

Abstract

DNA damage response (DDR) is a critical safeguarding system to protect genomic stability and integrality through a cascade of phosphorylation events of three PI-3-kinase-like kinases: ATM (ataxia telangiectasia mutated), ATR (ATM and Rad3 related), and DNA-PKcs (DNA-dependent protein kinase catalytic subunit). Although numerous studies have established that the DDR is mainly triggered by exposure to ultraviolet, ionizing irradiation and chemical treatment, which introduce DNA breaks into genomes, accumulating evidence has demonstrated that infections of most DNA viruses and some retroviruses are able to induce a DDR, which plays a critical role in the life cycle of the viruses.

Parvoviruses are small, non-enveloped and single-stranded DNA (ssDNA) viruses, and cause highly contagious diseases that are sometimes fatal in humans and animals. Parvoviral genomes are usually 5-6kb, and are flanked by two inverted terminal repeats. Two parvoviruses, minute virus of canines (MVC), a model virus for the study of human bocavirus that causes respiratory tract diseases in children worldwide, and human parvovirus B19 (B19V), a causative agent of several human diseases including bone marrow failure diseases and hydrops fetalis, were used in our study to probe the mechanisms of parvovirus infection-induced DDR. We found infection of both MVC and B19V triggers phosphorylation of the DDR upstream kinases in their host cells, and MVC mainly activates the ATM signaling pathway, while B19V activates the ATR signaling pathway. Moreover, we identified that inhibition of the kinases through inhibitor treatment or small interfering RNA knockdown significantly blocks viral DNA replication. These results indicate that, in contrast to turn on the protection effects of the DDR, parvovirus activates and hijacks the cellular DDR machinery for viral DNA amplification.

Following these studies, we next explored the mechanism by which the ATM signaling pathway contributes to MVC DNA replication. We discovered that MVC infection induces an intra-S phase arrest to block cellular DNA replication and to hijack the DNA replication machinery for viral DNA synthesis. The intra-S phase arrest is dependent on ATM signaling. Moreover, we

identified SMC1 (structural maintenance of chromosomes 1) as the key regulator of the viral infection-induced intra-S phase arrest. Either knockdown of SMC1 or complementation with a dominant-negative SMC1 mutant blocked both the intra-S phase arrest and viral DNA replication. Finally, we found that the intra-S phase arrest induced during MVC infection is neither caused by damaged host cellular DNA nor by viral proteins, but by replicating viral genomes, which are physically associated with the DNA damage sensor, the Mre11-Rad50-Nbs1 (MRN) complex.

Taken together, by using MVC and B19V as model organisms, we have probed the basic mechanism of the DDR induced during parvovirus infection. Our findings have greatly facilitated the understanding of the mechanisms underlying parvovirus DNA replication, and have provided a molecular basis for the novel strategy by which DNA viruses subvert the host cellular DDR signaling to make it conducive for viral DNA replication. Our study also sheds light on the identification of efficient anti-viral targets for the treatment of parvovirus-caused diseases.

Acknowledgements

I would like to take this opportunity to thank Dr. Joe Lutkenhaus and Dr. Jianming Qiu, who recruited me directly to the Ph.D. program of the department of Microbiology, Molecular Genetics and Immunology of the University of Kansas Medical Center. I wouldn't be at this point in my science career without their kind help.

I will forever be thankful to my advisor and mentor, Dr. Jianming Qiu. His truly scientific intuition has sparked my passion for science and inspired me to pursue a dream of becoming a virologist**.** I thank him for his guidance, encouragement and support during all my Ph.D. study. He spent tremendous time to teach me to think critically, to make a good presentation, and more importantly, to become an independent researcher. I enjoyed talking with him, not only for the topics about science, but also his advices on my career development. His mentorship made my Ph.D. study a beautiful journey in my life.

Besides my mentor, I would express my sincere gratitude to the rest of my thesis committee: Drs. Mohammad Ayoub Mir, Joe Lutkenhaus, Edward Stephens, Charlotte Vines and Nikki Cheng, for their insightful comments and hard questions, and for their valuable suggestions for my thesis writing.

Last but not the least important, I owe more than thanks to my family members, which include my parents and parents-in-law, for they everlasting love and support . I want to express my deepest gratitude to my wife Shan Yang, who sacrificed her career, coming along with me long way from our home country, to take care of me and our beloved daughters, Grace and Jessica. They are the driving force that has kept me working hard.

Table of Contents

Acceptance page ii

Abstract iii

Acknowledgements v

Table of Contents vi

Chapter I: Introduction 1

Introduction ……1

Dependovirus…… 5

Erythrovirus …….. 9

Parvovirus ……... 12

Bocavirus ……..... 15

Conclusion ……. 17

Objectives ……. 19

Chapter II: Bocavirus Infection Induces a DNA Damage Response That Facilitates Viral DNA Replication and Mediates Cell Death

Abstract 21

Introduction 22

Materials and methods 24

Results 28

Discussion 57

Chapter III: Parvovirus B19 infection of primary human erythroid progenitor cells triggers ATR-Chk1 signaling, which promotes B19 replication

Abstract 65

Introduction 66

Materials and methods 69

Results 73

Discussion 91

Chapter IV: ATM signaling facilitates autonomous parvovirus DNA replication through SMC1-mediated intra-S phase arrest

Abstract 96

Introduction 97

Materials and methods 100

Results 105

Discussion 135

Chapter V: Conclusions and discussion 142

References 147

Chapter 1
Introduction

Parvovirus infection-induced DNA damage response

Introduction

Parvoviruses are among the smallest DNA viruses and are widely spread in humans and many other species [1,2]. Parvovirus is non-enveloped with an icosahedral virion of 18-26 nm in diameter. It contains a linear single-stranded (ss)DNA genome of 5-6 kb, which is flanked by two terminal hairpin repeats. The *Parvoviridae* family is composed of two subfamilies: *Parvovirinae*, which infects vertebrates, and *Densovirinae, which* infects only invertebrates. The subfamily *Parvovirinae* contains five genera: *Amdovirus, Bocavirus, Dependovirus, Erythrovirus* and *Parvovirus* [3]. Adeno-associated viruses (AAVs), in the genus *Dependovirus*, replicate only during coinfection with other helper viruses, such as adenovirus or herpes virus [4]. All other parvoviruses replicate autonomously in their respective host cells and therefore are called autonomous parvoviruses [5,6].

Parvoviruses enter host cells through receptor-mediated endocytosis, and traffic into the nucleus, where viruses are uncoated and viral genomes are released. Released viral genomes are amplified by host cellular replication machinery; meanwhile, viral genomes are transcripted into viral mRNAs, which are spliced and exported into the cytoplasm. In the cytoplasm, viral mRNAs are translated into capsid proteins and non-structural proteins. Capsid proteins together with mature viral genomes are assembled in the nucleus and finally released from host cells through the lysis of both nuclear and cytoplasmic membrane. [2] (Figure 1)

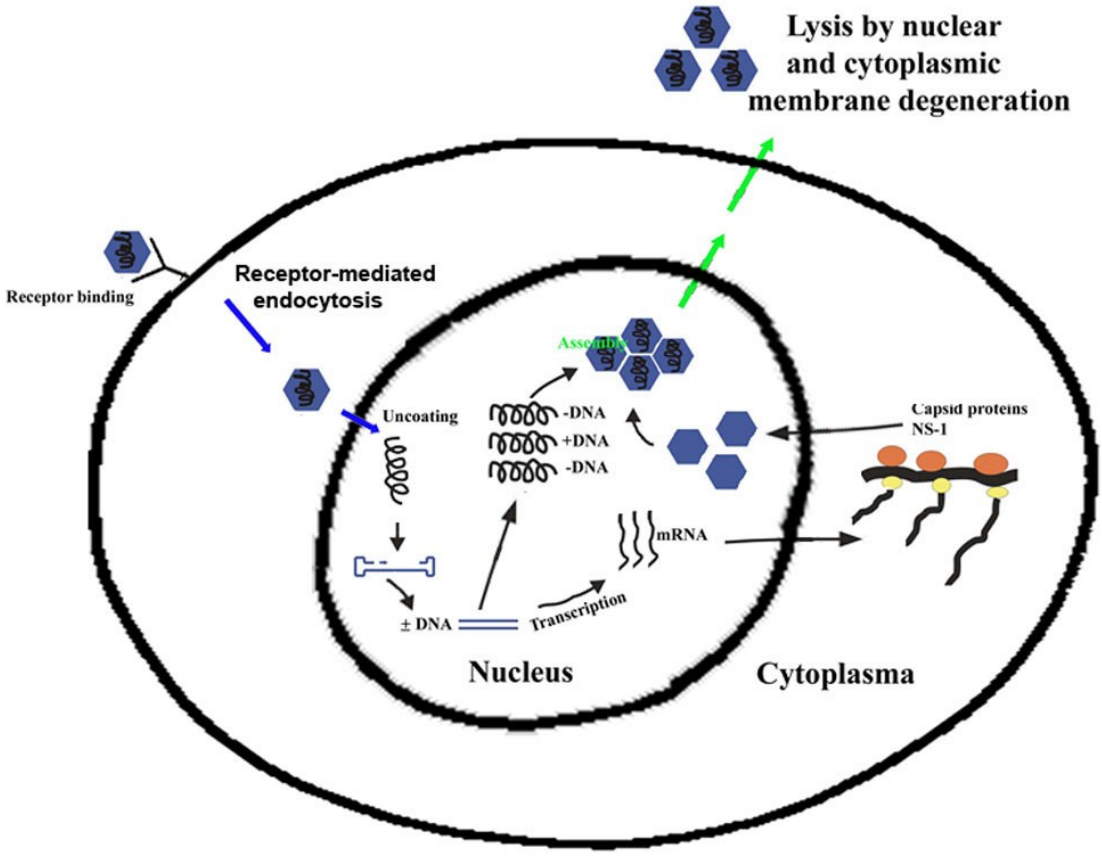

Figure 1 Parvovirus life cycle

As intracellular parasites, parvoviruses modulate the host cellular environment through the control of the cell cycle as well as the regulation of cell signaling pathways. Due to their simplistic gene expression profiles [3,7], parvoviruses largely rely on host cellular factors for productive infections. In order to propagate their DNA genomes, most parvoviruses arrest host cells at S phase for access to the cellular DNA replication machinery [8–14]; however, observations of G2/M arrest of host cells are also widely reported, especially during the late infection [14–18]. Moreover, parvovirus infections also induce cytopathic effects, which are characterized by their abilities to induce apoptosis, necrosis and autophagy [19–26]. The cell cycle arrest and cell death induced by parvovirus infections have been reviewed previously [27]. Although both *in vitro* and *in vivo* studies have suggested that basic cellular DNA replication factors are required for parvoviral DNA replication, accumulating evidence has suggested that the cellular DNA damage response (DDR) plays an important role in parvovirus replication [28–30].

DDR was originally identified as a cellular safeguarding system that protects cellular genome integrity and stability [31,32]. Mammalian cells are constantly challenged by many kinds of stresses that include intrinsic sources such as reactive oxygen species (ROS) produced from regular metabolisms, and extrinsic sources such as ultraviolet (UV), ionizing irradiation, and chemical treatment. These inducers create several types of damaged DNA structures, including single-stranded DNA breaks (SSBs), double-stranded DNA breaks (DSBs) and stalled replication forks [33,34]. The DDR signaling is a complex signal transduction pathway that is transduced by three components: sensors, mediators and effectors. The central mediators in the pathway are three phosphatidylinositol 3-kinase-like kinases (PI3KKs): ATM (ataxia telangiectasia-mutated kinase), ATR (ATM- and Rad3-related kinase), and DNA-PKcs (DNA-dependent protein kinase catalytic subunit) [34,35]. In response to different damaged DNA structures, different sets of DDR sensors are recruited. DSBs can be recognized by the

Mre11-Rad50-NBS1 (MRN) complex, which further activates the ATM kinase [36]. The ATM kinase has hundreds of substrates, which are effectors involved in cell cycle checkpoint, DNA repair and apoptosis [37–40]. DSBs can also be bound by the Ku70 and Ku80 complex, which recruits DNA-PKcs, a critical player in DNA repair of non-homologous end joining [41]. The ATR signaling pathway is in response to SSBs, stalled replication forks and DSBs resection. In SSBs and stalled replication forks, the ssDNA regions are coated with replication protein A (RPA), which loads Rad17 and the Rad9-Rad1-Hus1 (9-1-1) complex, to recruit TopBP1 (DNA topoisomerase 2-binding protein 1) [42–45]. TopBP1 further sequesters ATR, which is transformed into a hyperphosphorylated status by autophosphorylation at multiple sites [46]. Meanwhile during DSBs resection, single-stranded overhangs are formed, which promote an ATM-to-ATR switch [46,47]. Following the binding of sensors and activation of these three PI3KKs, a number of downstream effectors, including DNA repair proteins and cell cycle checkpoint proteins, are recruited and phosphorylated. Depending on the extent of DNA damage, cells are arrested at different phases of the cell cycle either for repairing the damage or triggering apoptosis if the damage is beyond repairing [33].

Interactions between DNA viruses and the host DDR machinery have been widely documented [48–51]. In contrast to triggering the protection effect of the DDR, viruses have evolved sophisticated strategies to redirect the DNA damage machinery. By selectively activating or suppressing components of the DDR, viruses are able to modulate the cellular environment for viral infections. Several reviews have summarized the relationship of different DNA virus species, especially double-stranded (ds)DNA viruses, to the DDR machinery [48–51]. The interaction between viruses and the DNA damage machinery not only significantly affects the viral life cycle but also play important roles in viral pathogenesis. Among the smallest DNA viruses, parvoviruses must exploit cellular machineries and signaling pathways, including DDR signaling pathways, for a productive viral infection. In addition, since parvoviruses contain

ssDNA genomes with unique hairpin structures at the ends (Figure 2), which are absent from cellular DNA, they are unique tools to study exogenous DNA-induced DDR. This review aims to summarize recent advance in parvovirus infection-induced DDR, with an emphasis on the diversity of signaling pathways utilized by different parvoviruses and the impact of the DDR machinery on the parvovirus life cycle as well as host cell fate decisions.

Genus *Dependovirus* (Adeno-associated virus type 2, AAV2)

Replication of AAV2 requires co-infection of a helper virus, such as adenovirus and herpes virus, via modulating the host cellular environment and activating viral gene expression [52]. In the absence of helper virus, the AAV2 genome can integrate into a specific locus on human chromosome 19 as latent infection [53]. AAV2 has not been associated with any human diseases and presents very low immunogenicity. Thus, it has been modified as one of the promising vectors in human gene therapy [54,55]. The AAV2 genome has identical inverted terminal repeats (ITRs), forming “T” shaped hairpins at each end (Figure 2) [56]. Studies about AAV2 infection-induced DDR have been performed under different conditions, i.e., infection of UV-inactivated AAV, transduction of recombinant AAV2 (rAAV2), coinfection of AAV2 and adenovirus, and coinfection of AAV2 and herpes virus type 1 (HSV1).

The MRN complex is a barrier to efficient AAV2 replication and rAAV2 transduction [57]. Adenovirus was the original identified helper virus for AAV2 productive infection [58]. The minimal set of adenovirus proteins required for AAV2 replication includes E1A, E1b55K, E4orf6, and VA RNA genes [59]**.** During adenovirus infection, E1b55K and E4orf6 proteins form a complex, which is important for export of viral mRNA [60,61]**.** The complex also causes the degradation of the MRN complex, promoting productive adenovirus infection by preventing the

concatemerization of adenovirus genomes [62]. During either AAV2 replication or processing of transduced rAAV2, the MRN complex was found to relocalize into the foci with AAV2 genomes [57,63]. Mre11 physically associated with rAAV2 genomes [63], and Mre11 and NBS1 bound to AAV2 ITR hairpin structures [57]. Thus, the MRN complex has an intrinsic ability to bind to the hairpin structures of AAV2 genomes. Notably, the MRN complex is not required for activation of the DDR signaling during AAV replication; conversely, it limits AAV2 replication and rAAV2 transduction efficiency. Silencing of NBS1 increased rAAV2 focus formation and rAAV2 transduction, while degradation of the MRN complex by E1b55K/E4orf6 created a more favorable environment for both wild type AAV2 replication and rAAV2 transduction [57]. Therefore, the MRN complex may initially function as an anti-virus cellular apparatus, while AAV2 requires the E1b55K/E4orf6 complex encoded from adenovirus to destroy this machinery.

During coinfection of AAV2 and adenovirus, DNA-PKcs signaling is the major mediator of the induced DDR [64,65]. The DDR is represented by phosphorylation of a number of DDR factors such as SMC1 (structural maintenance of chromosomes 1), Chk1 (checkpoint protein 1), Chk2 (checkpoint protein 2), H2AX, RPA32 [65]. Interestingly, although the MRN complex was destroyed during coinfection, autophosphorylation of the ATM kinase was observed [65], even it is not the mediator of the DDR. By contrast, DNA-PKcs is the primary mediator of the DDR in response to AAV2 and adenovirus coinfection. Along with its regulatory subunits, Ku70 and Ku86, DNA-PKcs localized to the AAV2 replication centers as well as the large non-structural protein Rep-mediated AAV2 replication compartments that only contain the AAV2 replication origins (p5 promoter and the ITR) [65]. In addition, DNA-PKcs plays an important role in AAV2 DNA replication *in vitro* as well as rAAV2 replication in the presence of adenovirus or HSV1 [66]. DNA-PKcs also has been reported to be involved in the formation of circular rAAV2 episomes [67,68]. However, during coinfection with adenovirus, wild type AAV2 DNA replication is not dramatically affected by DNA-PKcs inhibition [64]. Although it has not been shown whether the

ATR signaling is activated during AAV2 and adenovirus coinfection, expression of a kinase-dead ATR did not affect the downstream signaling, indicating that the ATR signaling is not involved [65]. Thus, during coinfection of AAV2 and adenovirus, both the ATM and the DNA-PKcs signaling pathways are activated, although the DNA-PKcs is the major mediator of the signaling.

During coinfection with HSV1, AAV2 replication activates the ATM and the DNA-PKcs signaling [69]. The helper proteins provided by HSV1 include UL5, UL8, UL52 and the DNA binding protein ICP8, which play important roles in HSV1 replication [70]. HSV1 infection alone activates the ATM signaling and inhibits ATR signaling [71,72]. Moreover, DNA-PKcs is inhibited through ICP0-dependent proteasomal degradation [73]. During coinfection with HSV1, AAV2 infection induced phosphorylation of all the three PI3KKs, and delayed the degradation of DNA-PKcs [69]. DNA-PKcs and ATM phosphorylated several downstream substrates such as NBS1, p53, Chk2, H2AX and RPA. Although ATR phosphorylation and recruitment of its binding component ATRIP (ATR-interacting protein) were observed, Chk1 was not phosphorylated, indicating that the ATR signaling is not activated [69]. However, whether phosphorylation of these kinases affects the AAV2 life cycle during the coinfection with HSV1 has not been studied.

Both the AAV2 genome and the large non-structural proteins Rep78/68 are able to induce a DDR. The structure of the AAV2 genome has a gap of ~4.4 kb between the two ITRs (Figure 2). This structure could mimic a SSB, and is a perfect trigger for the activation of the ATR signaling [42,74]. Indeed, studies on infection of UV-inactivated AAV2 proved that the AAV2 genome is able to induce a DDR, which arrests host cells at G2/M phase in the presence of p53, and apoptosis in the absence of p53 [75]. UV irradiation causes the formation of intra-strand cross-links in the AAV2 ssDNA genome, resulting in no expression of viral proteins. UV-inactivated AAV2 formed foci in infected cells, and DNA polymerase delta, ATR, TopBP1, RPA, and the 9-1-1 complex were found to colocalize within the foci, suggesting that

non-replicative AAV2 genome, by mimicking a stalled replication fork, provokes ATR-Chk1 signaling [76]. Activated Chk1 is required for the G2/M arrest following UV-AAV2 infection [77,78]. In addition, ectopic expression of the Rep proteins was able to activate the DDR signaling [10,65], possibly due to the endonuclease activity of the Rep proteins which creates non-specific nicks in chromosome DNA. However, during coinfection with adenovirus, the DDR signaling elicited by the Rep proteins was much weaker than that from AAV2 replication [65], suggesting that the majority of DDR signaling is generated from the replication event rather than from the Rep proteins or viral genome *per se*.

The consequences of DDR activation on virus life cycle and the host cell fate varies from different conditions of viral infection. Infection of UV-inactivated AAV2 triggers G2/M arrest of host cells and activates p84N5, a proapoptotic protein that further activates caspase-6 and induces p53-independent apoptosis in several cancer cell lines [78,79]. Notably, AAV2 can replicate autonomously (to a limited extent) in UV-treated host cells [80], suggesting that DDR signaling may trigger replication of AAV2 DNA. Additionally, ectopic expression of the large Rep proteins induced ATM-dependent S phase arrest that facilitated AAV2 replication [10]. However, during coinfection with adenovirus or HSV1, the consequences of DDR on the AAV2 lifecycle and host cell fate are still elusive, since these two helper viruses also interact with the cellular DNA damage machinery. Interfering with any DDR signaling alters the life cycle of these two viruses [81] and therefore indirectly affects AAV2 replication.

In conclusion, under different conditions of viral infection, AAV2 displays diverse patterns to interplay with the cellular DNA damage machinery. The MRN complex is a barrier to wild-type AAV2 replication and rAAV2 transduction. Although effects such as cell cycle arrest and apoptosis were observed during expression of the large Rep proteins and infection of UV-inactivated AAV, little is known about the impact of DDR signaling on the fate of host cells

and the life cycle of AAV2 during coinfection with its helper viruses. Nevertheless, study of AAV2-induced DDR will help us to better understand the biology of AAVs for enhancing rAAV transduction and preventing potential hazards of using AAV vectors in human gene therapy.

Genus *Erythrovirus* (Human parvovirus B19, B19V)

B19V belongs to the genus *Erythrovirus* and naturally only infects human erythroid progenitor cells (EPCs) of the human bone marrow and fetal liver [82–86]. Most commonly, B19V infection causes a mild disease called “fifth disease” [87]. In some conditions, B19V infection leads to more severe symptoms, e.g., in pregnant women during the second trimester, B19V infection induces hydrops fetalis [88]; in immunocompromised patients, it causes chronic pure red cell aplasia [89–91]; and in sickle cell disease patients, it induces transient aplastic crisis [92,93].

The B19V genome contains two symmetric ITRs (Figure 2). Under a single p6 promoter, it encodes three non-structural proteins (NS1, 11-kDa and 7.5-kDa) and two capsid proteins (VP1, VP2). The large non-structural protein NS1 is a multiple-functional protein with endonuclease, helicase, and transactivation activities [94]. NS1 *per se* is able to trigger G2/M arrest and apoptosis [18,95]. The 11-kDa protein has been shown to induce apoptosis [96], while the function of the 7.5-kDa remains unknown. *Ex vivo*-expanded EPCs are highly permissive to B19V infection [97], which was greatly increased under hypoxic conditions [98,99]. In contrast to other autonomous parvoviruses, whose infection induces S phase arrest during early infection [8–14], B19V infection induces G2/M arrest of infected UT-7/Epo-S1 cells [15] and EPCs [18,100,101] , a stage at which the arrested cells have a 4N DNA content as determined by DAPI (4′,6′-diamidino-2-phenylindole hydrochloride) staining. However, a more careful examination of

B19V-infected EPCs using a proliferation assay of BrdU-incorporation combined with DAPI staining [102,103] showed that B19V-infected EPCs were actually arrested at late S phase, which have a 4N DNA content (Y. Luo & J. Qiu, unpublished). This observation suggests replication of B19V, like other autonomous parvoviruses, requires cellular replication factors expressed in S phase.

B19V infection triggered a broad range of DDR, resulting in all three PI3KKs activated in infected EPCs, which localized to the B19V DNA replication centers [28]. Downstream effectors of the these kinases, such as Chk1, Chk2 and Ku70/Ku86 proteins, also colocalized within the replication centers, indicating that B19V has a powerful ability to activate the DNA damage machinery. This phenomenon is somehow similar to that observed during AAV2 and HSV1 coinfection [69]. The difference is that ATR phosphorylates Chk1 during B19V infection, whereas phosphorylated ATR did not contribute to Chk1 activation during AAV2 and HSV1 coinfection.

Replication of the B19V genome is required for triggering a DDR [101]. Expression of individual viral protein, including NS1, 11-kDa, 7.5-kDa, VP1 and VP2, in EPCs failed to induce a DDR [101]. Although studies in B19V-nonpermissive cells, e.g., the hepatocyte cell line HepG2, showed that B19V NS1 was able to nick cellular chromosome DNA and caused damage of cellular DNA [104], DDR in response to such potential DNA damage was not obvious during ectopic expression of the NS1 in EPCs as neither H2AX nor RPA32 was phosphorylated [101]. In UT7/Epo S1 cells, which are permissive to B19V infection [15], transfection of a B19V infectious DNA, but not a replication-deficient mutant that harbors mutation in the NS1 endonuclease motif, activated a DDR, indicating that the DDR induced by B19V is closely associated with the status of viral DNA replication [101]. The requirement of the viral replication process to trigger a robust DDR is similar to what was observed during AAV2 and adenovirus coinfection [65]. However, whether B19V ssDNA genome *per se* can induce a DDR warrants

further investigation. The ATR-Chk1 signaling facilitates B19V DNA replication [28]. Either inhibition of ATR activation by the treatment of an ATM/ATR-specific pharmacological inhibitor or transient knockdown of ATR significantly blocked B19V DNA replication. During B19V infection, Chk1 was phosphorylated and localized into the viral DNA replication centers. Inactivation of Chk1 phosphorylation by the treatment of a Chk1-specific pharmacological inhibitor also reduced B19V replication. Additionally, the DNA-PKcs signaling contributes to enhance B19V DNA replication but to a lesser extent. Interestingly, although the ATM signaling and its substrate Chk2 were activated during B19V infection, knockdown of ATM and inhibition of Chk2 phosphorylation did not affect B19V DNA replication significantly. Thus, the function of ATM signaling during B19V infection remains unknown.

Interestingly, B19V infection-induced DDR does not contribute to the G2/M arrest (a phase with a 4N DNA content) during infection [28,101]. Although both checkpoint kinases Chk1 and Chk2 have the ability to induce G2/M arrest [105–107], inhibition of either Chk1 or Chk2 activation in EPCs did not abolish G2/M arrest induced during B19V infection [28]. Additionally, knockdown of p53, which is phosphorylated at serine 15 by ATM, failed to abrogate B19V infection-induced G2/M arrest [101]. These results suggest that a p53- and Chk1/Chk2-indendeptnt pathway is involved in G2/M arrest induced during B19V infection. Indeed, the NS1 protein *per se* is able to induce G2/M arrest through deregulation of E2F family proteins [100]. A mutant infectious clone with a mutating putative transactivation domain of NS1 [101] replicated well in UT7/Epo S1 cells and induced a DDR, but not obvious G2/M arrest [101]. Thus, B19V infection-induced DDR is dispensable for the G2/M arrest induced during infection.

In conclusion, B19V infection not only triggers a broad range of DDR activation, but also hijacks ATR and DNA-PKcs for viral DNA replication. Viral DNA replication but not individual viral protein is required for B19V infection-induced DDR. The DDR has an unclear effect on the host

cellular environment since it is dispensable for the G2/M arrest of infected cells; however, it facilitates B19V DNA replication. It will be interesting to know whether the downstream effectors of ATR and DNA-PKcs signaling are involved in DDR-promoted B19V replication. Further study is warranted to examine the difference in the G2/M or late S (4N) phase arrest induced between by B19V infection and by the NS1 protein using the BrdU-incorporation/DAPI staining proliferation assay. Such an examination will reveal the role of the DDR in the cell cycle arrest during B19V infection.

Genus *Parvovirus* (Minute virus of mice, MVM; Parvovirus H-1, H1-PV)

-MVM

MVM has been used as a classic model to study the replication mechanism of autonomous parvoviruses [108,109]. Together with H1-PV, they are oncolytic parvoviruses due to their ability to selectively infect and kill various human tumor cells and inhibit tumorigenesis in animal models [110]. In contrast to AAV2 and B19V, the terminal hairpins of the MVM and H1-PV genomes are asymmetric (Figure 2). During MVM infection, MVM replicates in the viral replication centers, so called the autonomous parvovirus-associated replication (APAR) bodies, which include NS1, NS2 and several cellular DNA replication factors, i.e., polymerase delta, polymerase alpha, RPA and PCNA (proliferating cell nuclear antigen) [111]. Replication of MVM requires host cells at S phase, which was reported to be induced by NS1 protein [17].

MVM infection induces a DDR that is predominantly regulated by ATM signaling [29,112]. In both MVM-infected murine and human cells, DDR factors, e.g., H2AX, Nbs1, Chk2 and p53, were phosphorylated [29]. RPA32 is hyper-phosphorylated at multiple sites, including serines 4, 8 and 33; however, the function of the phosphorylation remains unknown [112]. Although many

of these phosphorylated proteins relocate into the APAR bodies, proteins such as γH2AX and phosphorylated MDC1 appeared to be diffused in some of the infected cells [112]. With treatment of an ATM-specific inhibitor, the majority of the phosphorylation events were reduced, indicating that ATM signaling is the major mediator of MVM infection-induced DDR [29]. By contrast, ATR signaling seems to be deregulated during MVM infection of asynchronous A9 cells, although it is not clear whether this is true in other cell lines [112]. In MVM-infected NB324K cells, DNA-PK components, Ku70 and Ku86, localized to the APAR bodies [29]. However, whether DNA-PKcs is phosphorylated during MVM infection was not examined.

Viral DNA replication is required for an MVM-induced DDR [29]. Ectopic expression of NS1, NS2 or NS1 plus NS2 did not generate significant levels of DDR signaling [29]. Infection of wild-type MVM and NS2-knockout mutant induced a similar DDR in asynchronous A9 cells, further suggesting that NS2 is not required for DDR induction [112]. Expression of NS1 induced a slightly increase in the level of γH2AX, which is likely due to the non-specific nicking function of NS1 [29,113]. The finding that UV-inactivated MVM at low MOI (multiplicity of infection) failed to induce an obvious DDR indicates that neither viral proteins nor viral genome alone is able to induce a DDR comparable to that observed during MVM replication [29].

ATM signaling contributes to MVM DNA replication [29]. Treatment of MVM-infected cells with an ATM-specific inhibitor significantly blocked MVM DNA replication [29]. However, Mre11, the sensor for ATM activation, was degraded during MVM infection [29]. DNA-PKcs signaling contributes minimally to MVM replication [29]. Whether the ATR signaling affects MVM DNA replication and host cell cycle arrest has not been studied. Inhibition of ATM signaling ameliorated MVM infection-induced G2/M arrest, indicating that ATM signaling partially contributes to MVM infection-induced cell cycle arrest [29]. Since Chk2 is phosphorylated during

MVM infection [29], it is likely that Chk2 plays a role in MVM infection-induced G2/M arrest during late infection.

Taken together, MVM infection mainly hijacks ATM signaling for viral DNA replication. We speculate that ATM- or Mre11-deficient cell lines do not support MVM replication. ATM signaling also partially contributes to MVM infection-induced G2/M arrest. The viral DNA replication event is required for the induction of DDR. It is not clear how ATM signaling promotes viral DNA replication. Since MVM replication is limited in cells at S phase [11,12,114], it is unknown yet whether ATM signaling regulates S phase arrest during early infection.

-H-1PV

H-1PV infection triggers a DDR that is mediated by reactive oxygen species (ROS) production [23]. ROS are chemically generated in cells treated with xenobiotic agents such as peroxides and oxidants, or by-products of the oxygen metabolism. Accumulation of such molecules causes oxidative stress, which damages cellular structures through initiation of apoptosis [115]. Recent studies also show that ROS production is a general source of DDR activation [116].

In contrast to the MVM NS1 protein, H-1PV NS1 *per se* induces apoptosis, ROS production and a DDR [23]. Either H-1PV infection or only NS1 expression in NS1-inducible stable cell line caused G2/M arrest and cytotoxic effects. NS1 expression-induced apoptosis was mediated through the activation of caspase-3 and -9. NS1 expression alone induced a high level of γH2AX, suggesting that the H-1PV NS1 protein has an intrinsic ability to induce a DDR. H-1PV infection increased ROS production. Treatment of H-1PV-infected or NS1-expressing cells with antioxidants blocked ROS production and decreased γH2AX expression, indicating that the NS1-induced ROS production contributes to DDR activation. In concert, antioxidant treatment

blocked the NS1-induced apoptosis. These results demonstrated that H1-PV NS1 has the ability to cause oxidative stress through upregulation of ROS production, which is likely due to cellular DNA damage, such as DSBs, induced by the NS1 non-specific nicking of chromosome DNA.

Collectively, H-1PV NS1 protein induces a DDR through regulating ROS production, which is responsible for the apoptosis induced during infection. It is unknown yet which DDR pathway is activated during H-1PV infection or by NS1 expression alone. More importantly, whether the DDR signaling plays a role in the H-1PV replication remains to be answered.

Genus *Bocavirus* (Minute virus of canines, MVC)

MVC belongs to the genus *Bocavirus*, which also includes bovine parvovirus 1 (BPV1) and the newly identified human bocavirus HBoV [117–119]. MVC contains two asymmetric terminal hairpins (Figure 2) [118]. Walter Reed/3873D (WRD) cells were widely used for MVC infection [120]. MVC infection of WRD cells triggered a gradual cell cycle change from S phase arrest in early infection to G2/M arrest in late infection as well as mitochondrion-mediated apoptosis [121]. MVC infection activates the ATM signaling [30]. In contrast to MVM infection, ATR was phosphorylated during MVC infection. γH2AX was distributed in a pannuclear pattern, while phosphorylated RPA32 colocalized within the MVC replication centers. Inhibition of ATM signaling blocked H2AX phosphorylation, while inhibition of both ATM and ATR signaling by pan-inhibitors blocked RPA32 phosphorylation, indicating that both ATM and ATR signaling pathways are activated. Whether DNA-PKcs is phosphorylated has not been confirmed, due to the lack of a suitable antibody. However, neither knockdown of DNA-PKcs nor treatment of MVC-infected cells with a DNA-PKcs-specific inhibitor affected phosphorylation of H2AX and RPA32, strongly suggesting that DNA-PKcs signaling is not activated during MVC infection. The

MRN complex colocalized with MVC NS1 at the early stage of infection, while at the late stage, the Mre11 protein appeared to be degraded.

MVC DNA replication is required for MVC infection-induced DDR [30]. Individual transfection of an infectious clone and its derivatives generated positive DDR signaling as long as the derivative plasmid is able to replicate [30], which is similar to that in MVM- or B19V-induced DDR [29,104]. We speculate that MVC proteins may not cause a significant damage to cellular DNA, and that DDR signaling may come mainly from viral DNA replication events, i.e., specific nicking of viral DNA by the MVC NS1 protein or production of the viral DNA intermediates that are aberrant from any cellular DNA structure.

MVC hijacks ATM signaling for viral DNA replication [30]. Progeny virus production was reduced when the ATM signaling was inactivated. Neither knockdown of ATR nor DNA-PK had a negative effect on MVC DNA replication. Ablation of Mre11 by its specific siRNA reduced MVC DNA replication, suggesting that the MRN complex functions as a mediator to activate ATM signaling in the early stage of MVC infection.

ATM signaling affects two aspects of host cells during MVC infection. On one hand, similar to MVM, inhibition of ATM signaling ameliorated but not diminished the G2/M arrest [30]; On the other hand, ATM phosphorylated p53 at serine 15, which contributed to MVC infection-induced cell death. Knockdown of p53 did not affect MVC infection-induced G2/M arrest but rescued about 50% of cells from cell death in the late stage of infection [30]. Since p53 is a well-established linker between DDR and apoptosis [39,122,123], and MVC infection does trigger a mitochondrion-mediated apoptosis [121], it was proposed that phosphorylation of p53 by the ATM signaling during MVC infection directly contributes to MVC infection-induced apoptosis, through which progeny virus can be quickly released from lysed host cells for another round of infection [30].

In summary, MVC hijacks ATM signaling to facilitate viral DNA replication and thereafter progeny virus production. Similar to MVM and B19V, MVC DNA replication is necessary for DDR induction. Activation of ATM signaling partially contributes to MVC infection-induced G2/M arrest, although it is not clear whether this is because of the direct activation of the G2/M checkpoint or a delay of S phase progression. Indeed, we observed that MVC infection trigged an intra-S phase arrest that is dependent upon the ATM signaling pathway (Y. Luo & J. Qiu, unpublished observation). The intra-S phase arrest not only blocked cellular DNA replication, but also delayed S phase progression. Therefore, we speculate that in the context of the intra-S phase arrest, MVC represses cellular DNA replication and continuously hijacks the cellular DNA replication machinery. These findings revealed the beneficial effects of the ATM activation on autonomous parvovirus DNA replication, and suggest a novel model for parvovirus DNA replication.

Conclusion

Parvoviruses have evolved sophisticated strategies to coexist with their host species. Although their genomes are aberrant from any cellular DNA structure, and the proteins expressed from the viral genome are limited, they are able to propagate in various host cells of different species. Studies about DDR induced during parvovirus infection have uncovered novel mechanisms underlying virus-host interactions. For *Dependovirus* AAV2, DDR proteins, such as the MRN complex, function as a barrier for viral infection, and this barrier can be destroyed by the helper virus. By contrast, in autonomous parvoviruses, the DDR machinery is hijacked by viruses in order to create a cellular microenvironment conducive for viral DNA replication. Therefore, parvoviruses are able to utilize different strategies to adapt to their host cells and modulate the host cellular environment. The DDR induced by different parvoviruses is summarized in Figure 2.

Both viral proteins and the ssDNA genome of parvoviruses are able to elicit a DDR. The nonstructural protein of parvoviruses, i.e., the NS1 protein of H1-PV and MVM, and the large Rep proteins of AAV2, are able to induce a DDR without the presence of viral genomes [10,23,29,65,113], indicating that they may create damaged cellular DNA though their endonuclease functions. The UV-inactivated AAV2 genome triggered ATR-Chk1 signaling [78,79]. However, during infection of MVM, MVC, B19V and coinfection of AAV2 and adenovirus, the DDR signaling is majorly activated from the DNA replication events [28–30,65], likely due to the specific nicking of viral DNA or generation of viral DNA intermediates that mimic damaged DNA.

During infection of autonomous parvoviruses, the DDR machinery is hijacked to facilitate viral DNA replication [28–30]. However, the MRN complex is a barrier to AAV2 replication and rAAV transduction when adenovirus is coinfected or its helper genes are expressed [57]. It is still unknown whether the three DDR pathways have an impact on the life cycle of AAV2 during coinfection, because both adenovirus and HSV1 interfere with the DDR machinery as well. The DDR machinery regulates cell cycle arrest and apoptosis induced during parvovirus infection. DDR triggered either by expression of the largest nonstructural viral proteins of parvoviruses [10,17,23,113] or by infection of autonomous parvoviruses [28–30] is able to arrest infected cells at S phase or G2/M phase. UV-inactivated AAV2-induced DDR not only arrests cells at G2/M [78], but also triggered apoptosis in tumor cells [79]. Viral infection-induced apoptosis was also observed following DDR activation during MVC infection, which activates the ATM-p53 signaling pathway [30]. Hence, parvovirus infection-induced DDR influences the host cell fate through cell cycle regulation and apoptosis induction. The mechanisms by which viral infection-induced DDR coordinates host cell cycle change and apoptosis require further investigation.

Objectives

Studies on parvovirus-induced DDR have greatly facilitated the understanding of parvovirus replication. Since using AAV2 as a model to study the relationship between the DDR and parvovirus DNA replication is very complicated due to the presence of the helper viruses, we aim to understand the basic mechanisms underlying autonomous parvovirus infection induced DDR by using MVC and B19V as model organisms.

In this study, in the first place, we aim to confirm that whether the DDR activation is a general feature of autonomous parvovirus infection. Next, we try to examine the detailed signaling pathways of DDR in each infection conditions of these two viruses. We also want to know the consequences of the DDR on infected host cells as well as viral life cycle.

Since autonomous parvovirus replicates in cells at S phase and induces a DDR, we also speculate that DDR-induced cell cycle arrest at either intra-S phase or late S phase (with a 4N DNA content) plays a critical role in DDR-promoted parvovirus DNA replication. The mechanisms by which parvoviruses induce S phase arrest by the DNA damage machinery and how DDR signaling facilitates viral DNA replication are also topics in this study.

Genus	Virus	Genome Structure	Mediator of the DDR	Consequence of the DDR
Dependovirus	AAV2	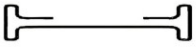	ATR (UV-AAV)	ATR triggers G2/M arrest and apoptosis in UV-AAV infected cells.
			DNA-PKcs (AAV2/Adenovirus)	The MRN complex limits AAV2 replication.
			DNA-PKcs (AAV/HSV-1)	Unclear
Erythrovirus	B19V	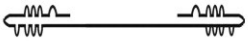	ATR and DNA-PKcs	Facilitates B19V replication; dispensable for B19V infection-induced G2/M arrest.
Parvovirus	MVM	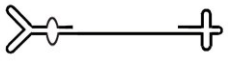	ATM	Facilitates MVM replication; partially mediates G2/M arrest.
	H-1PV		Unclear	Unclear
Bocavirus	MVC	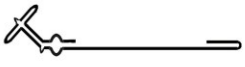	ATM	Facilitates MVC replication and triggers p53-dependent apoptosis; partially mediates G2/M arrest.
Amdovirus	AMDV (aleutian mink disease virus)	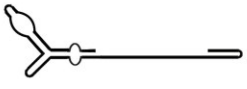	Unclear	Unclear

Figure 2 Summary of parvovirus infection-induced DDR.

Chapter 2

Bocavirus Infection Induces a DNA Damage Response That Facilitates Viral DNA Replication and Mediates Cell Death

Abstract

Minute virus of canines (MVC) is an autonomous parvovirus that replicates efficiently without helper viruses in Walter Reed/3873D (WRD) canine cells. We previously showed that MVC infection induces mitochondrion-mediated apoptosis and G2/M-phase arrest in infected WRD cells. However, the mechanism responsible for these effects has not been established. Here, we report that MVC infection triggers a DNA damage response in infected cells, as evident from phosphorylation of H2AX and RPA32. We discovered that both the ATM (ataxia-telangiectasia mutated) and ATR (ATM and Rad3-related) kinases were phosphorylated in MVC-infected WRD cells, and confirmed that ATM activation was responsible for the phosphorylation of H2AX, whereas ATR activation was required for the phosphorylation of RPA32. Both pharmacological inhibition of ATM activation and knockdown of ATM in MVC-infected cells led to a significant reduction in cell death, a moderate correction of cell cycle arrest, and, most importantly, a reduction in MVC DNA replication and progeny virus production. Parallel experiments with an ATR-targeted siRNA had no effect. Moreover, we identified that this ATM-mediated cell death is p53-dependent. In addition, we localized the Mre11-Rad50-Nbs1 (MRN) complex-the major mediator as well as a substrate of the ATM-mediated DNA damage response pathway to MVC replication centers during infection, and show that Mre11 knockdown led to a reduction in MVC DNA replication. Our findings are the first time to support the notion that an autonomous parvovirus is able to hijack the host DNA damage machinery for its own replication and for the induction of cell death.

Introduction

Bocavirus is a newly classified genus of the family *Parvovirinae*, and includes human bocavirus (HBoV), minute virus of canines (MVC) and bovine parvovirus (BPV). HBoV was recently associated with acute respiratory wheezing and pneumonia [124–126], and is commonly detected in association with other respiratory viruses [125,126]. In addition to being linked to respiratory illnesses, HBoV has been associated with gastroenteritic diseases [127–131]. Within their respective hosts, two closely related animal bocaviruses share these characteristics [132–137]. Although differentiated human airway epithelial cells were recently shown to support HBoV replication, the fact that this was at an extremely low level [138] makes this system a difficult one to study HBoV biology. MVC infection of Walter Reed/387D (WRD) cells, however, has been proven much more efficient [118,120]. Using this system, we have shown that MVC infection induces mitochondrion-mediated apoptosis, that this effect is dependent on replication of the viral genome, and that the MVC genome *per se* is able to arrest the cell cycle at the G2/M-phase [121].

Infection by many DNA viruses has been found to induce a cellular DNA damage response (DDR), which can either block or enhance viral DNA replication, as well as cell cycle arrest (in response to mild damage) or apoptosis (in response to irreparable damage), in infected cells [49]. DNA damage rapidly activates conserved DDR pathways [139,140] that involve three PI-3-kinase-like kinases (PI3Ks): ATM (ataxia telangiectasia mutated), ATR (ATM and Rad3 related), and DNA-PK (DNA-dependent protein kinase) [106,141,142]. ATM is primarily activated as a result of DNA double-strand breaks (DSBs), and is recruited to DSBs by the Mre11-Rad50-Nbs1 (MRN) complex. ATR, on the other hand, responds to the detection of single-stranded DNA (ssDNA) breaks and stalled DNA replication forks, and is recruited to RPA-coated ssDNA by an ATR-interacting protein (ATRIP) [140,143]. Like ATM, DNA-PK is activated in response to DSBs, but it is recruited to the damage site in complex with Ku70 and

Ku80. Once recruited to a site of damage, ATM, ATR and DNA-PK phosphorylate a number of substrates (including H2AX, RPA, CHK1 and CHK2, p53, SMC1, Nbs1 and BRCA1) that in turn target other proteins, with ultimate outcome being the silencing of CDKs and an arrest of cell-cycle progression to promote DNA repair or elimination of the potential hazardous cells by apoptosis [140,144,145].

Parvovirus contains a linear ssDNA genome with terminal repeat structures at both ends [146]. Adeno-associated virus 2 (AAV2), a member in the genus *Dependovirus* of the family *Parvovirinae*, in the case of infection by (UV-inactivated) AAV2 alone, provokes a DDR that mimics stalled replication forks, with both ATM and ATR being activated, resulting in the phosphorylation of CHK1 and H2AX and G2-phase arrest [75,76,147]. It is the p5 promoter sequence, rather than the AAV2 terminal repeats, that triggers DDR [147]. However, when AAV2 undergoes a productive infection in the presence of adenovirus, AAV2 DNA replication activates a DDR that is primarily mediated through DNA-PK pathway, and leads to phosphorylation of the downstream targets H2AX, RPA32, Nbs1, CHK1, CHK2 and SMC1 [64,65] in the absence of the MRN complex [65]. Replication of AAV2 requires degradation of the MRN complex, an upstream regulator essential for activation of the ATM pathway [57]. For this, AAV2 requires the help of another virus, such as adenovirus. Adenovirus *per se* can induce DDR and cell death [148]. Therefore, a simple model for studying the relationships among parvovirus DNA replication, DDR and induced cell death has not been established.

In the current study, we provide the first evidence that infection by MVC, an autonomous parvovirus, triggers a DDR that is represented by phosphorylation of both H2AX and RPA32. We show that both ATM- and ATR-mediated pathways are involved in the MVC infection-induced DDR, but that only the ATM-mediated pathway, which is sensed by the MRN complex, is critical for replication of the MVC genome and MVC-infection-induced cell death.

Materials and Methods

Cell and virus:

WRD canine cells were maintained in Dulbecco's modified Eagle's medium with 10% fetal calf serum in 5% CO_2 at 37°C. The MVC strain used in this study is the original strain GA3, which was isolated at the College of Veterinary Science, Cornell University. MVC was cultured and quantified as previously described, and the virus titer was determined as the number of fluorescence-focus forming units (ffu) per ml [121]. The WRD cell line and MVC strain were obtained as gifts from Dr. Colin Parrish at Cornell University. WRD cells were infected with MVC at a multiplicity of infection (MOI) of 5.

Chemicals and treatment:

Hydroxyurea (HU, Calbiochem) was diluted to deionized water as a stock solution at 250 mM. Inhibitors, CGK733, KU55933, NU7441 and Wortmannin, were bought from Calbiochem, and were diluted in DMSO as stock solutions at 10 mM. BrdU was purchased from Sigma and diluted in deionized water as a stock solution at 5 mM.

WRD cells were seeded on 60-mm dishes one day prior to chemical treatment. KU55933, CGK733, NU7441 and Wortmannin were applied to cells at a final concentration of 20 μM, 2.5 μM, and 10 μM, respectively, 3 hrs prior to infection. 0.25% DMSO was used as a DMSO control. HU was added to cells at a final concentration of 2.5 mM in parallel with MVC infection.

siRNA, plasmid and transfection:

siRNA oligos were synthesized as dicer-substrate RNAi at Integrated DNA technologies (IDT, Coralville, Iowa). The following siRNA sequences were chosen for targeting the genes of interest: siRNA specific to ATM (siATM): 5'-GUACUAGUUGCUUGUGUAACUGUA-3'; siRNA specific to ATR (siATR): 5'-AGAAAGGAUUGUAGGCUAAUGGAA-3'; siRNA specific to DNA-PK catalytic subunit (siDNA-PKcs): 5'-CUAGGAAAUCCAUCGGUAUCAUUAA-3'; siRNA specific to Mre11 (siMre11): 5'-GGUCUUCUACUCUUAGGGUUGUUCCUU-3'; siRNA specific to p53 (sip53): 5'- CCACCAUCCCUAAACUAAUGTG-3'. The following scrambled RNA (Scrambled) was used as a siRNA control: 5'CUUCCUCUCUUUCUCUCCCUUGUGA3'. Transfection of all the siRNAs was performed using Trifectin reagent (IDT) following the manufacturer's instructions. At 48 hrs post-transfection, the cells were fed with fresh medium and infected with MVC.

MVC plasmids, pIMVC, pIMVCNS1(-), pIMVCNP1(-), pIMVCVP1/2(-), and pMVCNSCap, and the method for transfection have been described previously [118,121].

Antibodies:

Anti-MVC NS1 and anti-MVC NP1 antisera were produced previously [118,121]. Anti-γH2AX (Millipore Corporate), anti-phospho(p)-RAP32(Ser33) (Bethyl Laboratories, Inc.), anti-phospho(p)-ATM (Ser1981) (Rockland Immunochemicals Inc.), anti-Rad50 (GeneTex Inc.), anti-p-SMC1(Ser957) (Genscript USA Inc.), and anti-ATM, anti-ATR and anti-DNA-PKcs (Calbiochem, EMD Chemicals Inc.) were used in this study. Both a monoclonal anti-Mre11 antibody (clone 12D7, GeneTex), which was generated by immunizing a truncated Mre11 from aa182 to 582, and a polyclonal anti-Mre11 antibody (C-16, Santa Cruz Biotechnology Inc.), which was raised against a peptide mapping near the C-terminus of human Mre11, were used to

detect Mre11. Anti-p-ATR(Ser428), anti-p-Nbs1(Ser343), and anti-p-p53(Ser15) were obtained from Cell Signaling Inc. Antibody dilutions used for Western blotting and immunofluorescence analysis were as suggested in the manufacturers' instructions.

Western blotting and immunofluorescence:

Western blotting and immunofluorescence assays were performed as previously described [121]. Confocal images were taken at a magnification of 100 × (objective lens), with an Eclipse C1 Plus confocal microscope (Nikon) controlled by Nikon EZ-C1 software.

For BrdU incorporation, WRD cells were seeded on a chamber slide and infected with MVC at an MOI of 5. At 18 hrs p.i., BrdU was added into the cell culture medium at a final concentration of 5 μM. At 24 hrs p.i., cells were fixed and co-immunostained with rat anti-MVC NS1 and mouse anti-BrdU to mark the MVC replication centers.

Southern blotting analysis:

Low-molecular-weight DNA (Hirt DNA) was extracted from WRD cells, and DpnI digestion and Southern blotting were performed as described previously using the MVC NSCap probe as described previously [118].

Virus titration assay:

WRD cells were transfected with siRNAs for 48 hrs, or treated with inhibitors for 3 hours prior to MVC infection (MOI = 5). At 48 hrs p.i., both the cells and medium were collected and

lysed by repeated freezing and thawing. After lysis, the samples were briefly centrifuged and the supernatants were collected for the virus titration assay.

WRD cells were seeded on 4 well-chamber slides (Lab-Tek, USA) 24 hrs prior to infection. Virus samples were serially diluted in ten-fold and added to each well. At 24 hrs p.i., cells were fixed in 100% acetone and stained with anti-MVC NS1 and then processed for immunofluorescence assay. The number of fluorescence-positive cells in each chamber was counted. This number of focus-forming units in each well was calculated by multiplying the number of fluorescence-positive cells per chamber by the dilution of the virus-containing supernatant. The viral titer is expressed as the average number of focus-forming units per ml of supernatant (ffu/ml)**.**

Flow cytometry analysis:

Live/Dead Violet staining for detection of cell death and DAPI staining for analysis of cell cycle were performed as described previously [121]. All of the processed samples were analyzed on a three-laser flow cytometer (LSR II; BD Biosciences) at the Flow Cytometry Core of the University of Kansas Medical Center. All flow cytometry data were analyzed using FACS DIVA software (BD Biosciences).

Results

MVC infection causes a DNA damage response (DDR) in infected cells.

To examine whether DDR is induced during MVC infection, we evaluated the phosphorylation status of H2AX and RPA32 in MVC-infected cells. First, we used BrdU incorporation to identify the MVC DNA replication centers, and inspected whether anti-BrdU staining colocalizes with the MVC NS1 protein. As shown in Fig. 1A, NS1 was present at active replication foci, as indicated by anti-BrdU staining. In subsequent experiments, we used anti-NS1 staining as a marker for the MVC DNA replication centers.

MVC-infected cells were co-immunostained with anti-NS1 and anti-phosphorylated H2AX (γH2AX) or with anti-NS1 and anti-RPA32 phosphorylated at serine 33 (p-RPA32). In parallel, we treated cells with hydroxyurea (HU), an agent known to induce DDR [149,150], as a positive control. At 48 hrs postinfection (p.i.), we found that MVC infection led to significant increases in the levels of both γH2AX and p-RPA32 in NS1-expressing cells (Fig. 1B&C, MVC-infected), with most of the NS1-expressing cells (red) also positive for anti-γH2AX or anti-p-RPA (green), respectively. Interestingly, p-RPA32 colocalized with NS1 at replication foci, but γH2AX did not (Fig. 1B&C, MVC-infected). In the HU-treated positive control cells, γH2AX and p-RPA32 were also expressed in the nuclei (Fig. 1B&C, HU-treated). Thus MVC infection specifically induces the phosphorylation of H2AX and RPA32. Western blot analysis revealed that H2AX and RPA32 were increasingly phosphorylated over time (Fig. 1D). Both H2AX and RPA32 were phosphorylated starting at 18 hrs p.i., and were maximally phosphorylated at 36 hrs p.i.; this correlated with the level of MVC replication as assessed NS1 expression (Fig. 1D). Collectively, these findings show that MVC infection induces a significant DDR that is correlated with MVC replication.

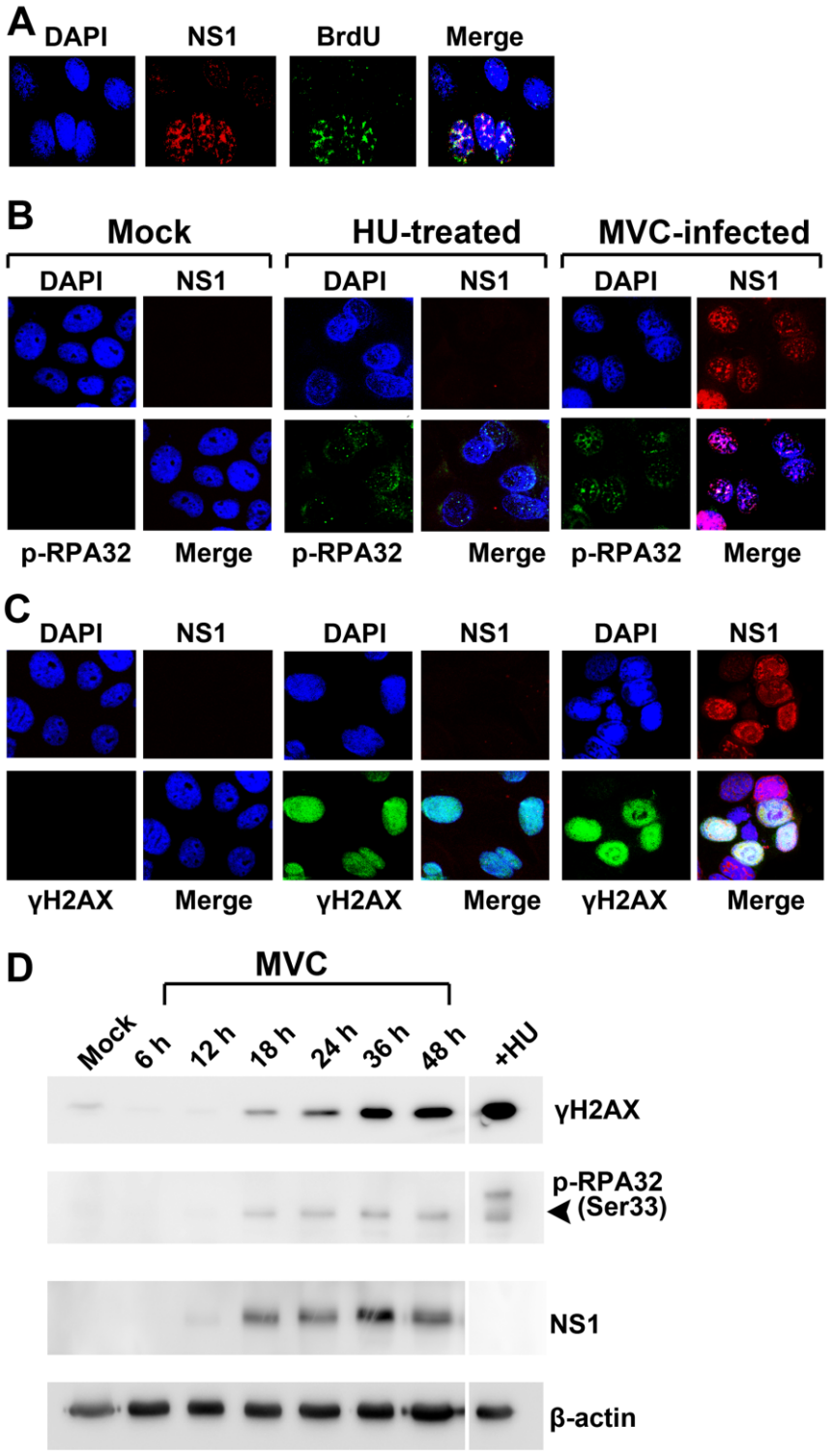
A
DAPI
NS1
BrdU
Merge
B
Mock
HU-treated
MVC-infected
DAPI
NS1
p-RPA32
Merge
C
γH2AX
D
MVC
Mock
6 h
12 h
18 h
24 h
36 h
48 h
+HU
γH2AX
p-RPA32
(Ser33)
NS1
β-actin

Figure 1. MVC infection induces a DDR.

(A) Detection of the MVC DNA replication foci using BrdU incorporation. Punctuate staining by anti-NS1 (red) or anti-BrdU (green) antibody indicates the replication foci. **(B&C)** Immunofluorescence analysis of MVC infection-induced DDR. At 48 hrs p.i., MVC-infected cells were co-immunostained with anti-MVC NS1 (red) and anti-γH2AX (green) **(B)** or anti-MVC NS1 (red) and anti-p-RPA(Ser33) (green) **(C).** Cells treated with hydroxyurea (HU) were used as a positive control for an induced DDR [149,150]. Nuclei were marked by DAPI staining. **(D)** Western blotting analysis of MVC infection-induced DDR. MVC-infected cells were harvested at the indicated time points and analyzed by Western blotting. In addition to the levels of the MVC NS1 protein, phosphorylation of the DDR markers H2AX and RPA32 was assessed using appropriate antibodies. The same membrane was reprobed with each antibody. HU-treated cells served a positive control, and anti-β-actin was used as a loading control. Arrow shows phosphorylated RPA32 at serine 33, two bands of phosphorylated RPA32 were detected in HU-treated cells.

Both ATM and ATR are activated in the MVC infection-induced DDR.

We examined which kinase pathway underlies the DDR induced during MVC infection. First, we used pharmacological inhibitors to ATM, ATR and DNA-PK to block the phosphorylation of these kinases. Both the ATM-specific inhibitor KU55933 [151] and the ATR/ATM-specific inhibitor CGK733 [152–157] reduced γH2AX levels by approximately 5-fold compared with those in untreated control cells (Fig. 2A, lanes 3&4 *vs.* 2); this did not hold true for the DNA-PK inhibitor NU7441 [158] (Fig. 2A, lane 5). CGK733 also significantly interfered with the phosphorylation of RPA32, whereas KU55933 and NU7441 did not (Fig. 2B). The pan-PI3K inhibitor Wortmannin [159] also inhibited the phosphorylation of RPA32, but not as potently as did CGK733 (Fig. 2B). Dephosphorylation of ATM by the inhibitors KU55933 and CGK733 was confirmed by anti-p-ATM staining (Fig. 2C, lanes 3&4), and ATR dephosphorylation by the inhibitor CGK733 was confirmed by anti-p-ATR staining (Fig. 2D, lane 4).

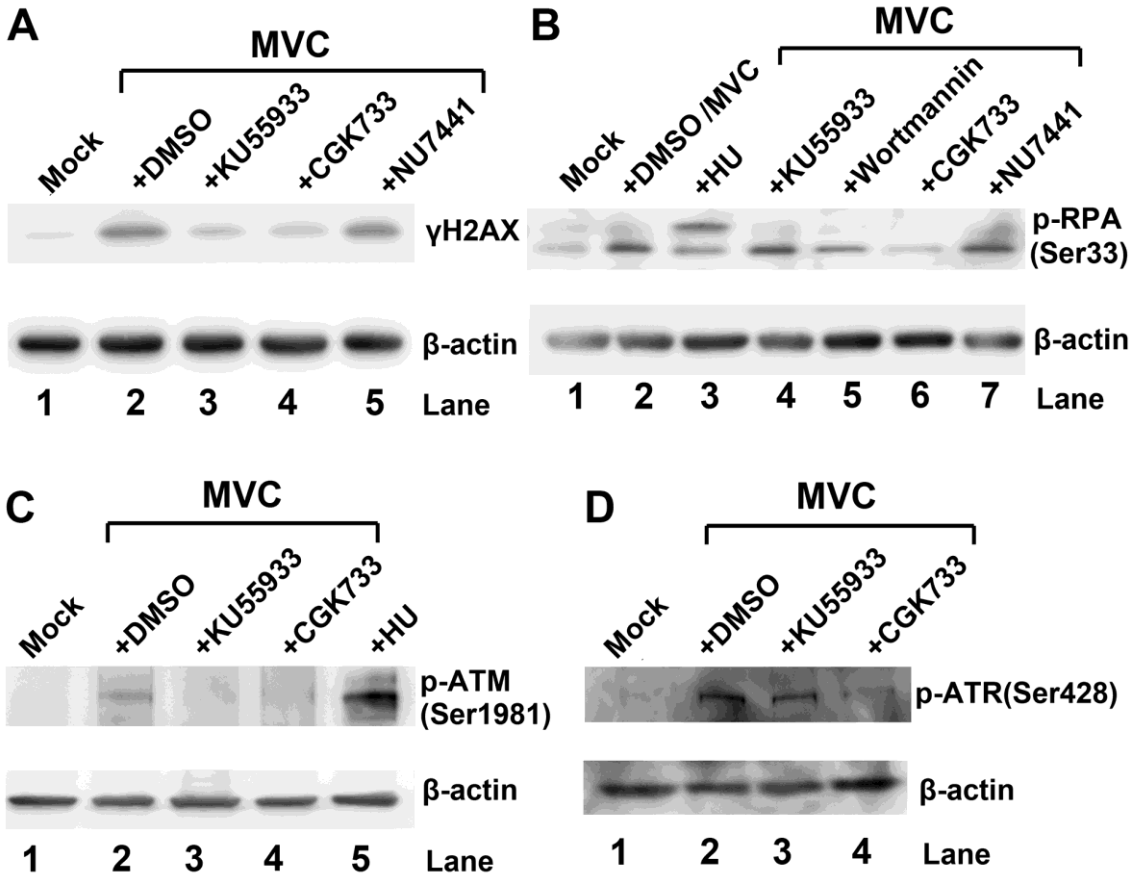
A
MVC
Mock
+DMSO
+KU55933
+CGK733
+NU7441
γH2AX
β-actin
1 2 3 4 5 Lane
B
MVC
Mock
+DMSO /MVC
+HU
+KU55933
+Wortmannin
+CGK733
+NU7441
p-RPA (Ser33)
β-actin
1 2 3 4 5 6 7 Lane
C
MVC
Mock
+DMSO
+KU55933
+CGK733
+HU
p-ATM (Ser1981)
β-actin
1 2 3 4 5 Lane
D
MVC
Mock
+DMSO
+KU55933
+CGK733
p-ATR(Ser428)
β-actin
1 2 3 4 Lane

Figure 2. Treatment with pharmacological inhibitors of ATM and ATR reduces MVC infection-induced phosphorylation of H2AX and RPA32, respectively.

WRD cells were treated with DMSO (at 0.25%) and inhibitors, and then infected with MVC at 3 hrs post-treatment. MVC-infected cells were harvested at 48 hrs p.i. and were lysed for immunoblotting using anti-γH2AX **(A)**, anti-p-RPA(Ser33) **(B)**, anti-p-ATM(Ser1981) **(C)**, and anti-p-ATR(Ser428) **(D).** In all blots, anti-β-actin was used to control for loading. Mock-infected and HU-treated cells were used as a negative and a positive control, respectively.

We next used siRNA molecules to specifically knock down ATM, ATR and the DNA-PK catalytic subunit (DNA-PKcs). As shown in Fig. 3A, the ATM-specific siRNA inhibited ATM expression by approximately 4-fold compared with the scrambled siRNA control (Fig. 3A). Consistent with an inhibition of ATM expression, the ATM siRNA reduced γH2AX by more than 5-fold to the background level (Fig. 3D, lane 3), but did not affect phosphorylation of RPA32 (Fig. 3E, lane 3). Similarly, the ATR-specific siRNA reduced ATR expression (Fig. 3B), and accordingly decreased the level of phosphorylated RPA32 to the background level in the mock control but not that of γH2AX (Fig. 3D&E, lane 4 *vs.* lane 1). However, neither phosphorylation event was diminished in MVC-infected cells treated with the DNA PKcs-specific siRNA (Fig. 3D&E, lane 5), in spite of the fact that the DNA-PKcs-specific siRNA inhibited nearly 90% of the DNA-PKcs (Fig. 3C, lane 3).

Together, these results show that the increase in γH2AX during MVC infection is mediated by ATM phosphorylation, whereas the increase in RPA32 phosphorylation is a consequence of ATR activation. Thus, MVC infection-induced DDR appears to involve activation of both the ATM and ATR pathways. Due to the lack of an antibody to detect phosphorylated canine DNA-PK, we were not able to test whether DNA-PK is phosphorylated during MVC infection. However, based on results using the DNA-PKcs-specific siRNA, we believe that DNA-PK is less likely to be involved in DDR induced by MVC infection.

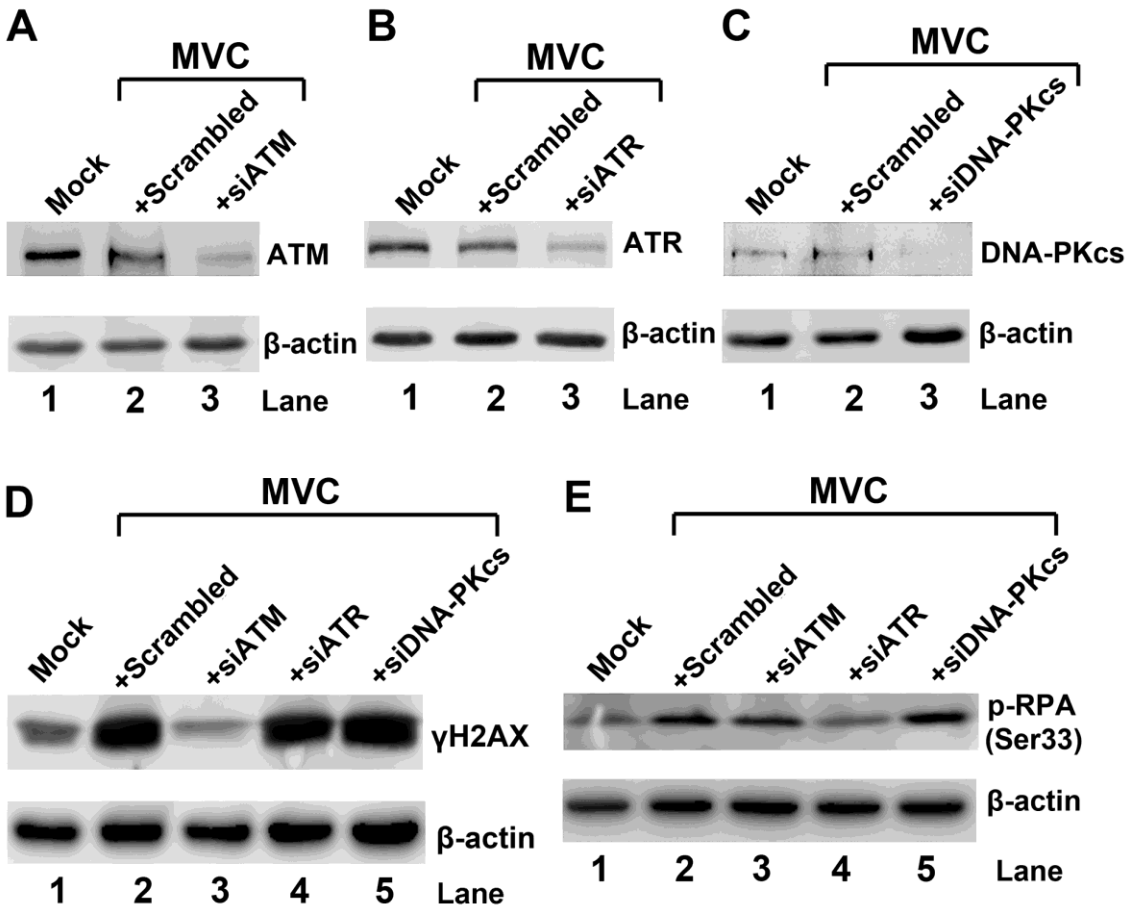
A
MVC
Mock
+Scrambled
+siATM
ATM
β-actin
1 2 3 Lane
B
MVC
Mock
+Scrambled
+siATR
ATR
β-actin
1 2 3 Lane
C
MVC
Mock
+Scrambled
+siDNA-PKcs
DNA-PKcs
β-actin
1 2 3 Lane
D
MVC
Mock
+Scrambled
+siATM
+siATR
+siDNA-PKcs
γH2AX
β-actin
1 2 3 4 5 Lane
E
MVC
Mock
+Scrambled
+siATM
+siATR
+siDNA-PKcs
p-RPA
(Ser33)
β-actin
1 2 3 4 5 Lane

Figure 3. Treatment with siRNAs targeting ATM and ATR reduces MVC infection-induced phosphorylation of H2AX and RPA32, respectively.

WRD cells were transfected with the indicated siRNA to silence ATM, ATR or DNA-PK. The cells were infected with MVC at 48 hrs post-transfection. **(A-C)** To confirm the efficiency of knockdown, at 48 hrs p.i., cells were collected and lysed for immunoblotting using antibodies against ATM **(A)**, ATR **(B)**, and DNA-PKcs **(C)**, respectively. A scrambled siRNA served as a negative control. **(D&E)** To assess the effect of the knockdown on the DDR, at 48 hrs p.i., cells were collected and lysed for immunoblotting using anti-γH2AX **(D)** and p-RPA(Ser33) **(E),** respectively. Both blots were reprobed with anti-β-actin antibody. Mock-infected cells were used as a background control.

The ATM-mediated DDR plays an important role in inducing the cytopathic effects that occur during MVC infection.

We used the above-described pharmacological inhibitors and siRNAs to examine the effects of inhibiting ATM, ATR and DNA-PK on the cell death that is triggered in WRD cells by MVC infection [121]. At 24 hrs and 48 hrs p.i., the cells were harvested for flow cytometry analysis with the cell death marker dye Live/Dead Violet and an anti-MVC NS1 antibody. NS1-expressing cells were selectively gated to determine the percentage of dead cells. We found that when either an ATM inhibitor (KU55933 or CGK733) or an ATM-specific siRNA was applied to MVC-infected cells, cell death at 48 hrs p.i. was significantly inhibited (Fig. 4). More specifically, treatment with KU55933 and CGK733 reduced cell death by 55% and 84%, respectively, over that seen in the DMSO control, and application of the ATM-specific siRNA reduced cell death by 70% compared to that achieved when the scrambled siRNA control was applied. Treatment of the cells with the ATR-specific siRNA resulted in only a slight inhibition of cell death, by approximately 11% (Fig. 4). In contrast, application of neither the DNA-PK inhibitor NU7441 nor DNA-PKcs-specific siRNA resulted in significant inhibition of the cell death induced by MVC infection at 48 hrs p.i. (Fig. 4). These results suggest that ATM activation is important to the cell death induced by MVC infection, whereas the ATR pathway contributes minimally. At 24 hrs p.i., cells in the DMSO control group did not undergo cell death at a significant level; therefore, inhibitory effects of the ATM inhibitor or of the siRNA could not be easily evaluated (Fig. 4). Moreover, application of the ATM-specific siRNA inhibited phosphorylation of p53 at serine 15 (Fig. 5A). Knocking down the p53 by a p53-speciifc siRNA reduced cell death by approximately 61%, compared to the treatment with the scrambled siRNA (Fig. 5B&C), but did not correct the cell cycle arrest (Fig. 5D). Thus our results suggest that MVC infection induces an ATM-mediated and p53-dependent cell death.

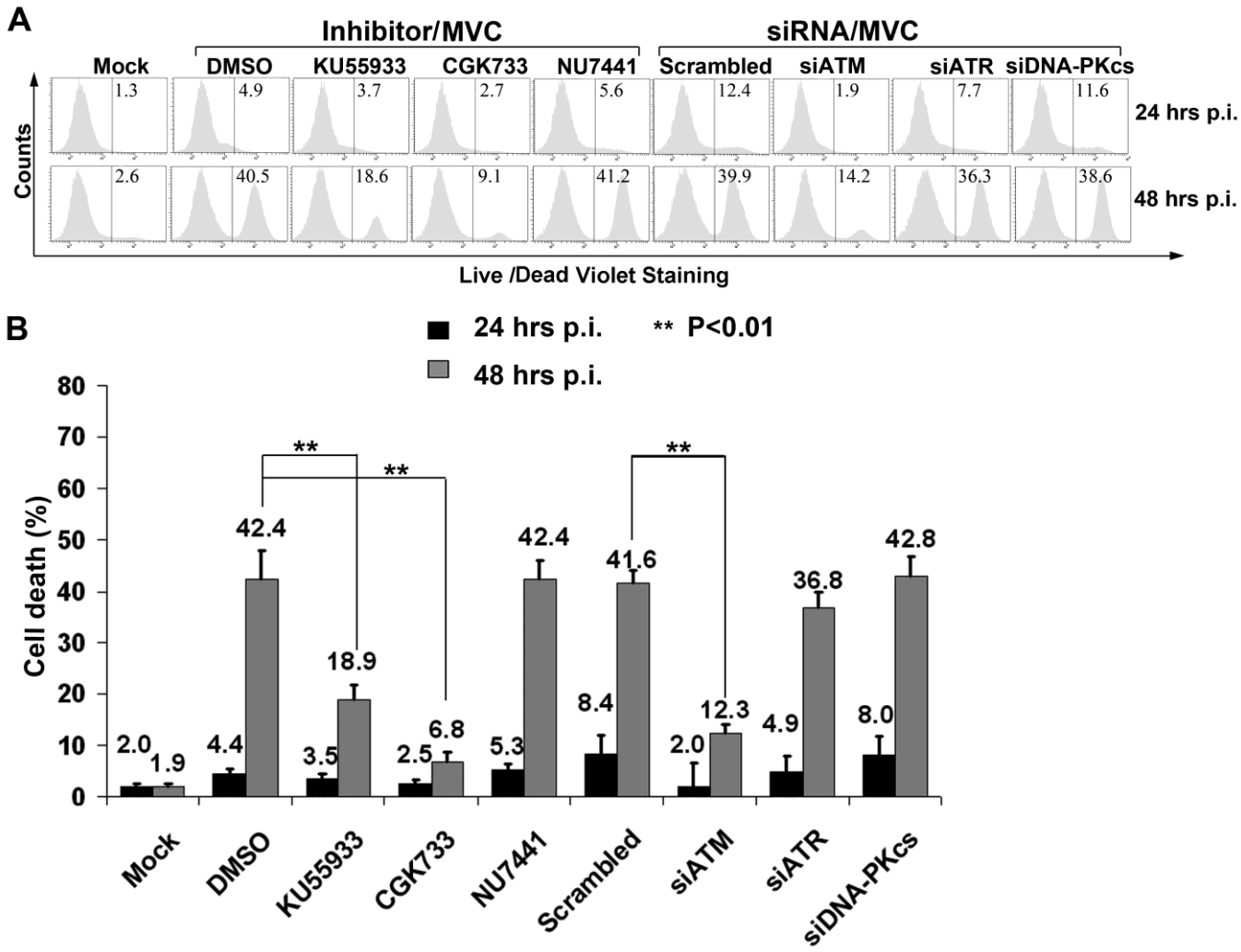
A
Inhibitor/MVC
siRNA/MVC
Mock
DMSO
KU55933
CGK733
NU7441
Scrambled
siATM
siATR
siDNA-PKcs
Counts
1.3
4.9
3.7
2.7
5.6
12.4
1.9
7.7
11.6
24 hrs p.i.
2.6
40.5
18.6
9.1
41.2
39.9
14.2
36.3
38.6
48 hrs p.i.
Live /Dead Violet Staining
B
24 hrs p.i.
** P<0.01
48 hrs p.i.
Cell death (%)
80
70
60
50
40
30
20
10
0
**
**
**
2.0
1.9
4.4
42.4
3.5
18.9
2.5
6.8
5.3
42.4
8.4
41.6
2.0
12.3
4.9
36.8
8.0
42.8
Mock
DMSO
KU55933
CGK733
NU7441
Scrambled
siATM
siATR
siDNA-PKcs

Figure 4. Both inhibiting ATM phosphorylation and knocking down ATM expression significantly reduce MVC infection-induced cell death.

WRD cells were treated with inhibitors for 3 hrs prior to MVC infection or transfected with the indicated siRNAs 48 hrs prior to MVC infection. **(A)** At 24 or 48 hrs p.i., cells were collected and analyzed using Live/Dead Violet and anti-NS1 co-staining by flow cytometry. The result shown is a representative one from three independent experiments. Percentages of dead cells in NS1-expressing cells are shown in each histogram. **(B)** Statistical analysis of the percentages of dead cells in NS1-expressing cells from three independent experiments. Average (numbers) and standard deviation ("T"-shaped bars) are shown for each treatment group.

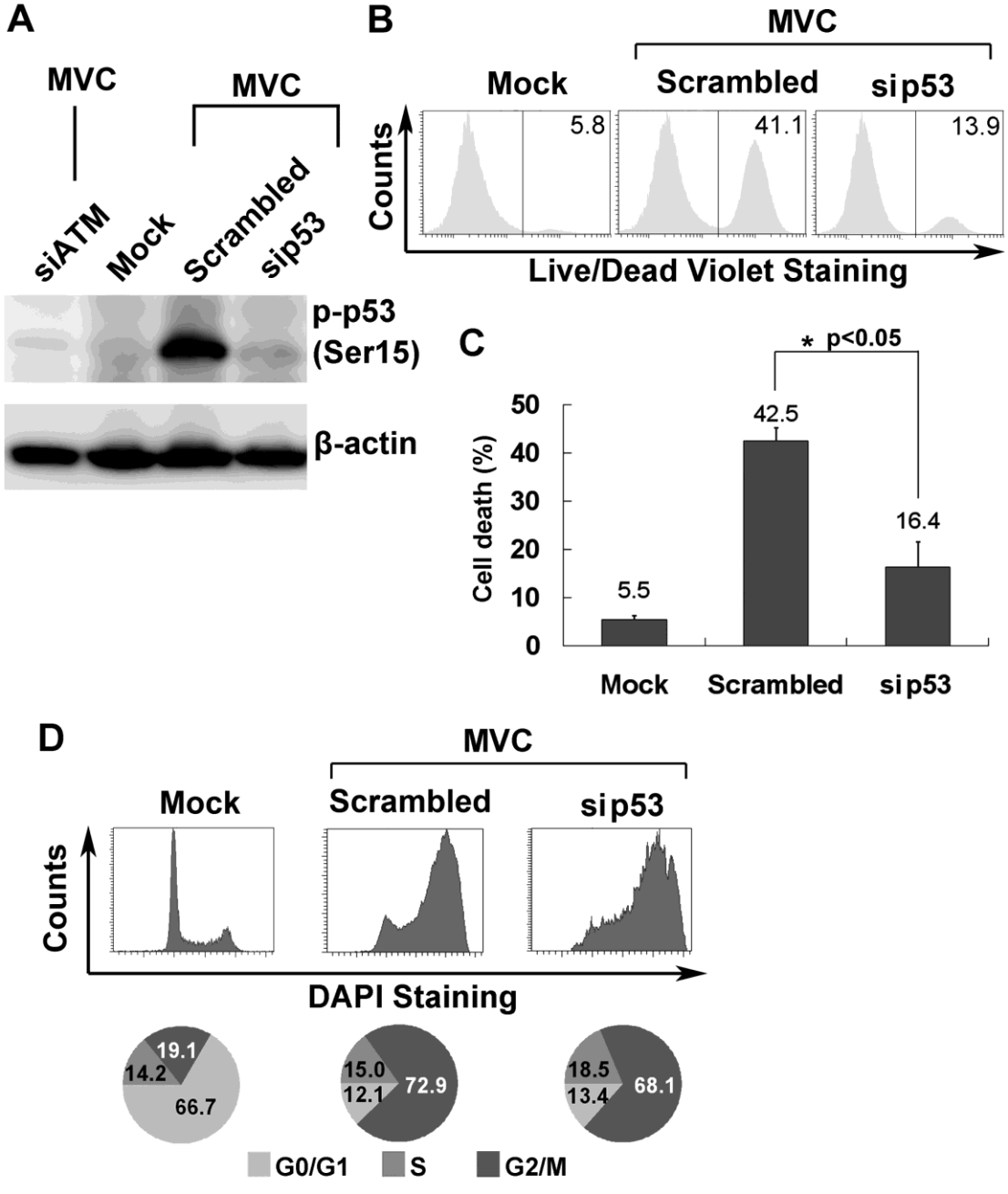
A
MVC
MVC
siATM
Mock
Scrambled
sip53
p-p53
(Ser15)
β-actin
B
MVC
Mock
Scrambled
sip53
5.8
41.1
13.9
Counts
Live/Dead Violet Staining
C
* p<0.05
42.5
16.4
5.5
Cell death (%)
50
40
30
20
10
0
Mock
Scrambled
sip53
D
MVC
Mock
Scrambled
sip53
Counts
DAPI Staining
19.1
14.2
66.7
15.0
12.1
72.9
18.5
13.4
68.1
G0/G1
S
G2/M

Figure 5. MVC infection-induced cell death is dependent on phosphorylation of p53.

WRD cells were transfected with the indicated siRNAs 48 hrs prior to MVC infection. **(A)** At 48 hrs p.i., cells were collected and lysed for immunoblotting using antibodies against phosphorylated p53 at serine 15. The blot was reprobed with anti-β-actin. **(B&C)** Cells were collected and analyzed using Live/Dead Violet and anti-NS1 co-staining by flow cytometry. A representative experiment is shown with percentages of dead cells in NS1-expressing cells in each histogram **(B)**, and average (numbers) and standard deviation ("T"-shaped bars) are shown for each treatment group **(C)**. **(D)** Cells were collected and analyzed for cell cycle using DAPI and anti-NS1 co-staining by flow cytometry. A representative experiment is shown with percentages of cells in each cell cycle.

We reported previously that a G2/M cell cycle arrest occurs during late MVC infection [121]. When KU55933 and CGK733 were applied to WRD cells prior to infection, the G2/M arrest that normally occurs at 48 hrs p.i., was inhibited to some extent; only approximately 56% (CGK733) and 67% (KU55933) were in the G2/M-phase compared to 76% in the DMSO control sample (Fig. 6). In contrast, the DNA-PK inhibitor had not effect (Fig. 6). Consistent with these results, only the ATM siRNA reduced the MVC infection-induced G2/M arrest, by approximately 16%, compared to that seen in the cells treated with the control scrambled siRNA (Fig. 6); neither the ATR- nor the DNA-PKcs-specific siRNA had an effect (Fig. 6). These results suggest that ATM activation is likely involved in the G2/M cell cycle arrest during MVC infection.

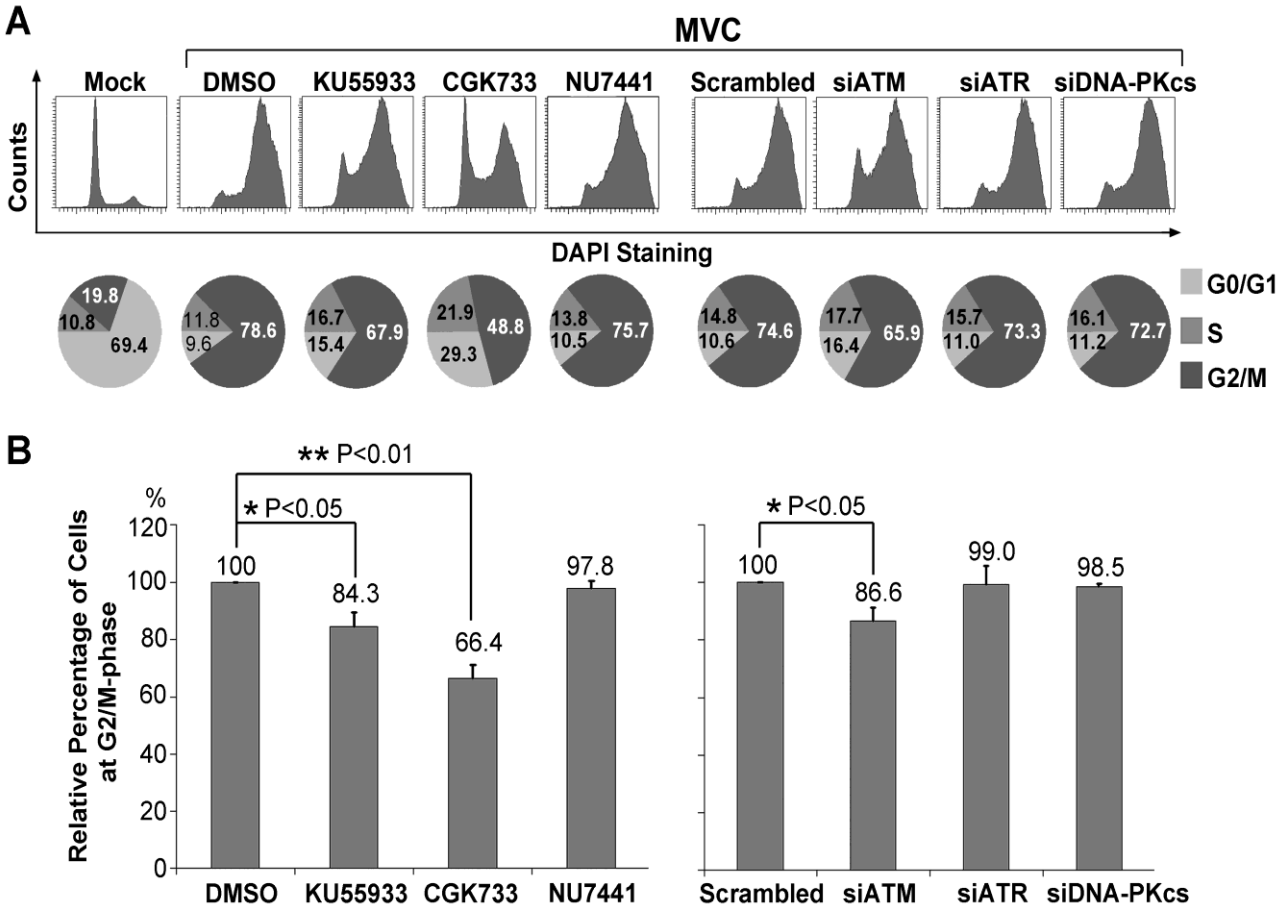
A
MVC
Mock
DMSO
KU55933
CGK733
NU7441
Scrambled
siATM
siATR
siDNA-PKcs
Counts
DAPI Staining
19.8
10.8
69.4
11.8
9.6
78.6
16.7
15.4
67.9
21.9
29.3
48.8
13.8
10.5
75.7
14.8
10.6
74.6
17.7
16.4
65.9
15.7
11.0
73.3
16.1
11.2
72.7
G0/G1
S
G2/M
B
** P<0.01
* P<0.05
%
Relative Percentage of Cells at G2/M-phase
120
100
80
60
40
20
0
100
84.3
66.4
97.8
DMSO
KU55933
CGK733
NU7441
* P<0.05
100
86.6
99.0
98.5
Scrambled
siATM
siATR
siDNA-PKcs

Figure 6. Both inhibiting ATM phosphorylation and knocking down ATM attenuate MVC infection-induced G2/M arrest.

(A) WRD cells were treated with inhibitors for 3 hrs prior to MVC infection or transfected with siRNAs 48 hrs prior to MVC infection. At 48 hrs p.i., the cells were subjected to flow cytometry for an assessment of G2/M arrest using DAPI and anti-NS1 co-staining. The percentage of cells in each phase of the cell cycle was quantified and is shown at the bottom. Significant changes in the numbers of cells in the G2/M-phase are shown. Mock-infected cells were analyzed as a normal cell cycle control. **(B).** Statistical analysis of the percentage of cells in the G2/M-phase in NS1-expressing cells from three independent experiments. Average (numbers) and stand deviation ("T"-shaped bars) are shown for each treatment group.

The ATM-mediated DDR is required for replication of the MVC genome.

To test whether MVC replication was impaired by deactivation of any of the three DDR pathways, we evaluated the percentage of MVC infected cells by intracellular staining using anti-NS1 antiserum. A typical experiment was shown in Fig. 7A, where at 48 hrs p.i., approximately 70% of WRD cells were infected with MVC (Fig. 7A, DMSO and Scrambled). In cells treated with KU55933 or CGK733, NS1-expressing cells were decreased to 41.6% and 11.6%, respectively, of the numbers seen in the control, indicating that ATM inactivation reduced MVC infection. Furthermore, knocking down ATM using an ATM-specific siRNA led to a 72% decrease in NS1-expressing cells compared to the number in the scrambled siRNA control group (Fig. 7A). However, treatment with either an ATR- or a DNA-PKcs-specific siRNAs failed to reduce the number of NS1-expressing cells significantly (Fig. 7A). These results indicate that ATM activation may facilitate MVC replication.

To confirm the role of ATM activation in MVC DNA replication, we treated WRD cells with our panel of kinase inhibitors and siRNAs and then analyzed MVC DNA replication by Southern blotting analysis. As shown in Fig. 7B, treatment of cells with either KU55933 or CGK733 reduced the level of the replicative form (RF DNA) of the MVC DNA by approximately 5-fold (Fig. 7B, lanes 2&3 *vs.* 5), whereas treatment with the DNA-PK inhibitor NU7441 did not (Fig. 7B, lane 4). Notably, both KU55933 and CGK733 inhibitors significantly blocked synthesis of the MVC ssDNA, by approximately 10-fold (Fig. 7B, lanes 2&3 *vs.* 5); this effect of ATM inhibition was more pronounced when the ATM-specific siRNA was applied (Fig. 7B, lane 8 *vs.* 7). In contrast, ATR- and DNA-PKcs-specific siRNAs failed to inhibit synthesis of both the RF DNA and ssDNA of MVC (Fig. 7B, lanes 9&10). The inhibition of ssDNA synthesis was confirmed by measuring progeny virus production from MVC-infected cells subjected to each treatment. As expected, the virus titers in the ATM-inhibited groups (KU55933-, CGK733- and siATM-treated) were reduced

more than 12-fold compared with those in their respective control groups (Fig. 7D, DMSO and Scrambled). Consistent with results from Southern blotting analysis, CGK733 treatment reduced progeny virus production by 32-fold; however, the inhibition of ATR alone using an ATR-specific siRNA did not significantly decrease the production of progeny virus (Fig. 7D, siATR). Likewise, treatments of cells with a DNA-PK-specific inhibitor or siRNA, however, did not affect the production of progeny virus compared to that seen in the respective controls (Fig. 7D, NU7441&siDNA-PKcs).

Taken together, these results show that the ATM-mediated DDR is essential to MVC DNA replication, and that this particular DDR is the most important with respect to synthesis of the MVC ssDNA genome during infection. This is the first time to demonstrate that an autonomous parvovirus is able to hijack the cellular DNA damage response machinery for its productive replication.

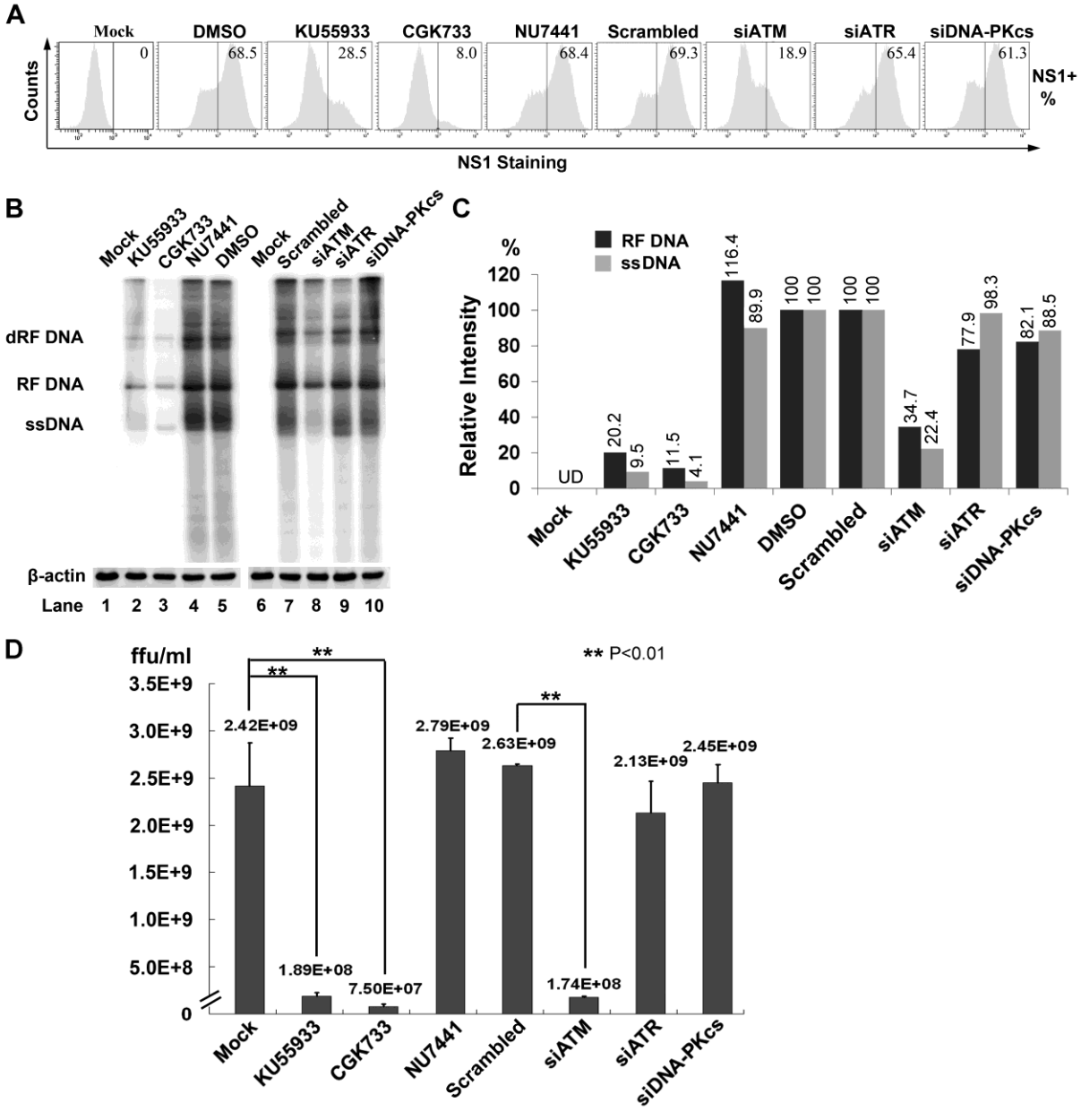
A
Mock
DMSO
KU55933
CGK733
NU7441
Scrambled
siATM
siATR
siDNA-PKcs
0
68.5
28.5
8.0
68.4
69.3
18.9
65.4
61.3
Counts
NS1+ %
NS1 Staining
B
Mock
KU55933
CGK733
NU7441
DMSO
Mock
Scrambled
siATM
siATR
siDNA-PKcs
dRF DNA
RF DNA
ssDNA
β-actin
Lane 1 2 3 4 5 6 7 8 9 10
C
%
RF DNA
ssDNA
Relative Intensity
120
100
80
60
40
20
0
UD
20.2
9.5
11.5
4.1
116.4
89.9
100
100
100
100
34.7
22.4
77.9
98.3
82.1
88.5
Mock
KU55933
CGK733
NU7441
DMSO
Scrambled
siATM
siATR
siDNA-PKcs
D
ffu/ml
** P<0.01
3.5E+9
3.0E+9
2.5E+9
2.0E+9
1.5E+9
1.0E+9
5.0E+8
0
**
**
2.42E+09
1.89E+08
7.50E+07
2.79E+09
2.63E+09
**
1.74E+08
2.13E+09
2.45E+09
Mock
KU55933
CGK733
NU7441
Scrambled
siATM
siATR
siDNA-PKcs

Figure 7. The ATM pathway is required for MVC DNA replication and progeny virus production.

WRD cells were treated with inhibitors as indicated 3 hrs prior to MVC infection or transfected with the indicated siRNAs 48 hrs prior to MVC infection. Mock-infected cells were analyzed as a negative control. **(A)** At 48 hrs p.i., the cells were assessed for MVC NS1 expression by flow cytometry. The percentage of NS1-expressing cells is shown in each histogram. **(B)** At 48 hrs p.i., one half of the cells were collected for extracting Hirt DNA, and the other half were collected and immunoblotted with anti-β-actin. Hirt DNA was normalized based on the level of β-actin in each sample, and subjected to analysis by Southern blotting. **(C)** Relative levels of the replicative form (RF DNA) and single-stranded (ssDNA) MVC DNA in each group were quantified using Image Quant TL software (GE Health). UD: undetectable. **(D)** At 48 hrs p.i., progeny virus was isolated and quantified as ffu/ml as described in Materials and Methods. The averages (numbers) and standard deviations ("T"-shaped bars) are shown.

The MRN complex facilitates MVC DNA replication.

To examine whether the MRN complex is involved in MVC DNA replication, we first evaluated whether this complex forms in early infection. At 24 hrs p.i., Mre11 in infected cells colocalized with the replication foci (punctuate patterns) as well as with Rad50 and phosphorylated Nbs1 (p-Nbs1) (Fig. 8A, 24 hrs); in uninfected cells, the Mre11, Rad50 and p-Nbs1 were broadly distributed throughout the nuclei without forming bright foci (data not shown). As MVC infection proceeded, Mre11 was degraded, as evident from a decrease in Mre11 in the MVC replication foci at 48 hrs p.i. (Fig. 8A, 48 hrs). Importantly, Rad50 and p-NBS1 remained at the same level in these locations as at 48 hrs p.i. (Fig. 8A, 48 hrs p.i.). Immunoblotting revealed a clear transition of Mre11 expression between 24 hrs and 36 hrs p.i. (Fig. 8B, Mre11); this period corresponds to the time point that is critical for replication of the MVC DNA (Fig. 8B, NS1). Notably, starting at 18 hrs p.i., we observed a smaller band of approximately 70 kDa (Fig. 8B, Mre11a). This small Mre11 band reached a maximal level at 24 hrs p.i., and decreased in late infection; this correlates with the timing of MVC DNA replication, as indicated by anti-NS1 staining (Fig. 8B, NS1). It was not expressed in HU-treated cells (Fig. 8B), and was confirmed not to be a viral protein (data not shown). We speculate that it is an active form of Mre11, which may play the important role of sensing DSBs and recruiting p-Nbs1 and Rad50 to the MVC replication foci. We used another anti-Mre11 antibody to confirm that Mre11 is degraded. Indeed, a slight reduction of the Mre11 band was observed, and only in infected cells, at 24 hrs and 36 hrs p.i. (Fig. 8B, Mre11b). In contrast, the level of Rad50 remained constant throughout MVC infection (Fig. 8B, Rad50).

To further explore the role of Mre11 in MVC DNA replication, we knocked down Mre11 and then measured MVC DNA replication. Unlike the loss of MRN complex function which occurs during AAV2 replication when it is co-infected with adenovirus [57], Mre11 knockdown led to a

significant decrease, approximately 3-fold, in MVC DNA replication (Fig. 8C&D). We speculated that this was caused by the failure to activate ATM, since the MRN complex acts an upstream regulator of the ATM pathway [36,160,161]. Indeed, we found that silencing of Mre11 reduced ATM phosphorylation significantly, to a level similar to that produced by ATM knockdown (Fig. 8E). Moreover, phosphorylation of the ATM substrate SMC1 [162–164] was reduced in this context (Fig. 8E). In addition, we found that in contrast to the results we obtained by silencing Mre11, knocking down ATM only reduced Nbs1 phosphorylation slightly, indicating that a low level of activated ATM is sufficient to phosphorylate Nbs1. As Nbs1 is essential for DSB repair and genome stability [165], the persistent presence of p-Nbs1 in the MVC replication foci (Fig. 8A) suggests that this activated form may play a role in replication of the MVC genome.

The results here show that the MRN complex localizes to the MVC replication foci, indicating that MVC genomes are sensed as DNA damage, likely as DSBs, by the MRN complex at the replication foci. On the other hand, colocalization of p-Nbs1 and Rad50 in the MRN complex within the MVC DNA replication foci may facilitate replication of the MVC genome.

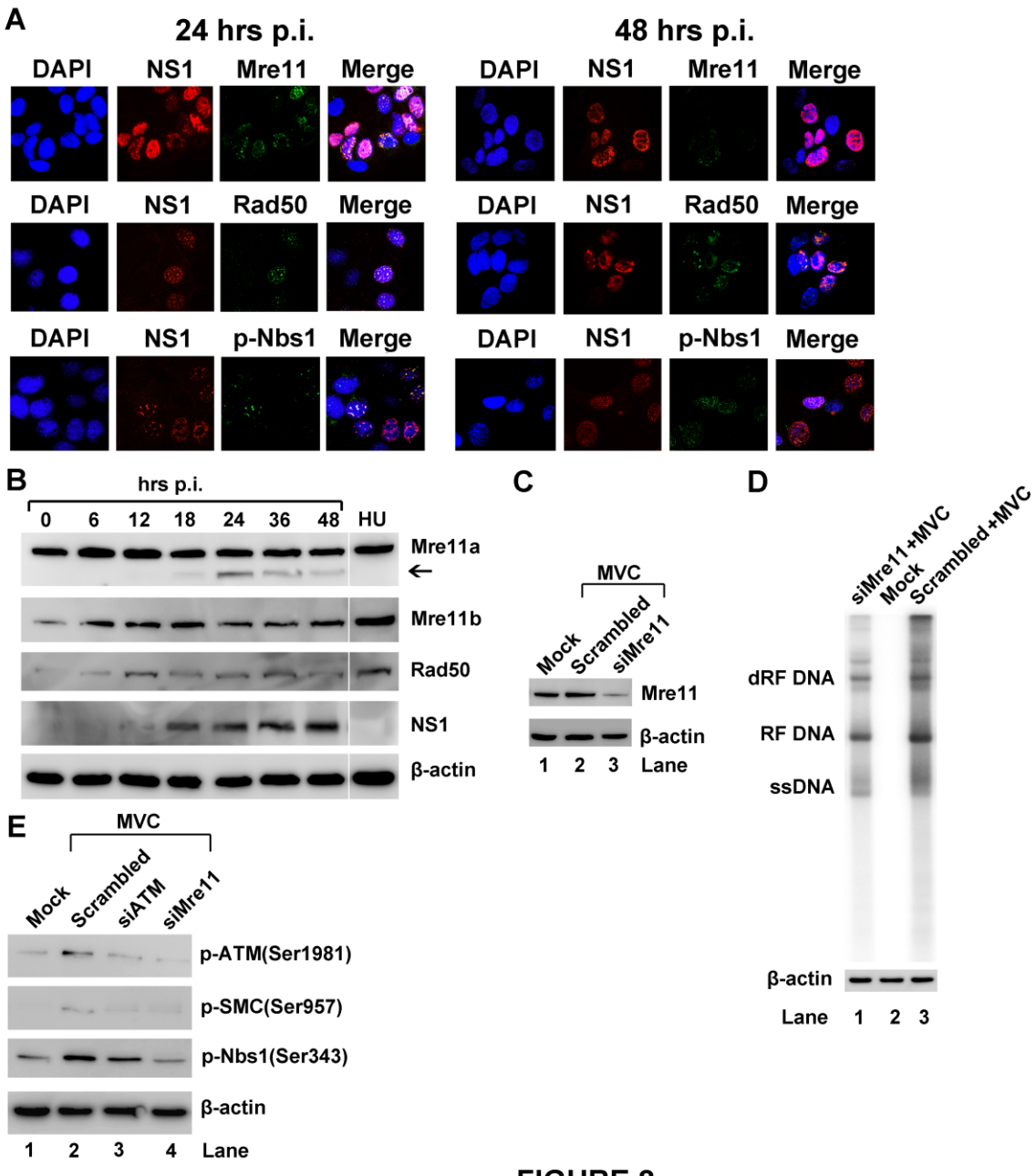
A
24 hrs p.i.
48 hrs p.i.
DAPI
NS1
Mre11
Merge
Rad50
p-Nbs1
B
hrs p.i.
0 6 12 18 24 36 48 HU
Mre11a
Mre11b
Rad50
NS1
β-actin
C
MVC
Mock
Scrambled
siMre11
Mre11
β-actin
1 2 3 Lane
D
siMre11+MVC
Mock
Scrambled+MVC
dRF DNA
RF DNA
ssDNA
β-actin
Lane 1 2 3
E
MVC
Mock
Scrambled
siATM
siMre11
p-ATM(Ser1981)
p-SMC(Ser957)
p-Nbs1(Ser343)
β-actin
1 2 3 4 Lane

FIGURE 8

Figure 8. The MRN complex is an upstream regulator of the ATM pathway and facilitates replication of the MVC genome.

(A) Immunofluorescence analysis of colocalization of the MRN complex in MVC replication center. At 24 or 48 hrs p.i. as indicated, Mre11, phosphorylated Nbs1 at serine 343 (p-Nbs1), and Rad50 were examined for co-localizing with MVC NS1 using their respective antibodies. A monoclonal anti-Mre11 antibody (clone 12D7) was used to detect Mre11. **(B)** Western blot analysis of MVC-infected cells. MVC-infected cells were collected at various times p.i. as indicated, and were analyzed by immunoblotting for the level of Mre11. Mre11 was examined using anti-Mre11 monoclonal antibody (Mre11a, upper panel) *vs.* a polyclonal antibody (Mre11b, middle panel). The blot was reprobed using anti-Rad50 (Rad50), and anti-NS1 (NS1), and anti-β-actin (β-actin) antibodies, sequentially. **(C&D)** WRD cells were transfected with the Mre11-speciifc siRNA (siMre11) and a scrambled siRNA as a control 48 hrs prior to MVC infection. Mock-infected cells were used as a negative control. At 48 hrs p.i., cells were collected and immunoblotted with anti-Mre11 and reprobed using anti-β-actin **(C)**; Hirt DNA was prepared from infected cells, normalized based on the level of β-actin in each sample, and analyzed by Southern blotting. **(E)** WRD cells were transfected with siRNAs as indicated 48 hrs prior to MVC infection. At 48 hrs p.i., the cells were collected and immunoblotted with anti-Mre11(C-16, Santa Cruz) and reprobed sequentially with anti-p-ATM(Ser1918), anti-p-SMC1(Ser957), anti-p-Nbs1(Ser343), and β-actin. Mock-infected cells were used as a background control.

Replication of the MVC genome induces the DDR.

We next sought to explore which viral components are involved in MVC infection-induced DDR. We transfected the MVC infectious clone, pIMVC, as well as its derivatives pIMVCNS1(-), pIMVCNP1(-), pIMVCVP1/2(-), and the NSCap-expressing construct pMVCNSCap, in which both terminal repeats were deleted, into WRD cells, separately (Fig. 9C). At 48 hrs p.i., we analyzed transfected cells for anti-γH2AX staining, and co-stained all samples except pIMVCNS1(-)-transfected cells with anti-NS1; pIMVCNS1(-)-transfected cells were co-stained with anti-NP1. Transfection of pIMVC induced phosphorylation of H2AX in ~80% of NS1-expressing cells at 48 hrs p.i. (Fig. 9A). H2AX was not phosphorylated in NP1-expressing cells and in NS1-expressing cells transfected with the replication-defective constructs pIMVCNS1(-) and pMVCNSCap, respectively [118,121] (Fig. 9A). Transfection of the NP1 knock-out construct, pIMVCNP1(-), which replicates poorly [118], also failed to induce significant phosphorylation of H2AX, whereas transfection of the pIMVCVP1/2(-) induced phosphorylation of H2AX in ~40% of NS1-expressing cells (Fig. 9A). Consistent with this result, transfection of the replicative constructs pIMVC and pIMVCVP1/2(-) phosphorylated p53 in ~10% and 5% in NS1-expressing cells, respectively, but transfection of the non-replicative MVC constructs did not (Fig. 9B), suggesting that activation of the death signaling cascade requires a high level of DDR. In the context of knockout of both VP1 and VP2, in pIMVCVP1/2(-)-transfected cells, the MVC genome was replicated at a level approximately 2 times less than that measured in pIMVC-transfected cells (Fig. 9C).

These results indicate that expression of the MVC protein(s) [NS1 in pIMVCNP1(-)-transfected cells, NP1 in pIMVCNS1(-)-transfected cells, or NS1, NP1 and VP1/2 in pMVCNSCap-transfected cells] is not sufficient to induce H2AX or p53 phosphorylation. Instead, H2AX and p53 phosphorylation is tightly associated with replication status of the MVC

genome. These results suggest that at least replication of the MVC genome is required to induce a DDR (Fig. 9D).

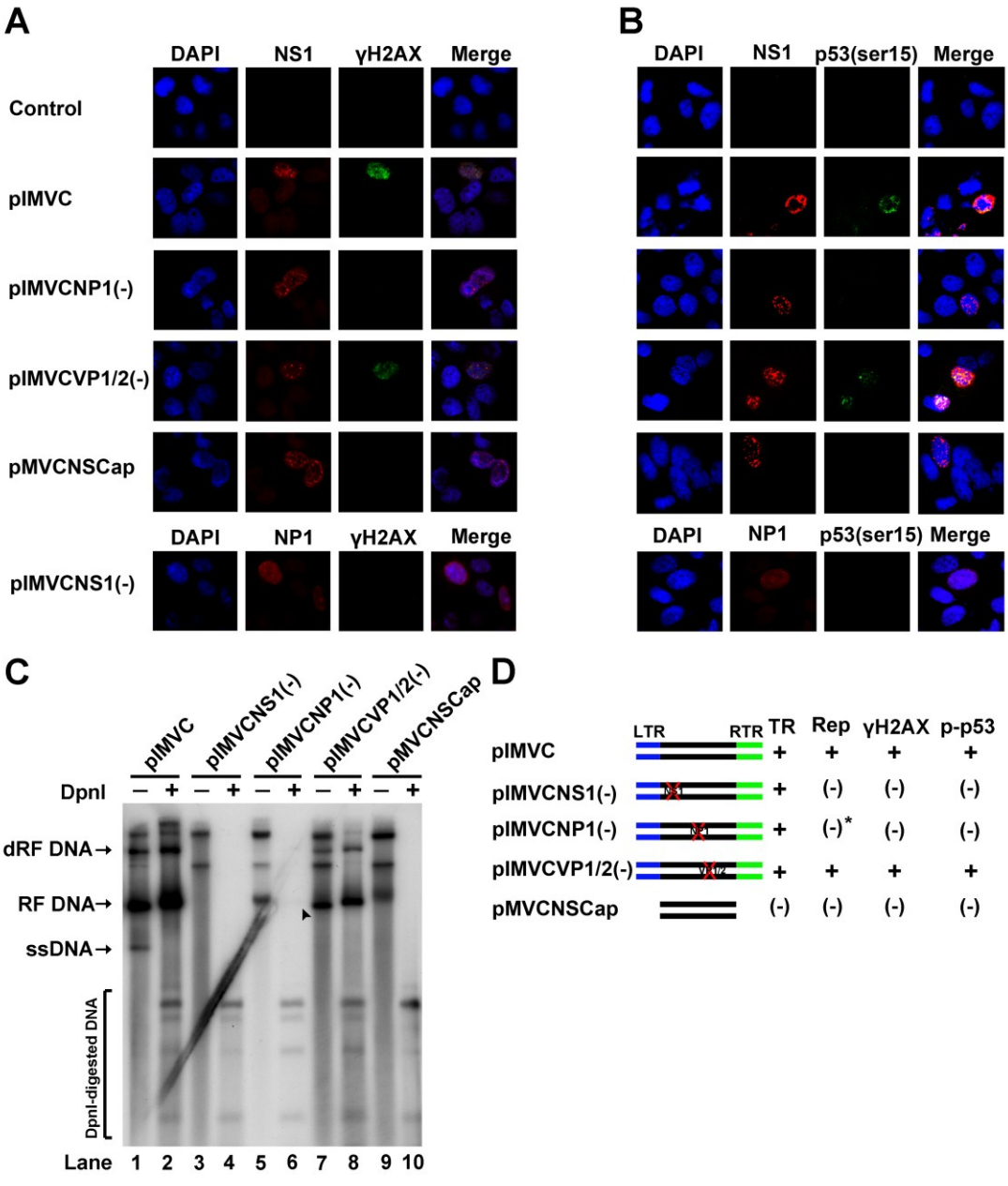
A
DAPI
NS1
γH2AX
Merge
Control
pIMVC
pIMVCNP1(-)
pIMVCVP1/2(-)
pMVCNSCap
DAPI
NP1
γH2AX
Merge
pIMVCNS1(-)
B
DAPI
NS1
p53(ser15)
Merge
DAPI
NP1
p53(ser15)
Merge
C
pIMVC
pIMVCNS1(-)
pIMVCNP1(-)
pIMVCVP1/2(-)
pMVCNSCap
DpnI
– + – + – + – + – +
dRF DNA→
RF DNA→
ssDNA→
DpnI-digested DNA
Lane 1 2 3 4 5 6 7 8 9 10
D
LTR
RTR
TR
Rep
γH2AX
p-p53
pIMVC + + + +
pIMVCNS1(-) + (-) (-) (-)
pIMVCNP1(-) + (-)* (-) (-)
pIMVCVP1/2(-) + + + +
pMVCNSCap (-) (-) (-) (-)

Figure 9. Replication of the MVC genome is required to trigger a DNA damage response.

WRD cells were transfected with pIMVC, its mutants pIMVCNP1(-),pIMVCNS1(-) and pIMVCVP1/2(-), and an MVC NSCap-expressing construct, indicated on left. Untransfected cells were set up as the control. **(A&B)** At 48 hrs p.i., cells were fixed and co-immunostained with anti-γH2AX, anti-NS1/NP1, and DAPI **(A)**, or anti-p-p53(ser15), anti-NS1/NP1, and DAPI **(B)**. **(C)** Hirt DNA was isolated from transfected cells, digested with DpnI and analyzed by Southern blotting. Arrowhead indicates a faint DpnI-resistant band [121]. **(D)** Transfected plasmids are illustrated, and results concluded from panels A-C are shown. Asterisk denotes a very low level of replication. LTR, left hand terminal repeat; RTR, right hand terminal repeat.

Discussion

In this study, we have demonstrated that MVC infection leads to phosphorylation of H2AX and RPA32, hallmarks of DDR [150,166–170], and that both the ATM- and ATR-mediated pathways are activated. In some respects, the DDR induced by MVC infection is beneficial to virus infection, i. e., facilitating replication of viral DNA, especially, synthesis of ssDNA, as well as inducing cell death, which is essential for virus egress. On the other hand, MVC infection-induced DDR is detrimental to the host in that it leads to activation of cell-cycle checkpoints and apoptosis of infected cells. Notably, the DDR was not triggered by expression of viral proteins and the delivery of plasmids containing the non-replicative MVC DNA, but rather by replication of the MVC DNA. Thus, we provide convincing evidence that a DDR induced by autonomous parvovirus plays critical roles in the virus life cycle and virus infection-induced cytopathic effects.

MVC infection induced a DDR mediated by both ATM and ATR pathways.

ATR and its downstream effector RPA32 were phosphorylated during MVC infection, and phosphorylated RPA32 colocalized with MVC NS1 in the replication centers (Fig. 1B). Interestingly, RPA32 is an ssDNA binding protein that is essential for replication of both the minute virus of mice (MVM) [171] and AAV2 [172] genomes. Activation of ATR and subsequent phosphorylation of RPA32 have been shown to play a pivotal role in the DDR induced by infection with UV-inactivated AAV2 [76,147]. Moreover, AAV2 DNA replication activates DNA-PK, which then phosphorylates RPA32 at multiple sites [65]. RPA32 phosphorylation also has been shown to increase as infection by EBV progresses [173]. However, in our study, we found that inhibition of RPA32 phosphorylation by silencing ATR did not affect MVC DNA replication. In fact, it has been reported that RPA32 phosphorylation appears to occur outside the

cellular replication sites [174]. CGK733 inhibits both ATM and ATR activation [152–157], and was the most effective inhibitor of DDR-mediated cell death and cell cycle arrest in MVC-infected cells. We believe that these potent inhibitory effects are due to the fact that CGK733 is a more potent inhibitor of ATM than is the ATM-specific inhibitor KU55933 in WRD cells, rather than due to its additional inhibition of ATR phosphorylation.

The DDR that is induced during SV40 infection has been suggested to be activated by the large T antigen *via* Bub1 binding [175]. The large T antigen also interacts with the MRN complex [176–178]. The HPV E7 protein directly binds to ATM, and this induces an ATM-mediated DDR upon HPV infection of differentiated epithelia [179]. In parvoviruses, both AAV2 Rep78 and parvovirus H-1 NS1 have been implicated in the phosphorylation of H2AX [10,23], which was hypothesized to occur as a response by either non-specific nicking of the cellular DNA by Rep78 [10], or NS1-induced reactive oxygen species (ROS) as a DNA damage agent [23]. However, Rep78 only accounts for a small portion of the DDR that is induced during AAV2 replication [65]. Notably, our results suggest that neither NS1 nor a stalled replication fork (Fig. 9), which would be potentially assembled in the region of the MVC replication origin to activate ATR [76,147], is responsible for DDR induced during MVC infection. The low level of DNA replication achieved by transfection of the NP1-deficient infectious clone [pIMVCNP1(-)] in WRD cells failed to induce a clear DDR. Given that a moderate level of genome replication is absolutely required for MVC-induced DDR, we hypothesize that specific nicking of the replicative form (RF) of the MVC genome by the helicase activity of NS1 may create lesions that mimics DSBs (Fig. 10, c), and that DDR is triggered when this signal accumulates to a certain level. In fact, ATM is a prime candidate for mediating the cellular damage response to DSBs [161], as DSBs are sensed by the MRN complex that triggers ATM-mediated H2AX phosphorylation [161,180]. How ATM is activated during virus infection is not clearly understood. Based on studies of HSV-1, it was proposed that DSBs may arise as a consequence of replication fork

collapse at sites of oxidative damage [181,182], possibly due to cleavage of the viral α sequences by endonuclease G during genome isomerization [183,184]. Parvovirus NS1 nicks only the positive strand of the RF DNA at the terminal resolution site [185], and it has been shown that opening of the DNA helix is required for MRN stimulation of functional ATM [36,161]. Self-complementary recombinant AAV2 (scAAV), of which the genome is a RF DNA, contains palindromic hairpin-structured terminal repeats, which resemble a repair intermediate of DSBs. Thus, NS1-nicked RF DNA and unpaired (replication) intermediates (Fig. 10, d&e) might be perfectly opened DNA helices that function as DSBs and trigger ATM activation.

In addition, delivery of the AAV2 genome by UV-inactivated AAV2 has been proven to induce ATM/ATR-mediated DDR [75,76,147], which differs from the DNA-PK-mediated DDR induced by AAV2 DNA replication [64,65]. In our study, we observed that the extent of DDR induced by MVC DNA replication somehow correlated with the replication efficiency and the accumulation of the ssDNA genome during infection. Interestingly, H2AX was significantly phosphorylated when cells were inoculated with UV-inactivated MVC at a high MOI of 40, but not at a low MOI of 5 (data not shown). Thus, we speculate that the accumulated ssDNA genome of MVC may also contribute to DDR induced during infection (Fig. 10, g), which warrants further investigation.

Based on the information summarized above, we hypothesize that during the virus life cycle, replication of the MVC genome leads to an accumulation of strand breaks, and that these are registered as DSBs and thus trigger ATM activation. RPA-coated ssDNA breaks, on the other hand, could potentially trigger ATR activation (Fig. 10, a&f) during replication [42]. Notably, MVM infection also induced an ATM-activated DDR that helps MVM DNA replication in MVM-permissive cells (David Pintel, personal communication). Both MVC and MVM are autonomous parvovirus, meaning that replication of their genomes does not require the function from a helper virus. Thus, both the MVC and MVM infection systems provide simple models in

which to study the DDR induced by the ssDNA genome of parvovirus. It is now clear that, like other DNA viruses [49,186], the autonomous parvovirus hijacks the cellular DDR machinery to facilitate replication of its genome.

Only ATM activation-mediated DDR facilitates MVC DNA replication and elicits cell death in MVC-infected cells.

Although MVC infection induces activation of both ATM and ATR, we found that only the ATM-mediated DDR contributes to MVC DNA replication and cell death. In response to DNA damage, cells activate a complex network of factors [144,145] that silence CDKs and thereby arrest the cell cycle, promoting DNA repair [187]. Interestingly, MVC-infection impaired cell proliferation and disturbed the cell cycle, allowing a transition from the S-phase accumulation to the G2/M arrest as the infection progresses [121]. Thus, MVC infection-induced DDR supports replication of the viral DNA by first arresting cell-cycle progression at the S-phase, and then impairing the cell cycle at the G2/M-phase to prevent mitosis, which would lead to apoptotic cell death. On the other hand, if the cell sustains DNA damage that cannot be repaired, the DDR triggers a cascade of apoptotic cell death, through either a p53-dependent or p53-independent pathway [122]. We found that p53 was phosphorylated upon MVC infection and that is dephosphorylated in the context of ATM inactivation (Fig. 5). Furthermore, replication of transfected MVC RF DNA induced phosphorylation of p53 albeit in a low level (Fig. 9), which presumably is due the low level of DNA replication by transfection compared with that during MVC infection. These findings suggest that phosphorylated ATM activates apoptosis in a p53-dependent manner (Fig. 10). Bax translocalization and caspase activation have been shown to occur during cell death triggered by MVC infection [121]. We hypothesize that phosphorylated p53 may activate the BH3-only molecules, e.g., tBID, BIM and PUMA, which further activate Bax/Bak [188].

We have demonstrated that ATM-mediated DDR is involved in cell cycle arrest to some extent, which is p53-independnet. We believe that CHK2 (checkpoint kinase 2) likely signals to activate this ATM-mediated G2/M arrest [145]. Notably, we did not observe a clear DDR in cells transfected with non-replicative and poorly replicating MVC constructs (Fig. 9). The cell cycle of these transfected cells, however, was arrested at G2/M-phase [121]. We think that the DDR induced replication of the MVC genome may not fully account for the cell cycle arrest during MVC infection, and that an unknown mechanism may contribute to the cell cycle arrest induced by the viral genome, specifically the terminal repeats [121]. Actually, both inhibition of ATM activation and knockdown of ATM only moderately rescued the cell cycle arrest. It could also be that a low level of DDR induced by the MVC genome, which is able to induce cell cycle arrest but not cell death [121], is not sufficient to induce a significant increase of γH2AX. Therefore, in the context of the DDR induced during MVC infection, it may be easier to prevent cell death than to prevent arrest of the cell cycle.

The MRN complex localizes to the MVC replication center.

MRN complex is involved in the initial processing of DSBs as a sensor, and is required for ATM activation by DNA damage [36,160,161,189]. It is also critical to the repair of DNA damage [190,191]. The MRN complex is required to signal DDR induction during HSV-1 infection [192], mutant adenovirus infection [193] and HPV infection [179]. In contrast, the MRN complex has to be destroyed during adenovirus [62], AAV2 [57], and SV40 [194] infections. During MVC infection, the MRN complex was assembled at early stages of infection, but Mre11 was slightly degraded at later stages, while the virus was actively replicating. A loss of Mre11 at later times following HSV-1 infection has also been reported [195]. However, the MRN complex was co-localized to the MVC replication center during the course of MVC infection. Further evidence that Mre11 knockdown reduced MVC replication by approximately 3-fold (Fig. 8) strongly

supports that the notion that the MRN complex is required for replication of the MVC genome (Fig. 10), and that its role may be to recruit DNA repair factors to the replication center [175], as the p-Nbs1 is essential to DSB repair [165]. On the other hand, the MRN complex senses ATM activation, which in turn may mediate proteasome-dependent degradation of the MRN subunit [194] at later stages of infection.

HSV-1, SV40 and HPV have all been shown to induce ATM-mediated DDR whereby a number of repair factors are recruited to the replication center [179,194,196,197]. Exactly, how the DDR microenvironment helps viral DNA replication is largely unknown. DSBs can be repaired by either of two distinct repair pathways: non-homologous end joining (NHEJ) or homologous recombination (HR) [198]. Components of these repair machineries have been shown to support viral DNA replication [49]. For example, DDR-induced Rad51 facilitates replication of the EBV and SV40 genomes [173,199]. Studying MVC replication-induced DDR and how this response feeds back to help MVC DNA replication will likely help us to understand the mechanism underlying virus infection-induced DDR.

In conclusion, MVC infection-caused cytopathic effects are unique, and are mediated by DDR induced by replication of the viral genome. We believe that the DDR is induced during parvovirus infection, and that the ensured cell death and cell cycle arrest maybe common, and potentially synergistic mechanisms underlying parvovirus infection-induced cytopathic effects. Understanding the mechanism underlying MVC-induced DDR, and the DDR-induced cell death and cell cycle arrest pathways will potentially elucidate the molecular pathogenesis of *Bocavirus* infection, as well as unravel the mechanism underlying the regulatory DDR pathways.

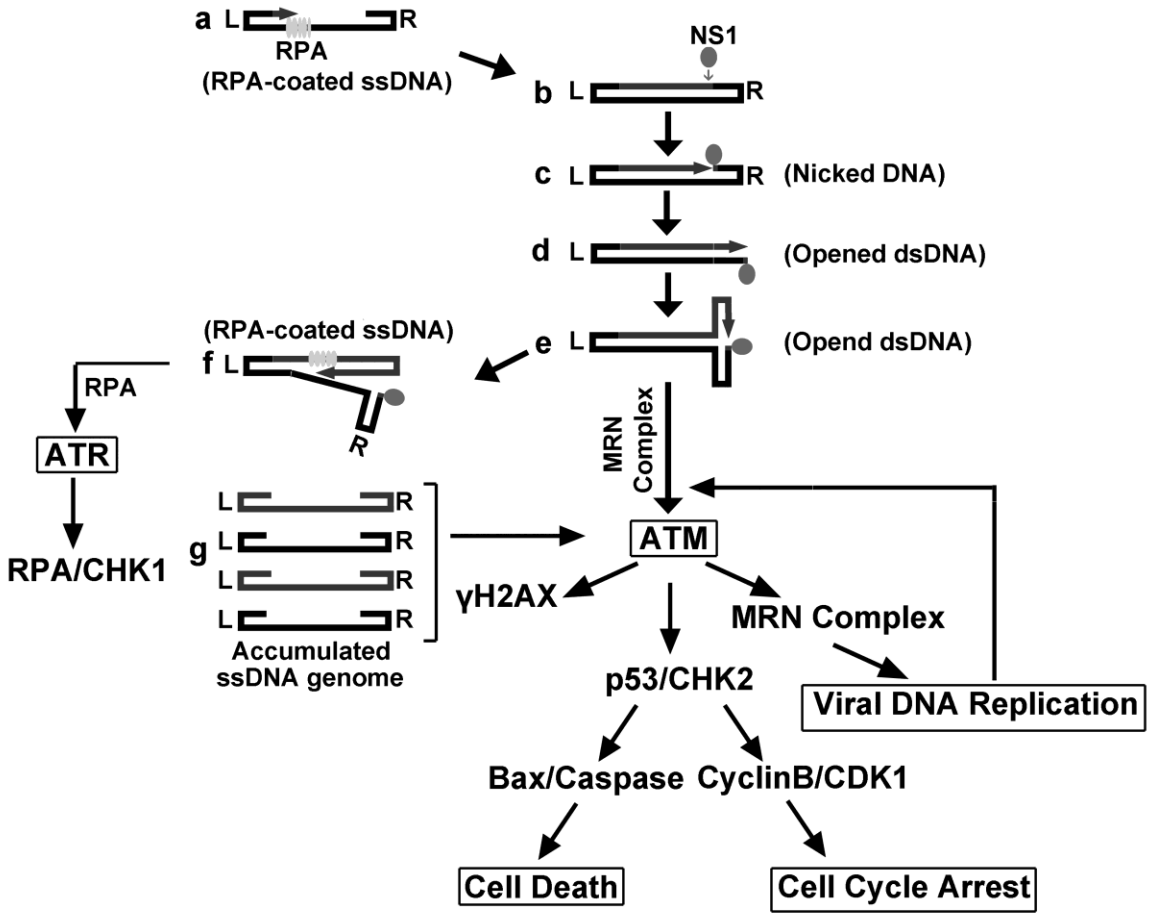
a
L
R
RPA
(RPA-coated ssDNA)
NS1
b
c
(Nicked DNA)
d
(Opened dsDNA)
e
(Opend dsDNA)
(RPA-coated ssDNA)
f
RPA
ATR
RPA/CHK1
MRN Complex
g
Accumulated ssDNA genome
ATM
γH2AX
MRN Complex
p53/CHK2
Viral DNA Replication
Bax/Caspase
CyclinB/CDK1
Cell Death
Cell Cycle Arrest

Figure 10. Proposed DNA damage response pathways induced during MVC infection.

The proposed pathways are described in detail in Discussion. Model of MVC DNA replication refers to DNA replication of the minute virus of mice [185]. Bax translocalization and caspase activation have been shown previously [121] to induce apoptotic cell death during MVC infection, and upregulation of cyclinB/CDK1 was confirmed to be responsible for the G2/M arrest that is induced during MVC infection [121]. L, left hand terminal repeat; R, right hand terminal repeat.

Chapter 3

Parvovirus B19 infection of primary human erythroid progenitor cells triggers ATR-Chk1 signaling, which promotes B19 replication

Abstract

Human parvovirus B19 (B19V) infection is restricted to erythroid progenitor cells of the human bone marrow. Although the mechanism by which the B19V genome replicates in these cells has not been studied in great detail, accumulating evidence has implicated involvement of the cellular DNA damage machinery in this process. Here, we report that, in *ex vivo* expanded human erythroid progenitor cells, B19V infection induces a broad range of DNA damage responses by triggering phosphorylation of all the upstream kinases of each three repair pathways: ATM (ataxia-telangiectasia-mutated), ATR (ATM and Rad3-related) and DNA-PKcs (DNA-dependent protein kinase catalytic subunit). We found that phosphorylated ATM, ATR and DNA-PKcs, and also their downstream substrates and components (Chk2, Chk1, Ku70/Ku80 complex, respectively) localized within the B19V replication center. Notably, inhibition of kinase phosphorylation (through treatment with either kinase-specific inhibitors or kinase-specific shRNAs) revealed requirements for ATR and DNA-PKcs, but not ATM, signaling, in virus replication. Inhibition of the ATR substrate Chk1 led to similar levels of decrease in virus replication, indicating that signaling *via* the ATR-Chk1 pathway is critical to B19V replication. Notably, the cell cycle arrest characteristic of B19V infection was not rescued by interference with the activity of any of the three repair-pathway kinases.

Introduction

Human parvovirus B19 (B19V), a member of the genus *Erythrovirus* within the family *Parvoviridae* [200], has been associated with a broad spectrum of human diseases. Most commonly, it causes a mild rash in children; this form is known as “fifth disease” [201]. However, in some circumstances, B19V infection leads to more severe symptoms. Examples of these diseases include hydrops fetalis, in pregnant women infected during the second trimester; chronic pure red cell aplasia, in immunocompromised patients; transient aplastic crisis, in sickle cell disease patients [88,201].

B19V contains a single-stranded DNA (ssDNA) genome; it is approximately 5.7-kb in length and features two identical terminal repeats (ITRs) at both ends [202]. Replication of the B19V genome is restricted to nuclei of human erythroid progenitor cells (EPCs) [173,203]. In *ex vivo* expanded EPCs, B19V infection induces apoptosis [21,96] and arrests cell cycle at the G2/M transition [100]. Analyses in *ex vivo* expanded EPCs infected with B19V have revealed that the large nonstructural protein NS1, which is multifunctional and essential to B19V DNA replication [94], causes the cell cycle arrest [100] and also plays a role in triggering infection-associated apoptosis [21,96]. In addition, we have demonstrated that cellular signaling pathways triggered by the binding of erythropoietin (Epo) to its receptor (EpoR) are critical to B19V infection of *ex vivo* expanded EPCs [204]. Beyond the fact that NS1 and EpoR signaling are involved, however, we know little about the mechanisms by which the B19V genome replicates in *ex vivo* expanded EPCs.

Several studies have shown that parvovirus infection induces a DNA damage response (DDR) that plays an important role in the replication of parvovirus DNA [29,30,112]. DDR is mediated by three PI-3-kinase-like kinases (PI3Ks): ATM (ataxia telangiectasia mutated), ATR (ATM and Rad3-related), and DNA-PKcs (DNA-dependent protein kinase catalytic subunit)

[32,35]. ATM is activated primarily by double-stranded DNA breaks (DSBs), and is recruited to DSBs by the Mre11-Rad50-Nbs1 (MRN) complex [38,205,206]; ATR responds to single-stranded DNA breaks (SSBs) and stalled DNA replication forks and is recruited by an ATR-interacting protein (ATRIP) to replication factor A (RPA)-coated ssDNA [207]; DNA-PK is activated in response to DSBs, and is recruited to damage sites in complex with both Ku70 and Ku80 [208]. After any of these kinases is recruited to a site of DNA damage, it phosphorylates a number of substrates (e.g., H2AX, RPA32, Chk1, and Chk2), which in turn target other proteins to silence cyclin-dependent kinases. This leads to the arrest of cell-cycle progression so that the damaged DNA can be repaired, or, in the case of irreparable damage, so that the potentially hazardous cells can be eliminated through apoptosis [32,209].

The kinases that control the DDR can be induced and hijacked by viruses to promote replication of the genomes [81]. For example, ATM signaling can be co-opted for this purpose by minute virus of canines (MVC) and minute virus of mice (MVM) [29,30,112], and DNA-PK is used in the same way by adeno-associated virus 2 (AAV2) during co-infection with adenovirus [64,65]. We reasoned that DDR may likewise contribute to the replication of the B19V genome during B19V infection of EPCs. The viral titer in the plasma of infected patients can be as high as 10^{13} genomic copies per ml [210,211], this overwhelming replication of the B19V genome may well lead to a replication stress and elicit a DDR.

In this report, we describe our investigation of the DDR in *ex vivo* expanded EPCs infected with B19V, in particular with respect to the possibility that DDR plays a role in virus replication. We discovered that B19V infection leads to a broad spectrum of DDR events, including phosphorylation of all three upstream kinases. We also found that these phosphorylated kinases, together with their downstream substrates or components, localize to the B19V replication center of the infected cell. In addition, disruption of either the ATR or

DNA-PKcs signaling pathway significantly reduces the efficiency of B19V DNA replication without disturbing the cell-cycle phenotype of infected EPCs.

Materials and Methods

Cell line and virus:

Ex vivo expanded $CD36^+$ EPCs were prepared as described previously [97,204]. B19V-containing viremic plasma sample P53 was obtained from ViraCor Laboratories (Lee's Summit, MO). The plasma sample was titrated 10-fold and infected $CD36^+$ EPCs. At 24 hrs postinfection (p.i.), the cells were fixed and stained with an anti-B19V NS1 antibody [96]. End point titers, fluorescence focus-forming units (FFU), were determined at the last dilution that gave unequivocal fluorescence. Virus infection was performed at a multiplicity of infection (MOI) of approximately 1 (FFU) per cell as described previously [204].

Chemicals and treatments:

Hydroxyurea (HU, Calbiochem, Darmstadt, Germany) was dissolved in deionized water to make a 250 mM stock solution. The pharmacological inhibitors of CGK733, KU55933, NU7441, SB218078 (Chk1 inhibitor, abbreviated as Chk1i) and NSC109555 (Chk2 inhibitor, abbreviated as Chk2i) were purchased from Tocris Bioscience (St. Louis, MO), and were dissolved in DMSO to make a 10 mM stock solution. Caffeine was purchased from Sigma (St. Louis, MO) and dissolved in deionized water as a stock solution at 100 mM.

Treatment with these pharmacological inhibitors was performed 3 hrs prior to infection with virus. KU55933, CGK733, NU7441 and caffeine were applied to cells at final concentrations of 10 μM, 2.5 μM, 10 μM and 1 mM, respectively. Chk1i and Chk2i were used at final concentrations of 150 nM and 5 μM, respectively. DMSO at 0.25% was used as a non-treatment control. EPCs treated with HU at a final concentration of 0.25 mM were used as positive control for DDR.

Lentiviral vectors and lentivirus transduction:

The oligos used to generate shRNAs were synthesized by Integrated DNA Technologies (IDT, Coralville, Iowa). shRNA oligos were annealed and ligated to the pLKO-GFP vector (Addgene, Inc.), and lentivirus was produced as described previously [204], following the manufacturer's instructions (http://www.addgene.org/plko). The following validated shRNA sequences (Sigma, St Louis, MO) were chosen for targeting the genes of interest: shRNA specific to ATM (shATM):
5'-CCGGTGATGGTCTTAAGGAACATCTCTCGAGAGATGTTCCTTAAGACCATCATTTTTG

-3'; shRNA specific to ATR (shATR): 5'-

CCGGAAAGAGGCTCCTACCAACGACTCGAGTCGTTGGTAGGAGCCTCTTTCTTTTTG

-3'; shRNA specific to DNA-PKcs (shDNA-PKcs):
5'-CCGGCCGGTAAAGATCCTAATTCTACTCGAGTAGAATTAGGATCTTTACCGGTTTTT

-3'; shRNA specific to Ku70 (shKu70):
5'-CCGGAAGAGTCTACCCGACATAAGCTCGAGCTTATGTCGGGTAGACTCTTCTTTTTG-3'.
The following scrambled shRNA (shScrambled) was used as a shRNA control:
5'CCGGCCTAAGGTTAAGTCGCCCTCGCTCGAGCGAGG GCGACTTAACCTTAGGTTTTTG
3'. At 48 hrs post-transduction, $CD36^+$ EPCs were infected with B19V.

Western blotting and immunofluorescence:

Western blotting and immunofluorescence assays were performed as described previously [30]. Confocal images were taken at a magnification of 40 × or 100 × (objective lens), with an Eclipse C1 Plus confocal microscope (Nikon) controlled by Nikon EZ-C1 software.

Antibodies used in this study:

Rat anti-B19V NS1 antibody was produced previously [96]. Other anybodies obtained commercially include: anti-γH2AX (Millipore Billerica, MA); anti-Ku70 and anti-phospho(p)-RPA32(Thr21) (Epitomics, Burlingame, CA); anti-p-ATM (Ser1981) (Rockland Immunochemicals Inc., Gilbertsville, PA); anti-p-DNA-PK(Ser2056) (Genescript, Piscataway, NJ); and anti-ATM, anti-ATR, anti-DNA-PK and anti-Ku80 (Calbiochem); anti-p-Chk1(Ser345) and anti-p-Chk2(Thr68) were purchased from Cell Signaling Inc. (Danvers, MA). In addition, two anti-p-ATR (Ser428) antibodies were obtained from Cell Signaling Inc. for immunofluorescence and Santa Cruz (Santa Cruz, CA) for Western blot analysis. Antibody dilutions used for Western blotting and immunofluorescence analysis were as suggested in the manufacturers' instructions.

Southern blot analysis:

Low-molecular-weight DNA (Hirt DNA) was extracted from $CD36^+$ EPCs as described previously [212]. Southern blotting was performed as described previously using the SalI digested pM20 probe which contains the full-length B19V genome [212].

Fluorescence in situ hybridization (FISH):

A B19V DNA fragment (nt 802-1295, Genbank accession no.: AY386330) was PCR-amplified and subsequently labeled using the Label IT FISH fluorescein Kit (Mirus, Madison, WI). In situ hybridization was performed following the manufacturer's instruction. Briefly, $CD36^+$ EPCs were cytospun onto slides, fixed in 1% paraformaldehyde for 30 min, and permeablized with 1% triton-100 for 10 min. After permeablization, slides were treated with 5 μg/ml RNase A at 37^{o}C for 1 hr and washed with 2×SSC (Sodium Chloride-Sodium Citrate) buffer. Slides were sequentially dehydrated with 70%, 85% and 100% ethanol in order for 2 min at room temperature, and then denatured with 70% formamide for 2 min. Sequentially, slides were dehydrated with 70% ethanol (pre-chilled at -20 ^{o}C), 85% and 100% ethanol at room temperature in order for 2 min each, and hybridized with fluorescein-labeled DNA probe at 37 °C overnight. After FISH, slides were treated with antibodies for immunofluorescence analysis.

Flow cytometry analysis:

We performed flow cytometry analysis as described previously [121]. Briefly, $CD36^+$ EPCs were fixed in 1% paraformaldehyde at room temperature for 30 min and permeablized with PBS containing 0.5% Tween-20. Cells were sequentially incubated with primary and secondary antibodies, and then with DAPI (4',6-diamidino-2-phenylindole) at 1 μg/ml in PBS containing 0.3% Tween-20. All processed samples were analyzed on a three-laser flow cytometer (LSR II; BD Biosciences) at the Flow Cytometry Core at the University of Kansas Medical Center. All flow cytometry data were analyzed using FACS DIVA software (BD Biosciences).

Results

B19V infection induces a DNA damage response (DDR) in B19V-infected EPCs.

To determine whether a DDR is induced during B19V infection of *ex vivo* expanded EPCs, we located the B19V DNA replication center using a FISH-based method with a B19V DNA-specific probe. Since the parvovirus large non-structural protein NS1 is essential to replication of the viral DNA [12,171,213], we co-stained the FISH-processed B19V-infected EPCs with an anti-NS1 antibody [96] to compare their localization. As shown in Fig. 1A, B19V NS1 (red) signal overlapped with that for the B19V DNA (green), indicating that the NS1 protein was expressed within the viral DNA replication center. In all of the subsequent experiments, we used anti-NS1 immunostaining to mark this center.

We next examined the expression levels and localization of phosphorylated H2AX (γH2AX) and Thr21-phosphorylated RPA32 (p-RPA32), a hallmark of DDR [214–216]. Both γH2AX and p-RPA32 were detectable as early as 12 hrs postinfection (p.i.), the time at which B19V NS1 first became visible (Fig. 1B&C). γH2AX either formed a ring at the edge of the nucleus and completely overlapped with NS1 expression, or was distributed evenly across the nucleus and thus had a broader expression domain than NS1 (Fig. 1D). In contrast, p-RPA32 consistently co-localized with NS1 (Fig. 1D). Overall, damaged foci were detected only in NS1-expressing cells. Upregulation of the expression of both γH2AX and p-RPA32 in infected cells *vs*. mock-infected cells was confirmed by Western blotting (Fig. 2B, compare lanes 2 and 1). Thus, our results demonstrate that B19V infection of EPCs induces a DDR.

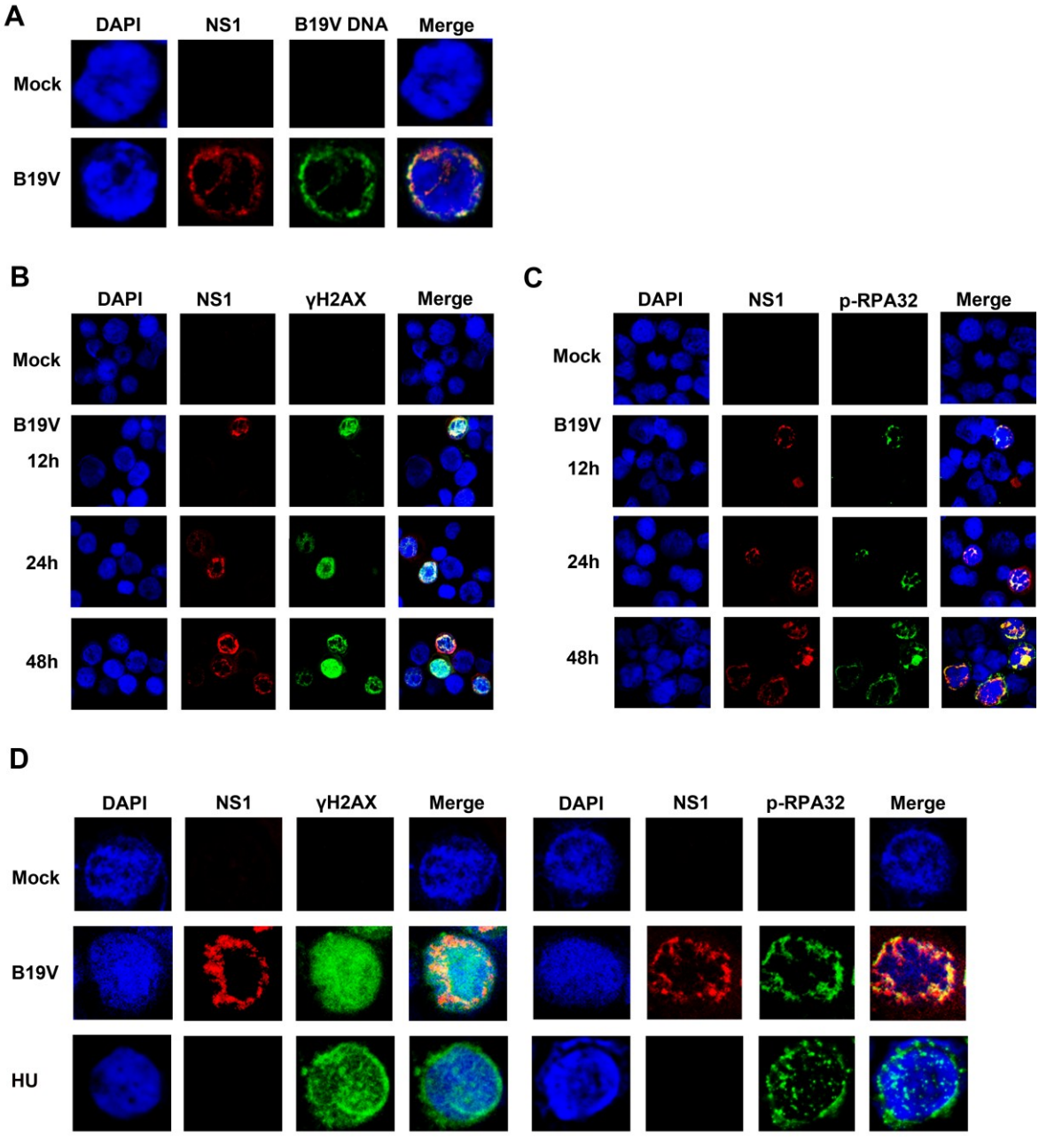
A
DAPI
NS1
B19V DNA
Merge
Mock
B19V
B
DAPI
NS1
γH2AX
Merge
Mock
B19V
12h
24h
48h
C
DAPI
NS1
p-RPA32
Merge
Mock
B19V
12h
24h
48h
D
DAPI
NS1
γH2AX
Merge
DAPI
NS1
p-RPA32
Merge
Mock
B19V
HU

Figure 1. B19V infection induces a DNA damage response in CD36$^+$ EPCs.

(A) Combined immunofluorescence- and FISH-based visualization of the B19V replication center. Mock- and B19V-infected CD36$^+$ EPCs were analyzed 48 hrs p.i. Replicated viral genome (green) were detected by hybridization with a B19V-specific DNA probe labeled with fluorescein. B19V NS1 (red) was immunostained with anti-B19V NS1 antibody. Nuclei were stained using DAPI. Confocal images were taken at a magnification of 100 ×. **(B-D) Immunofluorescence analysis of DDR in B19V-infected cells.** At the indicated times p.i., mock- and B19V-infected CD36$^+$ EPCs were co-immunostained with anti-B19V NS1 (red) and anti-γH2AX (green) (B), or with anti-B19V NS1 (red) and anti-p-RPA32 (green) (C). Confocal images in panels B&C were taken at a magnification of 40 ×. (D) Confocal images of the same 48 hrs p.i. samples as in panels B&C, but at a magnification of 100 ×. HU-treated EPCs were used as positive controls for γH2AX and p-RPA32 staining.

ATM, ATR and DNA-PK are activated in B19V-infected EPCs.

We next assessed which kinase pathway is activated in the B19V infection-associated DDR. Strikingly, we found that all three upstream kinases were phosphorylated, and the phosphorylated forms (green) localized to the B19V replication center (overlap with NS1, red; Fig. 2A). Specifically, we tested for the following markers: ATM phosphorylated on Ser1981, which typically responds to DSBs [38]; ATR phosphorylated on Ser428, which typically associates with SSBs and stalled replication forks [217]; DNA-PKcs phosphorylated on Ser2056, a form of the kinase known to be induced by DSBs [32]. The phosphorylation status of each protein was confirmed by immunoblotting with their respective antibodies (Fig. 2C, lane 3 and Fig. 2D, lane 2).

To determine which of the three upstream kinases is responsible for H2AX and p-RPA32 phosphorylation in B19V-infected EPCs, we blocked their kinase activities using a panel of pharmacological inhibitors that inhibit their phosphorylation. Use of the inhibitors at the specified concentration did not result in any obvious cytotoxicity (data not shown). As shown in Fig. 2B, the levels of γH2AX and p-RPA32 were more than 10-fold higher in whole cell lysates of B19V-infected cells than in lysates of mock-infected counterparts (Fig. 2B, compares lanes 1 and 2). Treatment with ATM-specific inhibitor KU55933 (at 10 μM) failed to cause a significant decrease in levels of γH2AX and p-RPA32 (Fig. 2B, compare lanes 2 and 4). However, treatment with the DNA-PK-specific inhibitor NU7441 (at 10 μM) reduced the levels of both by approximately (~) 60% (Fig. 2B, compare lanes 2 and 5). Notably, addition of the ATM and ATR pan-inhibitor CGK733 at 2.5 μM significantly decreased the levels of γH2AX and p-RPA32 (by more than 80%; Fig. 2B, compare lanes 2 and 3). The effectiveness of each inhibitors in preventing kinase phosphorylation was confirmed by Western blotting (Fig. 2C&D); KU55933 and NU7441 inhibited specifically the phosphorylation ATM and DNA-PK, respectively (Fig. 2C,

compare lanes 3 and 5; Fig. 2D, compare lanes 2 and 3), and CGK733 inhibited the phosphorylation of both ATM and ATR (Fig. 2C, compare lanes 3 and 4). Although an ATR-specific inhibitor is not available, the fact that specifically inhibiting ATM using KU55933 did not affect γH2AX and p-RPA32 expression, whereas inhibiting both ATR and ATM using CGK733 resulted in significantly reduced expression, suggests that ATR signaling is the major determinant of B19V infection-induced DDR, and that ATM does not play a major role in spite of its activation within the B19V DNA replication center. Moreover, our analysis suggests that the DNA-PK pathway also contributes to triggering of the DDR.

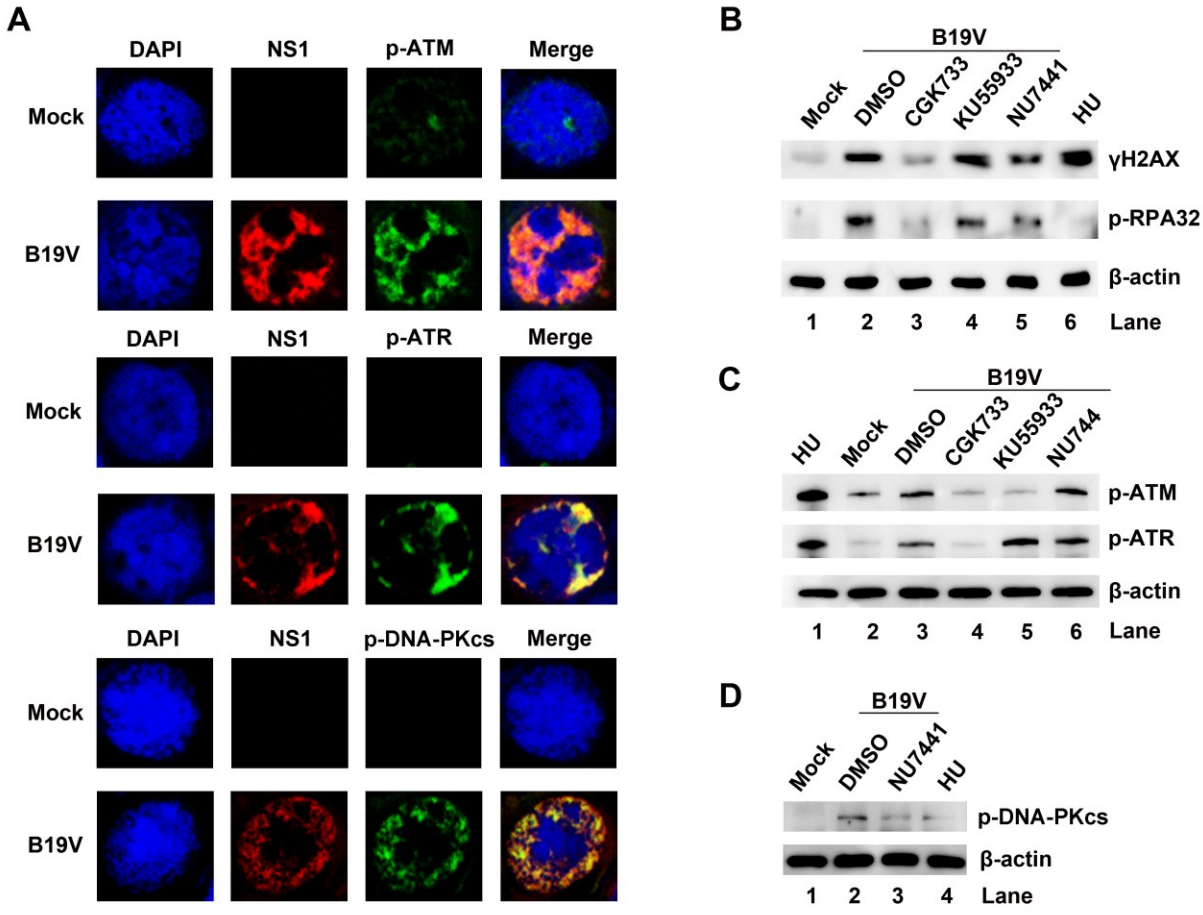
A
DAPI
NS1
p-ATM
Merge
Mock
B19V
DAPI
NS1
p-ATR
Merge
Mock
B19V
DAPI
NS1
p-DNA-PKcs
Merge
Mock
B19V
B
B19V
Mock
DMSO
CGK733
KU55933
NU7441
HU
γH2AX
p-RPA32
β-actin
1 2 3 4 5 6 Lane
C
B19V
HU
Mock
DMSO
CGK733
KU55933
NU744
p-ATM
p-ATR
β-actin
1 2 3 4 5 6 Lane
D
B19V
Mock
DMSO
NU7441
HU
p-DNA-PKcs
β-actin
1 2 3 4 Lane

Figure 2. All three upstream kinases of the DNA repair pathways are activated in response to B19V infection of CD36$^+$ EPCs.

(A) Immunofluorescence analysis. At 48 hrs p.i., mock- and B19V-infected CD36$^+$ EPCs were co-immunostained with anti-B19V NS1 (red) and anti-p-ATM (geen), anti-p-ATR (green) or anti-p-DNA-PKcs (green). Confocal images were taken at a magnification of 100 ×. **(B-D) Western blot analysis.** CD36$^+$ EPCs were treated with DMSO and the indicated inhibitors for 3 hrs prior to infection with B19V. Cells were harvested at 48 hrs p.i., lysed, and immunoblotted with anti-γH2AX and anti-p-RPA32 **(B)**, anti-p-ATM and anti-p-ATR **(C)** or anti-p-DNA-PKcs **(D).** In all blots, anti-β-actin was used as a loading control. HU-treated cells were used as a positive control for the DDR.

The ATR and DNA-PK signaling pathways are required for efficient B19V DNA replication in EPCs.

We and others have reported that DDR induced during infection by autonomous parvoviruses facilitates replication of the viral genome [29,30,112]. To determine whether this is true for B19V, we used flow cytometry to examine the effects of the DDR kinase inhibitors on the percentage of B19V-infected (NS1-expressing) cells. We found that the percentage of NS1-expressing cells was reduced by 60% when cells were treated with CGK733 (inhibitor of ATM and ATR) and ~25% when the cells were treated with NU7441 (inhibitor of DNA-PK), but was unaffected when the cells were treated with KU55933 (inhibition of ATM; Fig. 3A). In addition, treatment with 1 mM caffeine, another pharmacological inhibitor of ATM and ATR signaling [218], resulted in a 50% reduction in B19V-infected EPCs (Fig. 3A, Caffeine). Considering the importance of NS1 during parvovirus replication, we speculate that B19V DNA replication is impaired when the DDR signal is blocked as a consequence of ATR and DNA-PK pathway signaling.

We next performed Southern blot analysis to examine whether interference with DDR signaling impairs replication of the B19V genome. As shown in Fig. 3B, the levels of both replicative form DNA (RF DNA) and the ssDNA genome were significantly reduced by in B19V-infected EPCs that had been treated with CGK733 and caffeine, but not in those that had been treated with KU55933. Treatment with 2.5 μM CGK733 decreased B19V DNA forms ~3-fold, and treatment with 10 μM NU7441 reduced the RF DNA and ssDNA by ~30% (Fig. 3B). We further knocked down ATM, ATR and DNA-PKcs by transducing cells with lentiviruses expressing specific shRNAs. As shown in Fig. 3C, the efficiency of knockdown using these lentivirus-based shRNAs was high. We selected transduced cells based on the expression of GFP (encoded by the lentiviral vector), and found that the percentage of NS1-expressing cells in

the ATR-knockdown group was reduced by 50%, and in the DNA-PKcs group it was reduced by 27% (Fig. 3D). Taken together, the kinase inhibitor and knockdown results demonstrate that the ATR and DNA-PK signaling pathways contribute significantly to efficient B19V DNA replication.

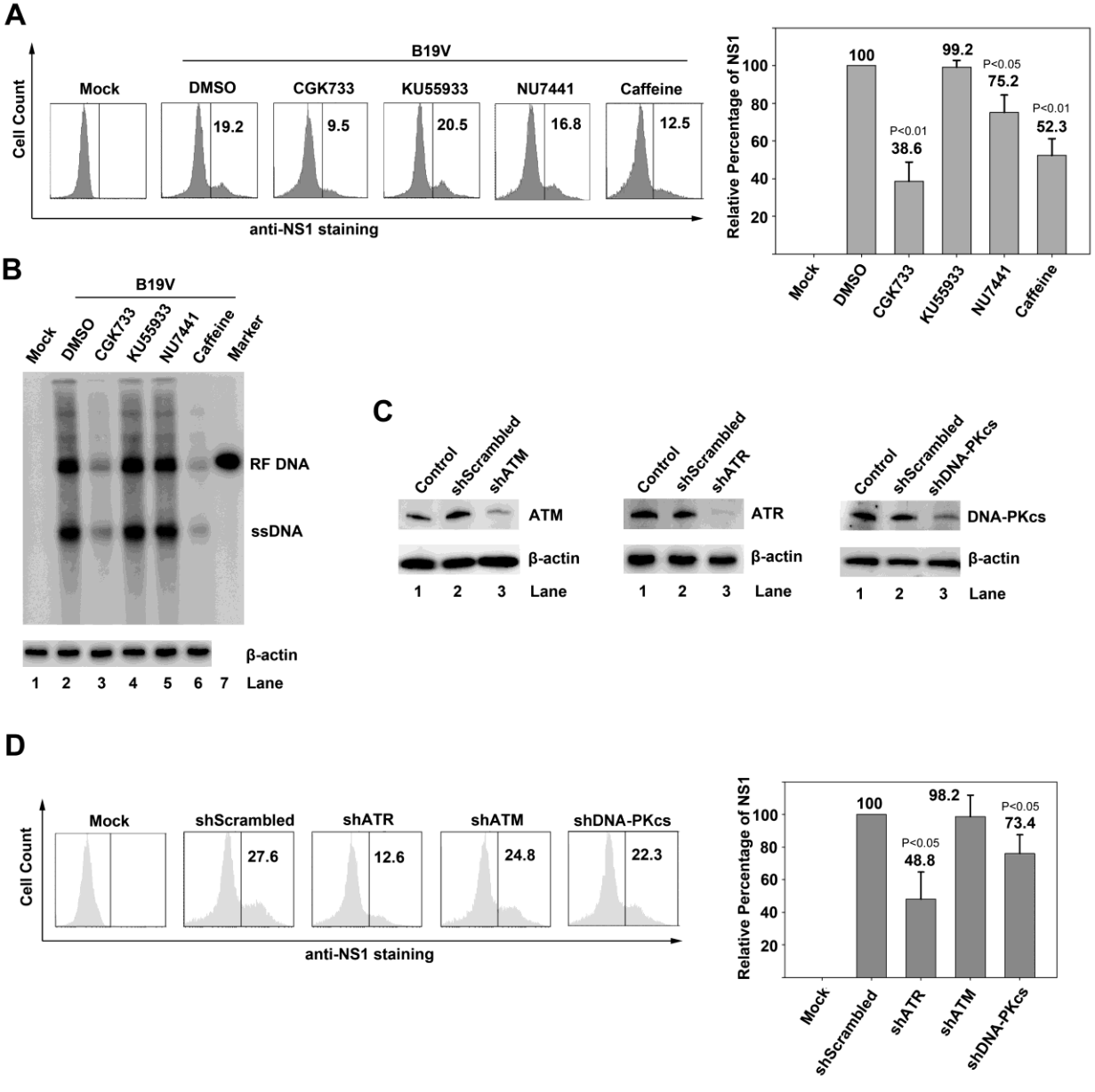
A
B19V
Mock
DMSO
CGK733
KU55933
NU7441
Caffeine
Cell Count
19.2
9.5
20.5
16.8
12.5
anti-NS1 staining
Relative Percentage of NS1
100
99.2
P<0.05
75.2
P<0.01
52.3
P<0.01
38.6
B
B19V
Mock
DMSO
CGK733
KU55933
NU7441
Caffeine
Marker
RF DNA
ssDNA
β-actin
1 2 3 4 5 6 7 Lane
C
Control
shScrambled
shATM
ATM
β-actin
1 2 3 Lane
Control
shScrambled
shATR
ATR
β-actin
1 2 3 Lane
Control
shScrambled
shDNA-PKcs
DNA-PKcs
β-actin
1 2 3 Lane
D
Mock
shScrambled
shATR
shATM
shDNA-PKcs
Cell Count
27.6
12.6
24.8
22.3
anti-NS1 staining
Relative Percentage of NS1
100
98.2
P<0.05
73.4
P<0.05
48.8

Figure 3. Inhibition of ATR and DNA-PK signaling reduces B19V replication.

(A&B) Effects of treatment with pharmacological inhibitors. $CD36^+$ EPCs were treated with the indicated inhibitors for 3 hrs prior to B19V infection. **(A) Flow cytometry analysis.** At 48 hrs p.i., mock- or B19V-infected cells were immunostained for intracellular B19V NS1, and analyzed by flow cytometry. Numbers indicate the percentages of cells expressing NS1 in each case. A representative result is shown. Bar graph shows statistical analysis with average and standard deviation based on at least three independent experiments, with the percentage of NS1-expressing cells in the DMSO-treated group being arbitrarily set as 100; relative percentages of NS1-expressing cells in the other groups are indicated. **(B) Southern blot analysis.** At 48 hrs p.i., half of the cells were collected for Hirt DNA extraction and analyzed by Southern blotting with a B19V DNA-specific probe (upper blot). The other half of each sample was used for Western blotting with the anti-β-actin antibody, which served as a loading control (lower blot). Bands representing replicative form DNA (RF DNA) and single-stranded DNA (ssDNA) are indicated. B19V full-length DNA digested from pB19-M20 [202] was used as a marker. **(C&D) Effects of treatment with kinase targeted shRNAs.** $CD36^+$ EPCs were transduced with shRNA-expressing lentiviruses, as indicated, at 48 hrs prior to infection. **(C) Western blot analysis**. At 48 hrs p.i., cells were collected and analyzed by Western blotting using the indicated antibodies. **(D) Flow cytometry analysis.** At 48 hrs p.i., cells were collected and analyzed for NS1 expression by flow cytometry, using anti-B19V NS1. Transduced (shRNA-expressing) cells were selected based on GFP positive population, and the percentages of NS1-expressing cells among the GFP-positive population are shown in each histogram. A representative result is shown. Statistical analysis from three independent experiments is also shown; the percentage of NS1-expressing cells in the shScrambled-transduced group was arbitrarily set as 100, and the relative percentages of NS1-expressing cells in other groups are indicated.

The ATR substrate Chk1 and the DNA-PKcs binding complex Ku70/Ku80 are required for B19V DNA replication in EPCs.

Given that ATM, ATR and DNA-PKcs were activated and also localized to the B19V replication center, we questioned whether their activated substrates or components also localized to this site. To answer this question, we examined the localization of: Ser345-phosphorylated Chk1 (p-Chk1), an ATR substrate; Thr68-phosphorylated Chk2 (p-Chk2), an ATM substrate [105,107,219,220]; and the Ku70/Ku80 heterodimer, which recruits DNA-PKcs and is part of the active DNA-PK holoenzyme [221]. As shown in Fig. 4A, Chk1 and Chk2 were phosphorylated and localized with NS1 within the nuclei of B19V-infected EPCs. Notably, although both Ku70 and Ku80 were evenly distributed across the nuclei in uninfected cells, they localized to the B19V replication center in infected cells (Fig. 4A, Ku80 and Ku70). These results confirmed that all the three signaling pathways (ATM-Chk2, ATR-Chk1, and DNA-PKcs-KU70/80) were activated in the B19V replication center.

We used Chk1- and Chk2-specific pharmacological inhibitors to further explore the roles of the ATR and ATM pathways in B19V DNA replication. The efficiency of each inhibitor was confirmed by flow cytometry, following staining for the phosphorylated, active forms of these proteins (Fig. 4B). Compared to cells in the mock group, those infected with B19V expressed ~4-fold more p-Chk1 and p-Chk2, as determined by the mean immunofluorescence intensity (MFI). When Chk1 and Chk2 inhibitors were applied, cell proliferation was not affected (data not shown) although the phosphorylation of Chk1 and Chk2 was inhibited by ~60-70%. Notably, only the inhibition of Chk1 led to reduced NS1 expression (~40% reduction; Fig. 4C). Consistent with this finding, application of the Chk1 inhibitor resulted in a ~70% decrease in replication of B19V genome, whereas application of the Chk2 inhibitor did not result in a significant change, relative

to that in cells treated with DMSO (Fig. 4D). Taken together, these results demonstrate that Chk1, a direct substrate of ATR signaling, plays an important role in B19V DNA replication.

To further examine the role of DNA-PK, we knocked down Ku70 by lentivirus-mediated shRNA. As shown in Fig. 4E, more than 70% of Ku70 was knocked down in shKu70-transduced EPCs compared with the scrambled shRNA control. Consequently, interference with Ku70 resulted in more than 50% reduction of NS1 expression, again suggesting that DNA-PK signaling plays a role in B19V replication.

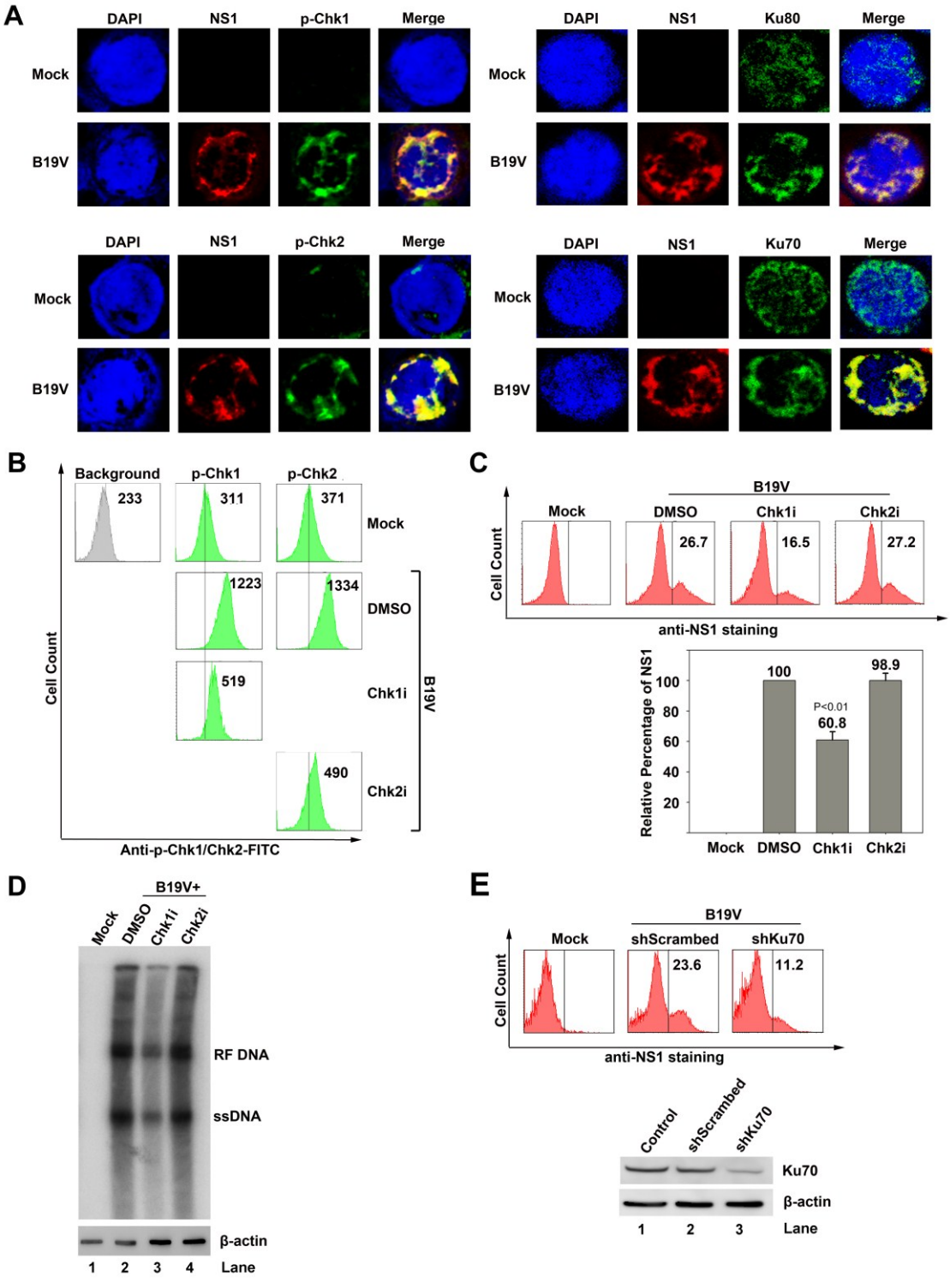
A
DAPI
NS1
p-Chk1
Merge
Mock
B19V
DAPI
NS1
Ku80
Merge
Mock
B19V
DAPI
NS1
p-Chk2
Merge
Mock
B19V
DAPI
NS1
Ku70
Merge
Mock
B19V
B
Background
p-Chk1
p-Chk2
233
311
371
Mock
1223
1334
DMSO
519
Chk1i
490
Chk2i
B19V
Cell Count
Anti-p-Chk1/Chk2-FITC
C
B19V
Mock
DMSO
Chk1i
Chk2i
26.7
16.5
27.2
Cell Count
anti-NS1 staining
Relative Percentage of NS1
100
98.9
P<0.01
60.8
Mock
DMSO
Chk1i
Chk2i
D
B19V+
Mock
DMSO
Chk1i
Chk2i
RF DNA
ssDNA
β-actin
1
2
3
4
Lane
E
B19V
Mock
shScrambed
shKu70
23.6
11.2
Cell Count
anti-NS1 staining
Control
shScrambed
shKu70
Ku70
β-actin
1
2
3
Lane

Figure 4. Inhibition of Chk1 and Ku70, but not Chk2, reduces B19V replication.

(A) Immunofluorescence analysis of localization of the substrates of ATR and ATM, and the DNA-PK components. At 48 hrs p.i., mock- or B19V-infected $CD36^+$ EPCs were co-immunostained with anti-B19V NS1 (red) and one of the following: anti-p-Chk1 (green), anti-p-Chk2 (green), anti-Ku70 (green) or anti-Ku80 (green). Confocal images were taken at a magnification of 100 ×. Nuclei were stained with DAPI. **(B-D) Treatment with pharmacological inhibitors of Chk1 and Chk2.** $CD36^+$ EPCs were treated with DMSO, a Chk1 inhibitor or a Chk2 inhibitor for 3 hrs prior to infection. **(B) Flow cytometry analysis of p-Chk1 and p-Chk2 expression.** At 48 hrs p.i., cells were stained for intracellular p-Chk1 and p-Chk2, and analyzed by flow cytometry. The Mean Fluorescence Intensity (MFI) is indicated. Background sample was treated with second antibody only. **(C) Flow cytometry analysis of NS1 expression.** At 48 hrs p.i., cells were stained for intracellular NS1, and analyzed by flow cytometry. Numbers show percentages of NS1-expressing cells in the population. A representative result is shown. Statistical analysis from three independent experiments is also shown. The percentage of NS1-expressing cells in the DMSO-treated group was arbitrarily set as 100; the values shown for the other cells are relative to the DMSO control. **(D) Southern blot analysis.** At 48 hrs p.i., Hirt DNA was extracted from one half of the cells and analyzed by Southern blotting (upper panel); the remaining cells were used for Western blot analysis with anti-β-actin, which served as a loading control (lower panel). **(E) Effect of treatment with Ku70-speciifc shRNA.** $CD36^+$ EPCs were transduced with lentiviruses expressing scrambled or Ku70-specifc shRNA, at 48 hrs prior to infection. At 48 hrs p.i., cells were collected and analyzed for NS1 expression by flow cytometry. Transduced (shRNA-expressing) cells were selected based on GFP positive population, and the percentages of NS1-expressing cells among the GFP-positive population are shown in each histogram. A representative result is shown. Western blot analysis at the bottom indicates knockdown efficiency of Ku70 in treated cells at 48 hrs p.i.

Inhibition of DDR signaling does not rescue B19V infection-induced G2/M cell cycle arrest.

DNA damage triggers biochemical pathways that arrest cell cycle progression [32,218]. Given that B19V infection of EPCs induces cell cycle arrest at the G2/M phase (Fig. 5A, DMSO) [100], we monitored cell cycle changes in response to infection-induced DDR in the presence of kinase inhibitors and kinase-specific shRNAs. We found that none of the inhibitors tested (KU55933, CGK733, NU7441, Chk1i and Chk2i) reduced the cell cycle arrest observed in B19V-infected cells (Fig. 5A, NS1+). Consistent with this finding, individual knockdown of ATM, ATR or DNA-PKcs failed to significantly change this phenotype (Fig. 5B, NS1+); in NS1-positive cells of both the treated and control groups, more than 90% of the cells were arrested at G2/M.

When we looked at infection-associated cell cycle changes across the entire cell population, we observed that inhibiting either ATR signaling (whether by applying CGK733, caffeine, or Chk1 inhibitor, or an ATR-targeted shRNA) or DNA-PK signaling (by applying a DNA-PKcs or Ku70 shRNA) reduced the number of G2/M-arrested cells across the whole population of B19V-inoculated EPCs (both NS1+ and NS1-) by ~10-15% (Fig. 5A, Total). Since B19V NS1 induces G2/M cell cycle arrest in B19V-infected EPCs [100], we believe that this reduction is due to a general decrease in NS1 expression in all of the cells (Fig. 3B&4D).

Collectively, these results suggest that during B19V infection of EPCs, a mechanism that is independent of DNA damage checkpoints regulates G2/M cell cycle arrest.

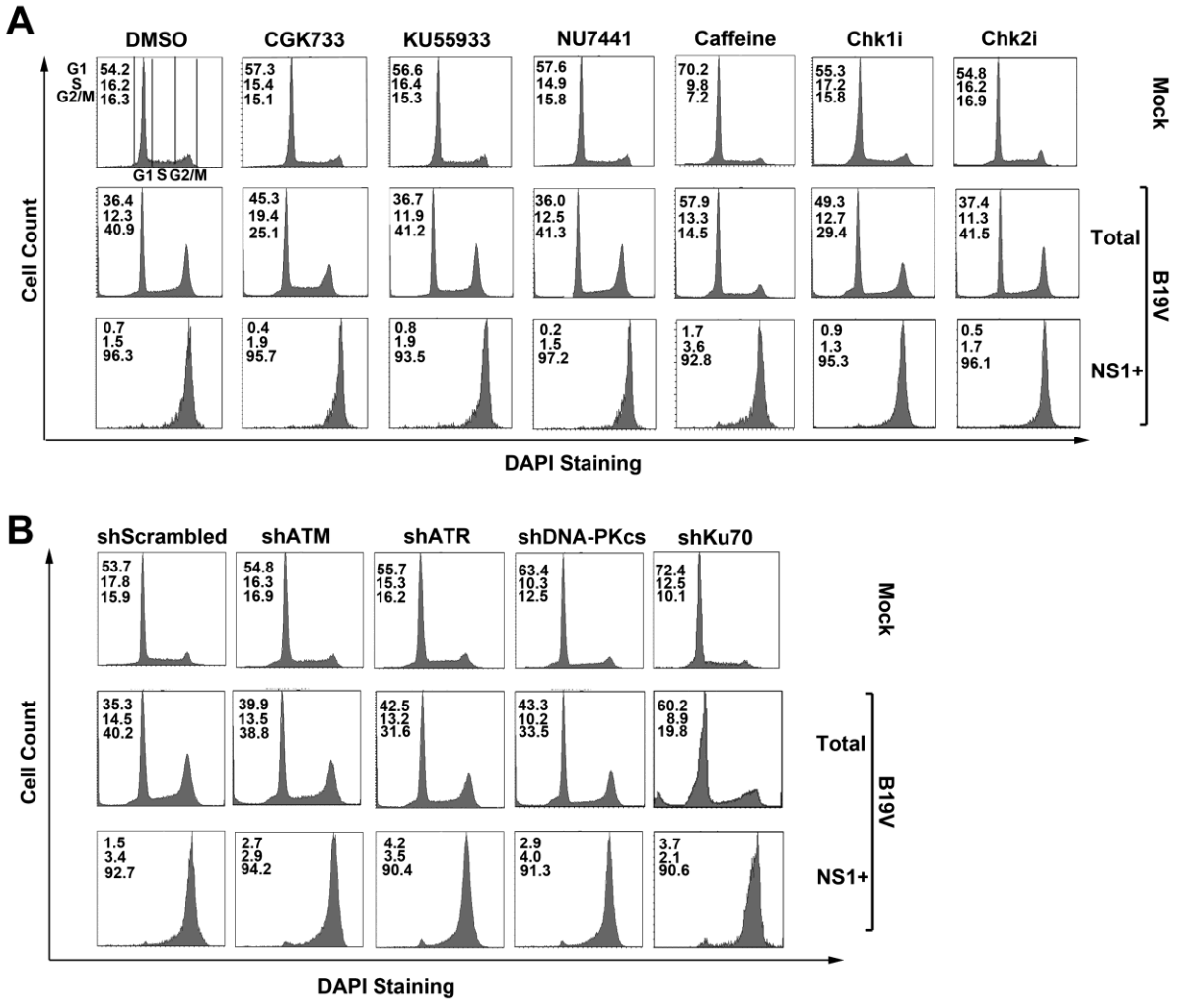
A
DMSO
CGK733
KU55933
NU7441
Caffeine
Chk1i
Chk2i
G1
S
G2/M
G1 S G2/M
54.2
16.2
16.3
57.3
15.4
15.1
56.6
16.4
15.3
57.6
14.9
15.8
70.2
9.8
7.2
55.3
17.2
15.8
54.8
16.2
16.9
Mock
36.4
12.3
40.9
45.3
19.4
25.1
36.7
11.9
41.2
36.0
12.5
41.3
57.9
13.3
14.5
49.3
12.7
29.4
37.4
11.3
41.5
Total
B19V
0.7
1.5
96.3
0.4
1.9
95.7
0.8
1.9
93.5
0.2
1.5
97.2
1.7
3.6
92.8
0.9
1.3
95.3
0.5
1.7
96.1
NS1+
Cell Count
DAPI Staining
B
shScrambled
shATM
shATR
shDNA-PKcs
shKu70
53.7
17.8
15.9
54.8
16.3
16.9
55.7
15.3
16.2
63.4
10.3
12.5
72.4
12.5
10.1
Mock
35.3
14.5
40.2
39.9
13.5
38.8
42.5
13.2
31.6
43.3
10.2
33.5
60.2
8.9
19.8
Total
B19V
1.5
3.4
92.7
2.7
2.9
94.2
4.2
3.5
90.4
2.9
4.0
91.3
3.7
2.1
90.6
NS1+
Cell Count
DAPI Staining

Figure 5. Inhibition of DDR signaling does not rescue the G2/M cell-cycle arrest associated with B19V infection.

(A) Effects of pharmacological inhibitors of DDR kinases on cell cycle arrest. $CD36^+$ EPCs were treated with DMSO or the indicated pharmacological inhibitor for 3 hrs prior to B19V infection, and the effects on the cell cycle were assessed by flow cytometry. **(B) Effect of shRNAs targeting DDR kinases on cell cycle arrest.** Cells were transduced with the indicated shRNA-expressing lentiviruses 48 hrs prior to infection, and the effects on cell cycle were assesses by flow cytometry. At 48 hrs p.i., GFP-expressing cells were selectively gated for anti-B19V NS1 staining and followed by DAPI staining for cell cycle analysis. Cell cycle in mock, infected cells with (NS1+) or without NS1 gating (total) are shown. In each panel, the percentages of cells in the G1, S and G2/M phases, respectively, are indicated (top left).

Discussion

In this study, we have demonstrated, for the first time, that infection of human primary EPCs by B19V leads to the phosphorylation of H2AX and RPA32, a hallmark of DDR, and that three DDR-mediating kinase pathways are activated. Nevertheless, only ATR-Chk1 signaling appears to have a strong influence on B19V DNA replication, with DNA-PKcs activation contributing to a lesser extent. We note that failure of ATM signaling to significantly influence B19V DNA replication and the induced DDR was surprising given the importance of this pathway in MVC- and MVM-induced DDR [29,30,112]. Finally, our results indicate that a DDR-independent checkpoint is responsible for the arrest of B19V-infected cells at the G2/M transition of the cell cycle.

Several members of the family *Parvoviridae* have recently been shown to induce DDR. During infection by the autonomous parvovirus MVC and MVM, ATM signaling is activated and required for replication of the viral genome [29,30,112]; ATR signaling is also activated in MVC-infected cells, but is not essential for MVC DNA replication [30]. In the case of infection by AAV2, a member in genus *Dependovirus* of the family *Parvoviridae*, it is predominantly the DNA-PK pathway that is activated in the presence of adenovirus, although ATM is also activated to some extent [64,65]. Notably in cells inoculated with UV-inactivated AAV2, only the ATR-Chk1 signaling is activated [76].

The DDR induced during B19V infection of primary human EPCs is unique in that all the three kinase pathways are activated. More importantly, B19V takes advantage of both the ATR-Chk1 and DNA-PK signaling pathways to promote replication of its genome. B19V contains an ssDNA genome with a long ITR of 383 nts at both ends, the gap between the two ends is quite large. This structure is a perfect trigger for the DDR, as the cellular DNA damage machinery recognizes the primered DNA as a SSB and activates ATR-mediated signaling [45]. In addition, parvovirus DNA replicates according to a strand-displacement model [114],

producing new ssDNA ends and mimicking SSBs. Thus, B19V DNA replication also contributes to ATR activation. Similarly, parvovirus DNA replication produces nicked DNA intermediates that could be recognized as a DSB [30], and may activate ATM and DNA-PK [32].

We observed that regular cell cycle of EPCs was moderately disturbed by knockdown of DNA-PKcs and Ku70 (Fig. 5B), indicating the importance of DNA-PK complex in sustaining EPC proliferation. Indeed, it has been shown previously that functional inactivation of either Ku70 or Ku80 in human somatic cell lines is lethal, and inactivation of DNA-PK causes proliferation deficit [222]. However, this notion does not affect the results obtained from using DNA-PK specific inhibitor, which did not affect the cell cycle of EPCs. Thus, we believe that inhibition of B19V replication by knocking down DNA-PKcs and Ku70 is a combined effect of inhibiting DNA-PK signaling pathway and partially blockage of G1/S transition.

DNA-PK, an enzyme that contributes to the repair of DSBs through nonhomologous end joining (NHEJ), plays an important role in persistence of recombinant AAV2 (rAAV2) in rAAV2-transduced tissues. It may exert its effects on promoting rAAV2 DNA circularization by recruiting Ku70 and Ku80, which bind directly to ITR structure of rAAV2 [67,68]. However, the role of DNA-PK in wild type AAV2 DNA replication is to recruit complex heterodimer Ku70 and Ku80 to the AAV2 ITR, which serves an origin of DNA replication, and facilitates AAV2 DNA replication *in vitro* [66]. Ku70 and Ku80 act in this context by executing their helicase activity, and as such function much like the MCM2-7 complex, to promote replication of the AAV2 DNA [66,223]. In the current study, we have shown during B19V infection, Ku70 and Ku80 are recruited to the B19V DNA replication center, likely as that also includes phosphorylated DNA-PKcs. Since the ITRs of B19V genome are identical, as is the case of those of the *Dependovirus* AAV2 [146], we speculate that the mechanism underlying DNA replication may be similar for these viruses, with Ku70 and Ku80 playing the same role.

The autonomous parvoviruses MVC and MVM hijack ATM signaling for their DNA replication [29,30,112]. Notably, infection by the autonomous parvovirus B19V activates ATM-Chk2 signaling. Both ATM and Chk2 were also recruited to the B19V DNA replication center; however, this activation had no significant effects on replication of the B19V genome. The structures of the MVC and MVM genomes are very similar; each contains a T-shaped palindromic repeat at the left end, and a U-shaped palindromic repeat at the right hand [118,146]. This could explain why they would use a similar DDR-based strategy to replicate their DNA. ATM activation during MVC infection activated p53, which is responsible for MVC infection-induced apoptosis [30]. Notably, p53 was phosphorylated during B19V infection of EPCs [100]. Thus, we speculate that the ATM-Chk2 activation may contribute to apoptosis of B19V-infected EPCs.

ATR signaling is responsible for the repair of SSBs and that associated stalled replication forks. Activation of its direct substrate, Chk1, results in slowed firing at the replication origin, and controls cell cycle arrest, replication fork stability and replication fork restart [217]. During parvovirus replication, NS1 creates a nick site at the terminal resolution site on the ITR [212], and the viral DNA undergoes replication according to a strand-displacement model [114], producing additional ssDNA ends that mimic SSBs structurally. Such events occur on multiple copies of the replicating B19V genome, and possibly trigger robust ATR activation. This leads to recruitment of ATR-dependent substrates (e.g., RFC, RPA32, MCM2-7, MCM10, PCNA and several DNA polymerases) to, or possibly their stabilization at, the replication fork [217]. Notably, the ATR-substrates also are important for AAV2 replication. A study involving an *in vitro* reconstitution assay has shown that RFC, PCNA, MCM2-7, polymerase δ and Rep78 are the minimum proteins required for efficient DNA replication of AAV2 [224,225]. In addition, one study revealed that infection with UV-inactivated AAV2 activates ATR-Chk1 signaling, and that activated ATR-Chk1 complexes then recruited polymerase δ to the AAV2 ITR by the

ATR-dependent substrates [76]. Unfortunately, it was not feasible to examine the role of this recruitment in AAV2 DNA replication in that study, since the genome of UV-inactivated AAV2 was crosslinked [76]. We have shown that ATR can phosphorylate both RPA32, a single-stranded DNA binding protein, that is directly involved in replication of eukaryotic cells, and MCM2 (data not shown), a helicase that initiates formation of the pre-replication complex. However, additional investigation will be required to understand the mechanism by which ATR-Chk1 signaling promotes B19V DNA replication.

DDR can lead to three distinct outcomes. When damage is severe and irreversible, the host cell may undergo apoptosis [226,227]. In the context of mild damage, it may recruit the repair machinery, through either non-homologous end joining (NHEJ) or mechanism involved in homologous recombination, and cell cycle arrest [32,228]. Our analysis of the effects of DNA repair pathway inhibitors that significantly reduced B19V DNA replication failed to detect a change in cell cycle pattern in infected cells. Moreover, although caffeine treatment caused a slight G1 arrest of the cell cycle in EPCs, it also failed to rescue the G2/M arrest in NS1+ cells. In addition, inhibiting Chk1 and Chk2 failed to interfere with G2/M cell cycle arrest in NS1+ cells, although these proteins normally function as checkpoint controls, regulating the cell cycle under stressful conditions [105,107]. Consistent with these findings, knockdown of ATM, ATR and DNA-PKcs did not affect B19V infection-induced G2/M arrest. All these lines of evidence strongly suggest that B19V infection-induced G2/M arrest is dependent on a DDR-independent cell cycle checkpoint. Indeed, it has been shown that B19V NS1 *per se* is able to arrest NS1-expressing cells at G2/M by deregulating E2F family transcription factors [100]. However, we cannot rule out the possibility that the ATR-Chk1 checkpoint, as well as the ATM-Chk2 checkpoint may be redundant with the E2F-mediated checkpoint in arresting cells at G2/M during B19V infection of EPCs. We are currently investigating this possibility.

In conclusion, we have identified a *de novo* role for ATR-Chk1 and DNA-PK signaling in B19V DNA replication in primary human EPCs. Components of these pathways can be explored as candidate drug targets for inhibiting B19V replication, and for the treatment of B19V-asociated diseases in patients infected with B19V.

Chapter 4

ATM signaling facilitates autonomous parvovirus DNA replication through SMC1-mediated intra-S phase arrest

Abstract

Activation of a host DNA damage response (DDR) is essential for DNA replication of Bocavirus minute virus of canines (MVC); however the mechanism by which DDR contributes to viral DNA replication is unknown. In the current study, we demonstrate that MVC infection triggers the intra-S phase arrest to slow down host cellular DNA replication and to recruit cellular replication factors for viral DNA replication. The intra-S phase arrest is regulated by ATM (ataxia-telangiectasia-mutated) signaling in a p53-independent manner. Moreover, we demonstrate SMC1 (structural maintenance of chromosomes 1) as the key regulator of the intra-S phase arrest induced during infection. Either knockdown of SMC1 or complementation with a dominant-negative SMC1 mutant blocks both the intra-S phase arrest and viral DNA replication. Finally, we show that the intra-S phase arrest induced during MVC infection was neither caused by damaged host cellular DNA nor by viral proteins, but by replicating viral genomes physically associated with the DNA damage sensor, the Mre11-Rad50-Nbs1 (MRN) complex. In conclusion, the feedback loop between MVC DNA replication and the intra-S phase arrest is mediated by the ATM-SMC1 signaling and plays a critical role in MVC DNA replication. Thus, our findings unravel the mechanism underlying DDR signaling-facilitated MVC DNA replication, and demonstrate a novel strategy of DNA virus-host interaction.

Introduction

Parvoviruses are small, non-enveloped and single-stranded DNA (ssDNA) viruses, and cause highly contagious diseases that are sometimes fatal in humans and animals [2,201]. The viral genome of parvoviruses is 5-6 kilobases (kb) and flanked by two terminal hairpin structures. Adeno-associated viruses (AAVs), in genus Dependovirus of the family Parvoviridae, require helper virus for replication, whereas autonomous parvoviruses, such as minute virus of mice (MVM) and minute virus of canines (MVC), in genera Parvovirus and Bocavirus, respectively, replicate autonomously in host cells. Because of its well-characterized reverse genetics system and efficient infection system, MVC has been used as a model to study the DNA replication mechanism of autonomous parvoviruses as well as the pathogenesis of bocavirus infection [30,118,121]. During infection of Walter Reed/3873D (WRD) canine cells, MVC induces a gradual cell cycle arrest, from S phase in early infection to G2/M phase at a later stage, and mitochondria-mediated apoptosis [121]. Additionally, MVC hijacks the cellular DNA damage response (DDR) machinery to facilitate viral DNA replication [30]. The MVC genome shares 50-60% identity with the genome of human bocavirus type 1 (HBoV1) [118,229], a newly identified human pathogen that causes acute respiratory tract infections in children worldwide [124,229–233]. Therefore, MVC has been used as a model for studying bocavirus replication.

Infections of many DNA viruses are able to subvert the cellular DDR machinery [49,51,81,234], a safeguarding system triggered by damaged cellular DNA structures such as ssDNA breaks (SSBs), double-stranded DNA breaks (DSBs) and stalled replication forks [32,180]. The central role of the DDR is to protect genome stability and integrity through a cascade of phosphorylation events initiated by three phosphatidylinositol 3-kinase-like kinases (PI3Ks), ATM (ataxia telangiectasia-mutated kinase), ATR (ATM- and Rad3-related kinase), and DNA-PKcs (DNA-dependent protein kinase catalytic subunit) [34,35]. In the presence of

damaged DNA structures, these three kinases are recruited and auto-phosphorylated, and further recruit a number of effector proteins to coordinate cell cycle arrest, DNA repair, and apoptosis. ATM signaling has been reported to be co-opted by many DNA viruses, including autonomous parvoviruses MVC and MVM [29,30,112], papillomaviruses [179,235], and herpes viruses [71,236–239], to help their productive infections. However, the beneficial effects of ATM signaling on viral DNA replication have not been well-understood [49–51].

In replicating cells in S phase, one of the most important outcomes of the DDR is the intra-S phase arrest [145,240,241]. The intra-S phase arrest plays a crucial role in preventing damaged DNA to enter mitosis by slowing the rate of S phase progression and stabilizing stalled replication forks [145,242]. The signaling proteins involved in the intra-S phase arrest include a large number of checkpoint proteins and DNA repair factors. Intra-S phase checkpoint proteins are activated to slow down cellular DNA replication through degradation of replication proteins or regulator factors such as Cdc25A [241,243–247], while DDR signaling recruits repair factors to the damaged DNA foci for the rapid resumption of replication following DNA repair [248]. ATM signaling plays a central role in regulating DSB-induced intra-S phase arrest. Damaged DNA is first recognized by the Mre11-Rad50-NBS1 (MRN) complex sensor and further recruits ATM kinase. Following ATM autophosphorylation, several proteins such as Chk2 (checkpoint protein 2), BRCA1 (breast cancer type 1 susceptibility protein) and SMC1 (structural maintenance of chromosomes 1) are phosphorylated and recruited as checkpoint proteins [145]. SMC1 was originally identified as a subunit of the cohesion complex that ensures proper segregation of sister chromatids [249]. Further studies confirmed that it is an intra-S phase checkpoint protein that is phosphorylated at serines 957 and 966 by ATM kinase [163,250–253]. However, it is not clear how SMC1 interferes with cellular DNA replication proteins or regulator factors through its checkpoint function. Although replication of many DNA viruses occurs during the S phase of host

cells and induces a DDR, the link between viral infection-induced DDR and the intra-S phase arrest has not been well-established.

Modulation of the host cellular environment through cell cycle control is an important strategy for replication of DNA viruses. By arresting cells in S phase, viral DNA synthesis is facilitated by the cellular DNA replication machinery; however, many DNA viruses also block cellular DNA synthesis for productive infection [254–256]. Autonomous parvovirus MVM has been reported to inhibit host cell growth through p53-dependent inhibition of cyclin A, and the large nonstructural protein NS1 plays a key role in inhibiting host cell DNA synthesis [16,17,113]. However, we found that expression of the non-structural proteins of MVC, NS1 and NP1, failed to interfere with host cell cycle regulation [121], indicating that a mechanism without a direct involvement of viral proteins is involved in MVC-induced cell cycle arrest.

In this study, we aim to determine whether DDR signaling and cell cycle modulation coordinate to facilitate MVC DNA replication. Our results confirm that MVC infection triggers the intra-S phase arrest that is mediated by the ATM-SMC1 pathway and facilitates viral DNA replication. Moreover, our results provide direct evidence that MVC infection-induced DDR is elicited by the MRN complex that senses replicating viral genomes. These findings reveal a novel strategy by which MVC exploits cellular DNA replication and DDR machineries for its own DNA replication, and provide new insights in the mechanisms of virus-host interaction that directly contribute to viral DNA replication.

Materials and Methods

Cell culture and virus infection.

WRD cells [120] were maintained in Dulbecco's modified Eagle's Medium (DMEM) with 10% fetal calf serum (FCS) in 5% CO2 at 37°C. MVC (GA3 strain) was cultured and titrated as previously described [30,118,121]. WRD cells were infected with MVC at a multiplicity of infection (MOI) of 3. Both WRD cells and MVC were gifts from Collins Parrish at Cornell University).

Chemicals and treatment.

ATM kinase Inhibitor KU55933 (Tocris Bioscience, Bristol, UK) was prepared in dimethyl sulfoxide (DMSO) as a stock solution at 10 mM. Bromodeoxyuridine (BrdU; Sigma) was diluted in deionized water as a stock solution at 10 mM. WRD cells were seeded on 60-mm dishes 1 day prior to chemical treatment. KU55933 was applied to cells at a final concentration of 10 μM upon virus infection.

Antibodies used.

The rat anti-MVC NS1 polyclonal antibody was developed previously [118]. All the other antibodies used in this study were purchased from companies listed as follows: anti-BrdU and anti-PCNA antibodies (BD Biosciences, San Jose, CA), anti-γH2AX antibody (Novus, Littleton, CO), and anti-Rad50 (Epitomics, Burlingame, CA), anti-p-p53(Ser15) and anti-Flag epitope (Cell signaling, Danvers, MA), anti-β-actin (Sigma,), anti-cyclin A, anti-RFC1, anti-pol δ and anti-Mre11 antibodies (Santa Cruz Biotechnology, Santa Cruz, CA), anti-p-Nbs1(Ser343) and

anti-p-SMC1(Ser957) antibodies (Genscript, Piscataway, NJ), and anti-SMC1 antibody (Genetex, Irvine CA). All the secondary antibodies were purchased from Jackson ImmunoResearch Laboratories, Inc. (West Grove, PA).

siRNA, plasmids, and transfection.

Small interfering RNA (siRNA) oligonucleotides were synthesized as dicer substrate RNA interference (RNAi) at Integrated DNA Technologies (IDT, Coralville, IA). The following siRNA sequences were chosen for targeting the genes of interest: siRNA specific to canine ATM (siATM), 5'-GUA CUA GUU GCU UGU GUA ACU GUA-3'; siRNA specific to canine SMC1A (siSMC1), 5'-CUC UCC CAA UCU CUG GAU AUU UGG-3'; siRNA specific to canine p53 (sip53), 5'-CCA CCA UCC CUA AAC UAA UGT G-3'. The following scrambled RNA (scrambled) was used as an siRNA control: 5'-CUU CCU CUC UUU CUC UCC CUU GUG A-3'. Transfection of all siRNAs was performed using Hiperfect reagent (Qiagen, Valencia, CA) following the manufacturer's instructions. At 48h post-transfection, the cells were fed with fresh medium and infected with MVC.

Plasmids pcDNA3-5'cMyc-SMC1wt and pcDNA3-5'cMyc-SMC1(S957A/S966A) [250], expressing wild-type human hSMC1wt and hSMC1(S957A/S966A) mutant, respectively, were purchased from Addgene (Cambridge, MA). MVC plasmids pIMVC, pIMVCNP1(-), pIMVCVP1/2(-), and pMVCNSCap and control vector pBB have been described previously [118]. Nucleofection was used to transfect plasmid DNA using an AMAXIA Nucleofector (Lonza In., NJ) at program T030.

Southern blot analysis.

Low molecular weight (Hirt) DNA was extracted from infected cells [257,258] and analyzed by Southern or Dot blotting using an MVC NSCap probe as described previously [30,118,121].

BrdU incorporation and BrdU pulsing assays.

For BrdU incorporation assay [102], BrdU was added to the cell culture medium at the final concentration of 30 μM and incubated for 1h. After BrdU incorporation, cells were collected, fixed in 3.7% paraformaldehyde for 30 min and permeabilized with 0.1% Triton X-100 for another 30 min. After permeabilization, two procedures were followed to differentiate the cell cycle (cellular DNA replication) from viral DNA replication. For the detection of the cell cycle, cells were treated with 1 M HCl for 30 min to denature chromosome DNA for the binding of the BrdU epitopes with an anti-BrdU antibody (clone B44) [259]. For viral DNA replication analysis, the HCl treatment step was skipped [260] since parvovirus replication generates ssDNA viral genome a well as replication intermediates that contain partial ssDNA [114]. The cells were co-stained with anti-BrdU and anti-MVC NS1 antibodies followed by secondary antibodies and DAPI to analyze the cell cycle and the percentage of NS1-positive (NS+) cells, respectively.

For the BrdU pulsing assay, at 18h p.i., mock- or MVC-infected cells were incubated with BrdU at 30 μM for 20 min. Incubated cells were collected immediately after BrdU labeling and every hour thereafter. Collected cells were fixed, permeabilized and treated with 1 M HCl as described above. Treated cells were then co-stained with DAPI and anti-BrdU and anti-MVC NS1 antibodies, and were assessed by flow cytometry. Mock- and MVC-infected cells were gated according to NS1 staining, and the change in DNA content in the BrdU-labeled cells was monitored by DAPI staining.

Flow cytometry analysis.

The above stained cell samples were analyzed on a three-laser flow cytometer (LSR II; BD Biosciences) at the Flow Cytometry Core of the University of Kansas Medical Center. All flow cytometry data were analyzed using FACSDiva software (BD Biosciences).

Comet assay.

A Comet assay kit was purchased from Cell Biolabs Inc. (San Diego, CA) and used according to the manufacturer's instructions. Briefly, at 18h p.i., mock- or MVC-infected cells were trypsinized and diluted in PBS. Mock-infected cells were treated with 100 μM H2O2 at 4ºC for 20 min as positive controls. Mock- and MVC-infected, and H2O2-treated cells were mixed with 1% low melting-point agarose, respectively, and coated on slides. Then, the slides were treated in an alkaline condition, electrophoresed and stained with the VISTA green dye. Stained slides were visualized under a confocal microscope (Eclipse C1 Plus, Nikon, Melville, NY) with Nikon EZ-C1 software. Images were taken at a magnification of ×40.

BrdU-based dot blot analysis of DNA replication.

WRD cells were mock- or MVC-infected. At 12h, 18h, 24h and 48h p.i., the infected cells were collected. Half of the cells were used to purify total DNA (both genomic DNA and viral DNA) using the DNeasy Blood & Tissue Kit (Qiagen). The other half of the infected cells were used to extract low molecular weight DNA (viral DNA) using the Hirt DNA extraction method [257,258]. Extracted DNA was diluted in 100 μl of deionized water. The BrdU-based dot blot assay was

performed as previously described [261]. Briefly, to expose the BrdU epitopes in cellular DNA, the DNA samples were denatured by heating at 95ºC for 5 min and immediately kept on ice; 5 µl of the DNA samples were pipetted onto a nitrocellulose membrane. The DNA on the membrane was cross-linked by UV treatment at a dose of 700 mJ/cm2 in a Hoefer UVC 500 UV cross-linker (Hoefer, Inc., Holliston, MA). The membrane was then blocked in 5% non-fat milk in TBST (Tris-buffered saline, pH 7.4, with 0.1% Tween 20) at room temperature, after which a Western blotting procedure was followed.

Western blotting and immunofluorescence staining.

Western blotting was performed as previously described [30,121]. Immunofluorescence staining was performed as previously described [30,212]. Briefly, cells were fixed in 3.7% paraformaldehyde and permeabilized in 0.1% Triton X-100, except for the staining with an anti-PCNA antibody, in which 90% methanol was used. Images were taken at a magnification of ×100 or ×40 under a confocal microscope (Eclipse C1 Plus, Nikon) with Nikon EZ-C1 software.

BrdU-based immunoprecipitation (IP) assay.

At 18h p.i., mock- or MVC-infected cells were pulsed with BrdU at 100 µM for 1h and collected. IP was performed using the Pierce Crosslink IP kit (Thermo Scientific, Rockford, IL). Briefly, treated cells were lysed and centrifuged; the supernatant that contained viral DNA was incubated with protein A/G-coated resins pre-incubated with an anti-BrdU antibody. The resins were then rinsed and diluted in protein loading buffer followed by Western blotting using an anti-Mre11 antibody.

Results

MVC DNA replication arrests host cells in S phase during early infection.

We have shown previously that MVC infection induces a host cell cycle change from S phase in early infection to G2/M phase in later infection [121]; however, whether such a change is related to viral DNA replication is unknown. To determine the relationship between viral and cellular DNA replication, we performed a BrdU pulse labeling assay. BrdU is a thymidine analog that can be incorporated into replicating DNA [260,262]. For the detection of cellular DNA replication by BrdU incorporation, a denaturation process, such as treatment with hydrochloride (HCl), is necessary because the BrdU epitopes are only detectable in a ssDNA form by the monoclonal anti-BrdU antibody (B44 clone) [259]. As anticipated, without denaturation, incorporated BrdU was undetectable in mock-infected cells (Fig. 1A, -HCl). In contrast, MVC-infected cells showed punctate foci of anti-BrdU staining that co-localized with the foci stained for MVC NS1 (Fig. 1A, -HCl), which represent active viral DNA replication centers. Thus, denaturation is not necessary for the detection of parvoviral ssDNA synthesis in this assay as previously reported for replication of parvovirus Aleutian mink disease virus (AMDV) [260]. This is presumably because parvovirus DNA replication generates replicative intermediates that contain partial ssDNA and viral ssDNA genome [114]. Notably, with denaturation, both mock- and MVC-infected cells showed a much broader distribution of BrdU-incorporated foci, which presumably contained both newly synthesized cellular DNA and both dsDNA and ssDNA forms of viral DNA (Fig. 1A, +HCl).

To determine the relative levels of incorporated BrdU in cellular DNA vs. viral DNA under the denaturation condition, total DNA and lower molecular weight DNA (Hirt DNA) of infected cells were extracted, respectively, from equal numbers of cells, and were analyzed by a dot blot assay. Incorporated BrdU in Hirt DNA of MVC-infected cells was detected at a background level

as that seen in Hirt DNA of mock-infected cells (Fig. 1B, Hirt DNA), except for the Hirt DNA prepared from MVC-infected cells at 18h post-infection (p.i.; Fig. 1B, arrow), suggesting a peak of viral DNA replication. At this peak, the incorporation of BrdU into Hirt DNA was over 20 times lower than that into cellular DNA (Fig. 1B, 18h). Notably, the Hirt DNA samples contained nearly all the viral DNA in the total DNA of MVC-infected cells (Fig. 1C), and were contaminated only with a very low level of cellular DNA (Fig. 1B, 48h/Mock). Hence, these results confirm that the majority of incorporated BrdU signaling resulted from cellular DNA replication in infected cells. In following studies, denaturation of infected cells was used to differentiate cellular DNA replication from viral DNA replication.

The cell cycle change was then examined in MVC-infected cells. At all the times points p.i., approximately 36% of NS1-negatvie cells (NS1-) were in S phase (Fig. 2A, NS1-). At 12h p.i., MVC-infected (NS1+) cells showed 81% in S phase. The majority of these NS1+ cells were actually in early S phase as shown by a lower DNA content (Fig. 2A, NS1+/12h). NS1+ cells progressed to mid-S phase at 18h p.i. and late S phase at 24h p.i. (Fig. 2A, NS1+/18h and 24h). At 48h p.i., viral DNA replication slowed down; only 16% of NS1+ cells were in S phase, and the majority of NS1+ cells had moved to G2/M phase (Fig. 2A, NS1+/48h). A statistical analysis of the cell cycle over the course of MVC infection was summarized (Fig. 2B). Overall, MVC infection induced 80% of NS1+ cells in S phase from 12h to 24h p.i. but only 35-37% of mock-infected cells.

We next detected BrdU incorporation in infected cells without denaturation to probe viral DNA replication. Approximately 40% of the total cell population produces a significant level of viral ssDNA/replication intermediates, which suggests active viral DNA replication, at 18h and 24h p.i. At 48h p.i. viral DNA replication had slowed down to 9% of the total cell population, although most of the cells (approximately 72%) were MVC-infected as shown by NS1+ staining

(Fig. 2C). These results indicate that active viral DNA replication occurs from 18h to 24h p.i. (Fig. 2D).

Taken together, these results show that MVC infection induces accumulation of infected cells in S phase during early infection, which supports active viral DNA replication. Notably, we observed that at early infection (18h-24h p.i.), cellular DNA replication was active but at a lower rate (Fig. 1B, compare dots in lines between Mock and MVC for Total DNA), indicating that S phase progression was perturbed during early infection.

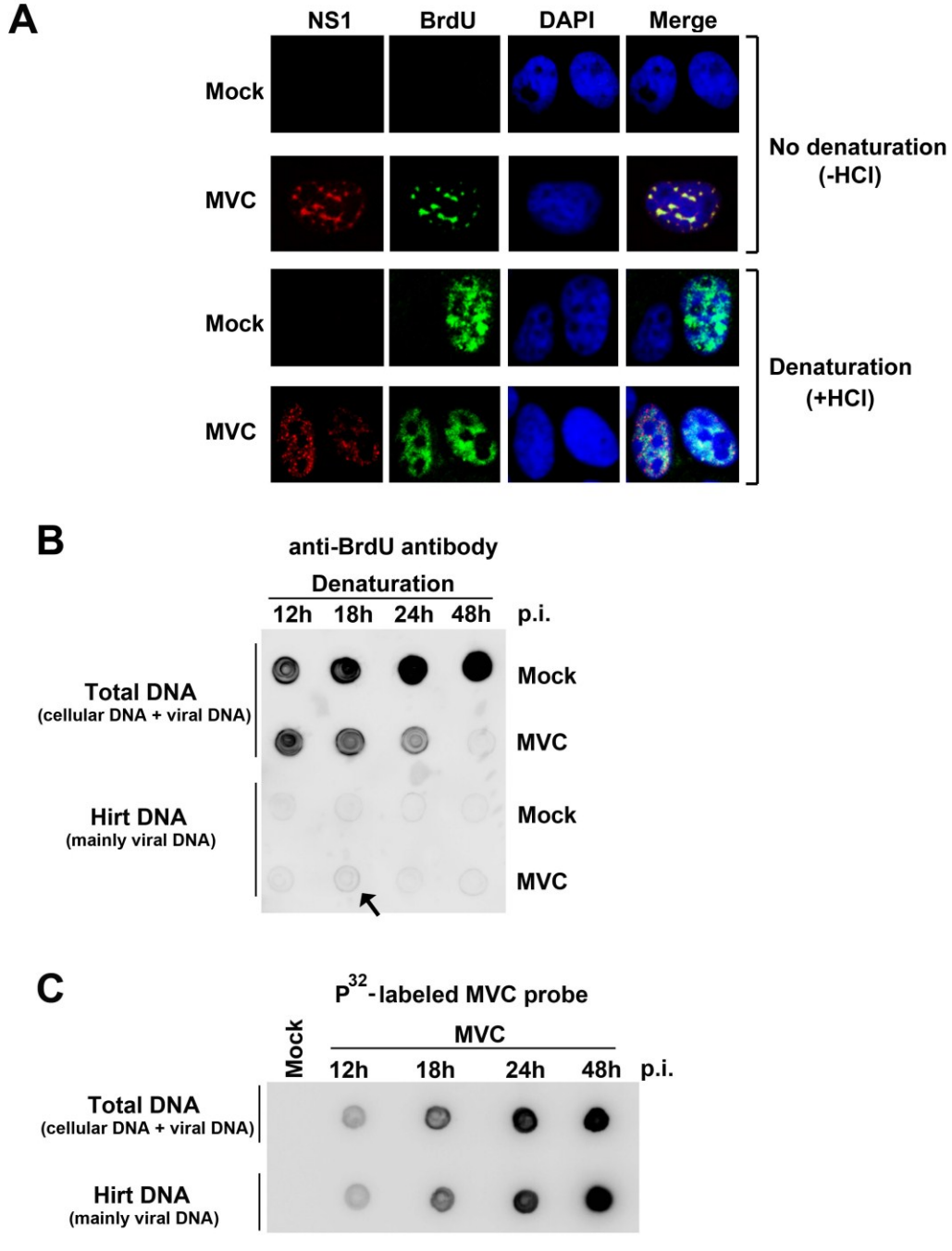
A
NS1
BrdU
DAPI
Merge
Mock
MVC
Mock
MVC
No denaturation
(-HCl)
Denaturation
(+HCl)
B
anti-BrdU antibody
Denaturation
12h
18h
24h
48h
p.i.
Total DNA
(cellular DNA + viral DNA)
Mock
MVC
Hirt DNA
(mainly viral DNA)
Mock
MVC
C
P32-labeled MVC probe
Mock
MVC
12h
18h
24h
48h
p.i.
Total DNA
(cellular DNA + viral DNA)
Hirt DNA
(mainly viral DNA)

Fig. 1. Cellular DNA replication decreases, but still prevails over viral DNA replication during early infection of MVC.

(A) Immunofluorescence analysis of DNA replication. WRD cells were seeded on chamber slides 24h prior to MVC infection. At 18h p.i., cells were incubated with BrdU for 1h. The cells on slides were fixed and treated with (+HCl) or without HCl (-HCl) as indicated. Fixed cells were co-stained with anti-MVC NS1 and anti-BrdU antibodies and DAPI. Confocal images were taken at a magnification of ×100. **(B) Dot blot analysis of viral and cellular DNA replication**. At the indicated times p.i., mock- or MVC- infected cells were incubated with BrdU for 1h. BrdU-labeled cells were collected and extracted for total DNA and Hirt DNA (lower molecular weight DNA), respectively. The DNA samples were denatured and dot blotted and immunostained with an anti-BrdU antibody. **(C) Southern blot analysis of viral DNA in preparations of total DNA and Hirt DNA**. The total DNA and Hirt DNA samples extracted from MVC-infected cells were denatured and dot blotted and hybridized with a 32p-lablled MVC NSCap probe [118].

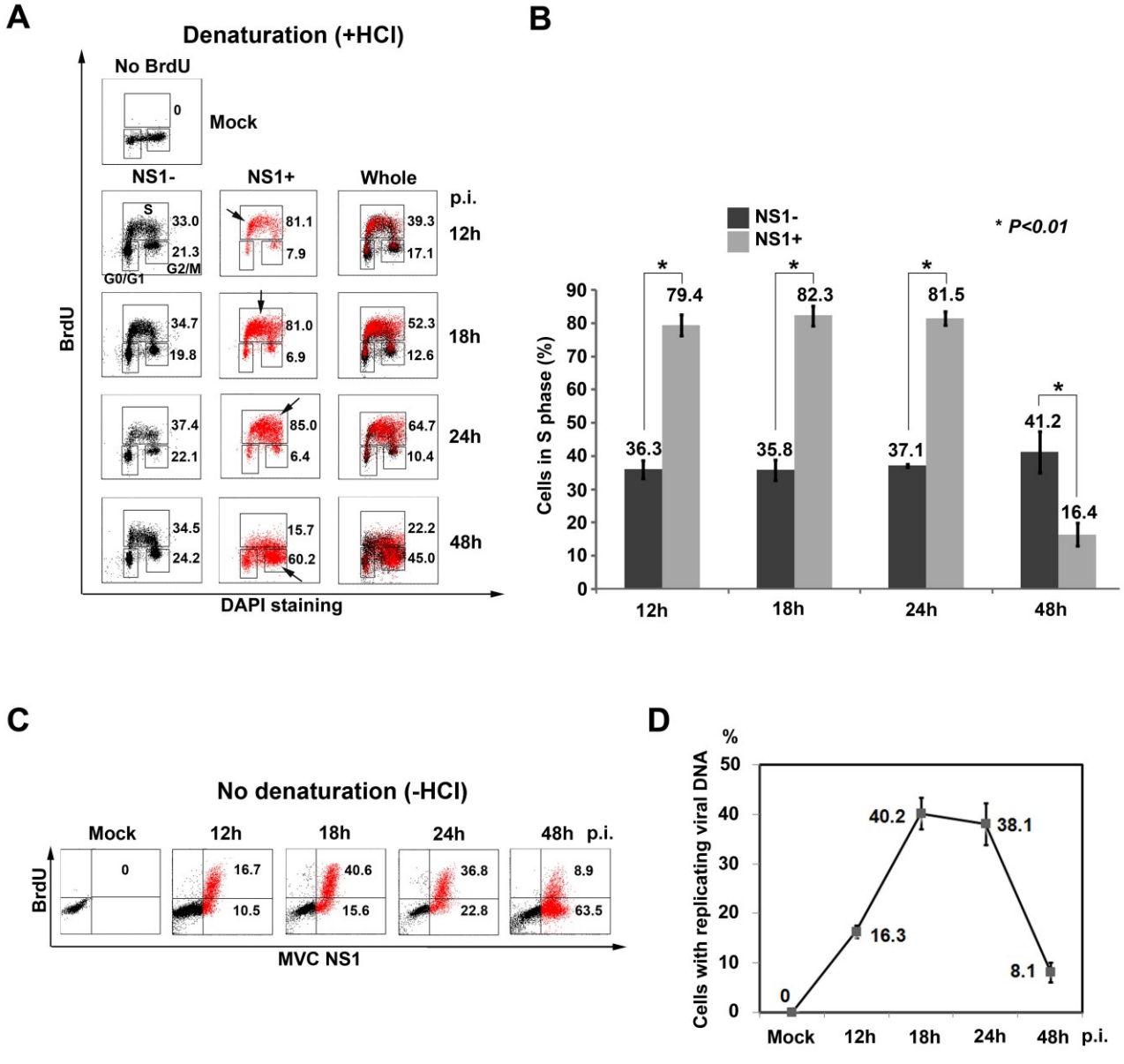
A
Denaturation (+HCl)
No BrdU
Mock
NS1-
NS1+
Whole
p.i.
12h
18h
24h
48h
S
G0/G1
G2/M
BrdU
DAPI staining
B
NS1-
NS1+
* P<0.01
Cells in S phase (%)
79.4
82.3
81.5
41.2
36.3
35.8
37.1
16.4
C
No denaturation (-HCl)
Mock
12h
18h
24h
48h p.i.
BrdU
MVC NS1
D
Cells with replicating viral DNA
%
40.2
38.1
16.3
8.1
0
Mock
12h
18h
24h
48h p.i.

Fig. 2. MVC DNA replication arrests host cells in S phase.

(A&B) Flow cytometry analysis of the cell cycle. (A) At the indicated times p.i., mock- or MVC-infected cells were BrdU-labeled, treated with HCl (+HCl), stained and analyzed by flow cytometry. Unlabeled mock-infected cells were used as a negative control for anti-BrdU staining. Both the NS1-positive (NS1+, marked in red) and negative (NS1-, marked in black) cell populations were gated. The percentage of cells in each phase was gated in the NS1+ and NS1- cell populations and in the whole population (whole) based on the intensity of BrdU staining and DNA content. Numbers show percentages of cells in S phase (upper) and G2/M phase (lower) in each histogram. Arrows indicate the most concentrated cell population. (B) The percentages of cells in S phase are shown as means (numbers) and standard deviations (error bars) and were generated from at least three independent experiments. P values were determined using Student's t-test. (C&D) Flow cytometry analysis of viral DNA replication. **(C)** At the indicated times p.i., mock- or MVC-infected cells were incubated with BrdU for 1h. The cells were co-stained with anti-NS1 and anti-BrdU antibodies and DAPI, and analyzed by flow cytometry. NS1+ cells were marked in red. Numbers shown in the histograms indicate percentages of cells with BrdU incorporation from one representative experiment. **(D)** The percentages of BrdU+ cells are plotted to the time points p.i. Averages and standard deviations are shown at each time point on the right side, and were obtained from at least three independent experiments.

MVC DNA replication prolongs S phase.

To further investigate whether S phase accumulation is due to a prolonged S phase progression, we performed a BrdU pulsing assay to analyze the rate of S phase progression. Immediately after labeling (0h post-labeling), infected cells (at 18h p.i.) with 2N, intermediate (Interm.) and 4N DNA contents were all labeled in the mock group for cellular DNA synthesis in early, mid and late S phase, respectively (Fig. 3C, Mock/0h). In contrast, the majority of the labeled infected cells had an intermediate DNA content immediately after labeling (Fig. 3C, MVC/0h), which was consistent with the cell cycle arrest in mid-S phase at 18h p.i. (Fig. 2A). Labeled mock-infected cells were able to synthesize DNA smoothly, as evidenced by the fast increase in cells with a 4N DNA content every hour post-labeling. At 5h post-labeling, approximately 90% of the cells had a DNA content of 4N. At 6h post-labeling, a large portion of cells finished mitosis and became 2N cells, indicating that those cells had finished one round of replication and the daughter cells had entered G1 phase (Fig. 3C, Mock). By contrast, MVC-infected cells synthesized DNA slowly as the increase in 4N cells was much slower than in the mock-infected group. At 12h post-labeling, only 55% of the labeled cells had a DNA content of 4N. All the labeled cells were not able to pass G2/M phase even after 24h post-labeling (approximately 48h p.i.). It took at least 12h for infected cells to move from early S to late S phase, suggesting that the S phase of MVC-infected cells is prolonged.

Collectively, these results confirm that MVC DNA replication induces S phase arrest. Moreover, cellular DNA synthesis in MVC-infected cells is still active but slower, which is consistent with the fact that BrdU was less incorporated in MVC-infected cells than in mock-infected cells (Fig. 1B). Thus, we hypothesized that MVC infection creates a prolonged S phase to block cellular DNA replication and to facilitate viral DNA replication.

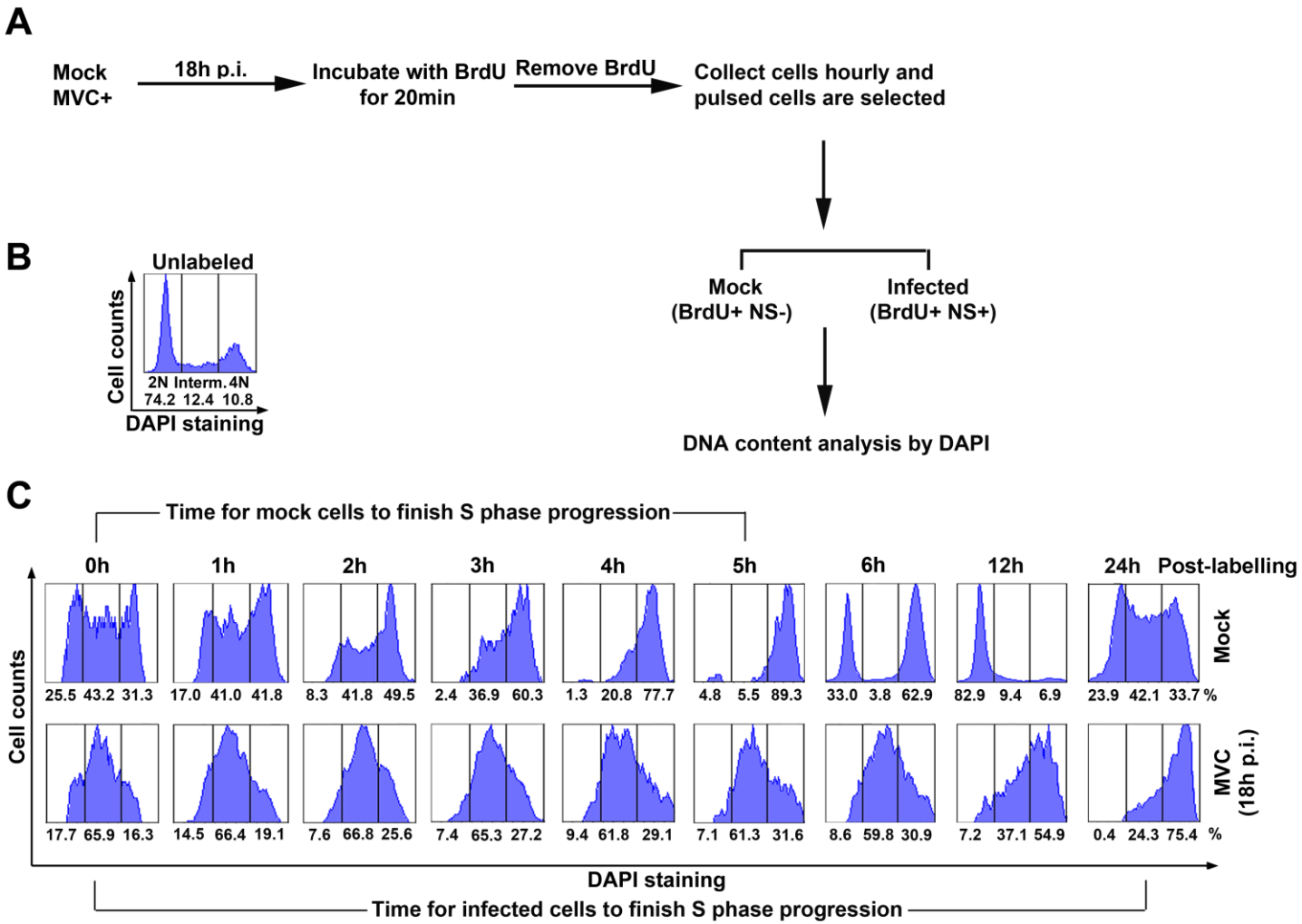
A
Mock
MVC+
18h p.i.
Incubate with BrdU for 20min
Remove BrdU
Collect cells hourly and pulsed cells are selected
Mock (BrdU+ NS-)
Infected (BrdU+ NS+)
DNA content analysis by DAPI
B
Unlabeled
Cell counts
2N Interm. 4N
74.2 12.4 10.8
DAPI staining
C
Time for mock cells to finish S phase progression
0h
1h
2h
3h
4h
5h
6h
12h
24h
Post-labelling
Mock
25.5 43.2 31.3
17.0 41.0 41.8
8.3 41.8 49.5
2.4 36.9 60.3
1.3 20.8 77.7
4.8 5.5 89.3
33.0 3.8 62.9
82.9 9.4 6.9
23.9 42.1 33.7 %
MVC (18h p.i.)
17.7 65.9 16.3
14.5 66.4 19.1
7.6 66.8 25.6
7.4 65.3 27.2
9.4 61.8 29.1
7.1 61.3 31.6
8.6 59.8 30.9
7.2 37.1 54.9
0.4 24.3 75.4 %
Cell counts
DAPI staining
Time for infected cells to finish S phase progression

Figure 3. MVC replication delays host cell S phase progression.

(A) Diagram of BrdU pulsing assay. WRD cells were infected with MVC or mock-infected. At 18h p.i., infected cells were incubated with BrdU for 20 min. After removing BrdU, cells were taken every hour as indicated in panel C. The cells were treated with HCl and then co-stained with an anti-NS1 antibody, an anti-BrdU antibody and DAPI for flow cytometry analysis. (B&C) DNA content analysis. DNA content was gated as 2N, 4N, and intermediate (Interm.; between 2N and 4N) in unlabeled cells based on DAPI staining (B), which was used as a reference to gate labeled cells with 2N, 4N and intermediate DNA content (C). Numbers under histograms show percentages of the cell population in each gate.

MVC hijacks host cellular DNA replication factors for viral DNA replication.

S phase is critical for parvoviruses to hijack the cellular replication machinery [5,11,13]. Previous studies on MVM and H-1 parvovirus have shown that the DNA replication factors PCNA (proliferating cell nuclear antigen), RFC1 (replication factor C 1), cyclin A, pol α and pol δ were recruited into the viral DNA replication compartments during infection [111,263]. Since MVC infection delays S phase progression, we assessed the localization of these DNA replication factors in the nuclei of infected cells. At 18h p.i., PCNA, RFC1, pol δ and cyclin A co-localized with MVC NS1 (Fig. 4A), suggesting that these replication factors were hijacked for viral DNA synthesis in the environment of prolonged S phase. Notably, the level of RFC1, a component of the clamp loader RFC complex that drives PCNA and polymerase loading onto the replication fork, disappeared gradually in the viral DNA replication centers during infection (Fig. 4A, RFC1). Western blot analysis confirmed that the total RFC1 level was significantly reduced at 18h and 24h p.i. (Fig. 4B). The levels of other replication factors, such as cyclin A and PCNA, were also decreased but to a lesser extent than that of RFC1.

Since ATM signaling-mediated intra-S phase arrest has been reported to be involved in inhibition of cellular DNA replication during S phase [163,250–253], and since ATM signaling is also required for MVC replication [30], we assessed the protein levels of these replication factors in ATM-inactivated infected cells. The reduction in the replication factors was obviously diminished by an ATM-specific inhibitor, KU55933 [151] (Fig. 4B), indicating that the reduction is dependent on ATM signaling.

Taken together, these results further confirm that S phase is required for MVC DNA replication. MVC infection not only creates a prolonged S phase environment for hijacking cellular DNA replication factors, but also reduces the overall levels of cellular DNA replication factors to inhibit cellular DNA synthesis. Since the reduction in replication factors was blocked by

an ATM-specific inhibitor, we hypothesized that ATM signaling may play a critical role in the inhibition of cellular DNA synthesis that contributes to the delay in S phase progression and to the intra-S phase arrest [145,241].

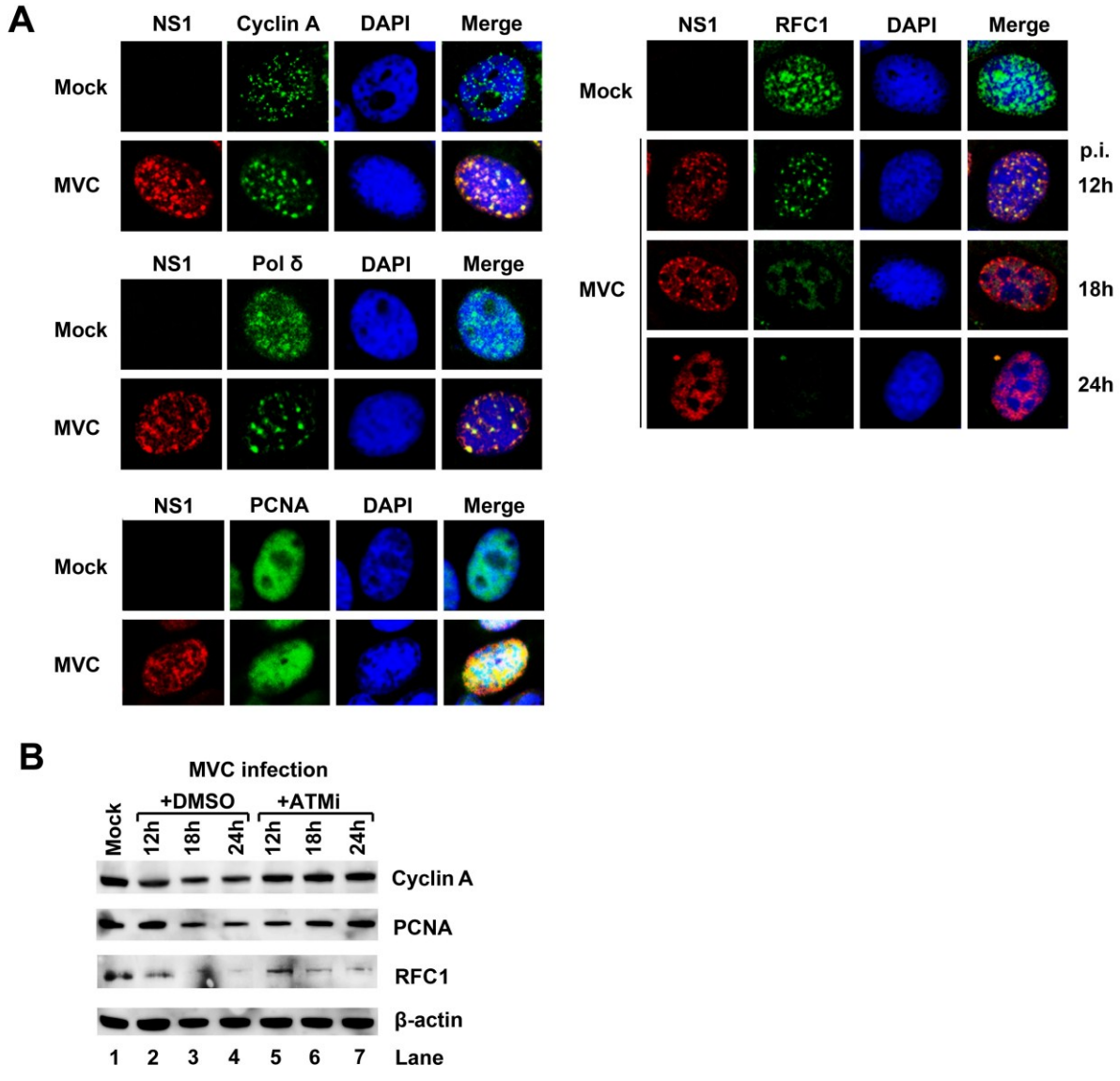
A
NS1
Cyclin A
DAPI
Merge
Mock
MVC
NS1
Pol δ
DAPI
Merge
Mock
MVC
NS1
PCNA
DAPI
Merge
Mock
MVC
NS1
RFC1
DAPI
Merge
Mock
MVC
p.i.
12h
18h
24h
B
MVC infection
+DMSO
+ATMi
Mock
12h
18h
24h
12h
18h
24h
Cyclin A
PCNA
RFC1
β-actin
1 2 3 4 5 6 7
Lane

Fig. 4. MVC hijacks host DNA replication factors for viral DNA replication.

(A) Immunofluorescence staining of cellular DNA replication factors. At 18h p.i., mock- and MVC-infected cells were fixed and stained with the indicated antibodies and DAPI. For RFC1 staining, infected cells were also analyzed at 12h and 24h p.i. **(B) Western blot analysis of cellular DNA replication factors.** Mock- and MVC-infected cells were either treated with ATM inhibitor KU55933 (ATMi) or DMSO control. At the indicated times p.i., the cells were collected and analyzed by Western-blot using antibodies against proteins as indicated.

ATM signaling regulates MVC infection-induced intra-S phase arrest.

To further examine the correlation between S phase arrest and ATM signaling, we pulse-chased infected cells with BrdU, and analyzed BrdU-labeled cells under denaturation for expression of γH2AX, which is induced by ATM activation during MVC infection [30]. As shown in Fig. 5A, nearly all γH2AX-positive cells were also BrdU-positive, suggesting that ATM activation correlates with the infection-induced S phase arrest, whereas treatment with an ATM-specific inhibitor blocked this correlation (Fig. 5A, MVC/ATMi). As a control, treatment with the ATM inhibitor did not change the cell cycle pattern in mock-infected cells (Fig. 5A, Mock/ATMi).

To define the function of ATM signaling in the MVC infection-induced intra-S phase arrest better, we examined the cell cycle status of infected cells treated with the ATM inhibitor or DMSO (as a control). In ATM inhibitor-treated groups, the population of the cells in S phase was almost reduced to the level of mock-infected cells (Fig. 5B). Thus, inhibition of ATM signaling significantly blocked the infection-induced S phase arrest. These results strongly suggest that the S phase arrest, which occurs in replicating cells, is ATM activation-dependent. Hence, we conclude that the MVC infection-induced S phase arrest mimics the intra-S phase arrest elicited by cellular DSBs. Inhibition of the S phase arrest by the ATM inhibitor significantly blocked viral DNA replication (Fig. 5C), which is consistent with our previous observations [30].

Altogether, these results show that MVC infection-induced S phase arrest is regulated by ATM signaling, and is the intra-S phase arrest. Importantly, in addition to UV-, chemical- or irradiation-induced intra-S phase arrest, our results supply a *de novo* example that replication of a DNA virus is able to induce the intra-S phase arrest that plays an essential role in viral DNA replication.

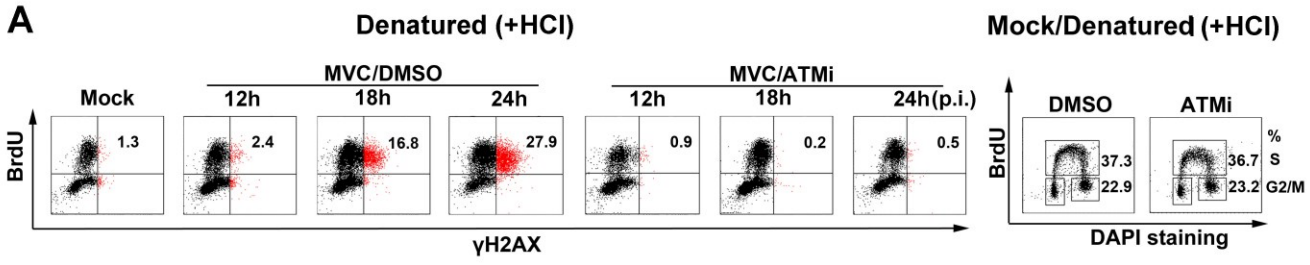
A
Denatured (+HCl)
Mock/Denatured (+HCl)
MVC/DMSO
MVC/ATMi
Mock
12h
18h
24h
12h
18h
24h(p.i.)
1.3
2.4
16.8
27.9
0.9
0.2
0.5
BrdU
γH2AX
DMSO
ATMi
37.3
22.9
36.7
23.2
%
S
G2/M
DAPI staining

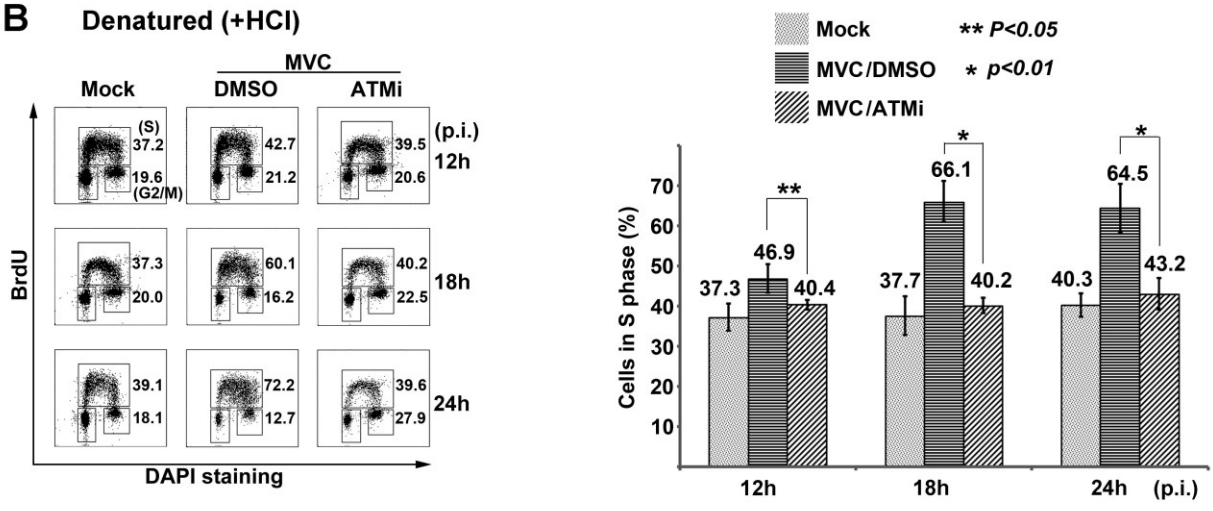
B
Denatured (+HCl)
MVC
Mock
DMSO
ATMi
(p.i.)
(S)
37.2
19.6
(G2/M)
42.7
21.2
39.5
20.6
12h
37.3
20.0
60.1
16.2
40.2
22.5
18h
39.1
18.1
72.2
12.7
39.6
27.9
24h
BrdU
DAPI staining
Mock
MVC/DMSO
MVC/ATMi
** P<0.05
* p<0.01
Cells in S phase (%)
37.3
46.9
40.4
37.7
66.1
40.2
40.3
64.5
43.2
12h
18h
24h
(p.i.)

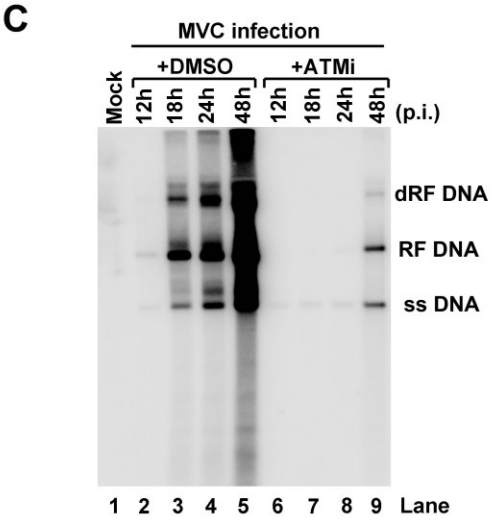
C
MVC infection
+DMSO
+ATMi
Mock
12h
18h
24h
48h
12h
18h
24h
48h
(p.i.)
dRF DNA
RF DNA
ss DNA
1 2 3 4 5 6 7 8 9 Lane

Figure 5. MVC infection-induced S phase arrest is regulated by ATM signaling.

(A&B) Flow cytometry analysis of DDR. WRD cells were infected with MVC or mock-infected, and were treated with ATMi or DMSO. At the indicated times p.i., the cells were incubated with BrdU for 1h. (A) Labeled cells were treated with HCl and then co-stained with anti-γH2AX and anti-BrdU antibodies for flow cytometry analysis. Numbers in each histogram show percentages of both BrdU- and γH2AX-positive cells. A cell cycle analysis of ATMi-treated mock-infected cells is shown on the right side. Treated cells were co-stained with an anti-BrdU antibody and DAPI. Numbers show percentages of cells in S phase (upper) and G2/M phase (lower), respectively. (B) Labeled cells were treated with HCl, then co-stained with an anti-BrdU antibody and DAPI for cell cycle analysis. The whole cell population in S phase, either treated with ATMi or DMSO, and mock-infected cells, was quantified at the indicated times p.i., and is shown as mean ± standard deviation. *P* values were determined using Student's t-test. (C) Southern blot analysis of viral DNA replication. MVC-infected cells either treated with DMSO control or ATMi were collected for preparation of Hirt DNA at the indicated times p.i. Samples were analyzed by Southern blot. Mock-infected cells were used as a negative control.

MVC infection-induced intra-S phase arrest is p53-independent.

ATM-dependent accumulation of p53 plays a pivotal role in regulating G1 phase arrest to block cellular DNA synthesis following DNA damage [264]. It has also been reported that p53 is involved in MVM NS1-mediated S phase arrest [17]. In addition, our previous study also showed that p53 was phosphorylated at serine 15 in the late stage of MVC infection [30]. To explore whether p53 activation plays a role in MVC infection-induced intra-S phase arrest, we assessed the cell cycle pattern and viral DNA replication of MVC-infected cells knocked down p53. We confirmed that p53 was phosphorylated at serine 15 at 18h p.i. (Fig. 6A). Transfection of either p53 siRNA or ATM siRNA reduced p53 phosphorylation to the background level (Fig. 6A), indicating that p53 was phosphorylated by ATM signaling during MVC replication. However, while knockdown of ATM significantly reduced the cell population in S phase, knockdown of p53 did not change the cell population in S phase (Fig. 6B). In parallel, knockdown of ATM but not of p53 significantly blocked MVC DNA replication (Fig. 6C).

Taken together, we conclude that p53 is not involved in MVC infection-induced intra-S phase arrest. This result is also consistent with the notion that p53 is not associated with the intra-S phase arrest induced by cellular DNA damage [145].

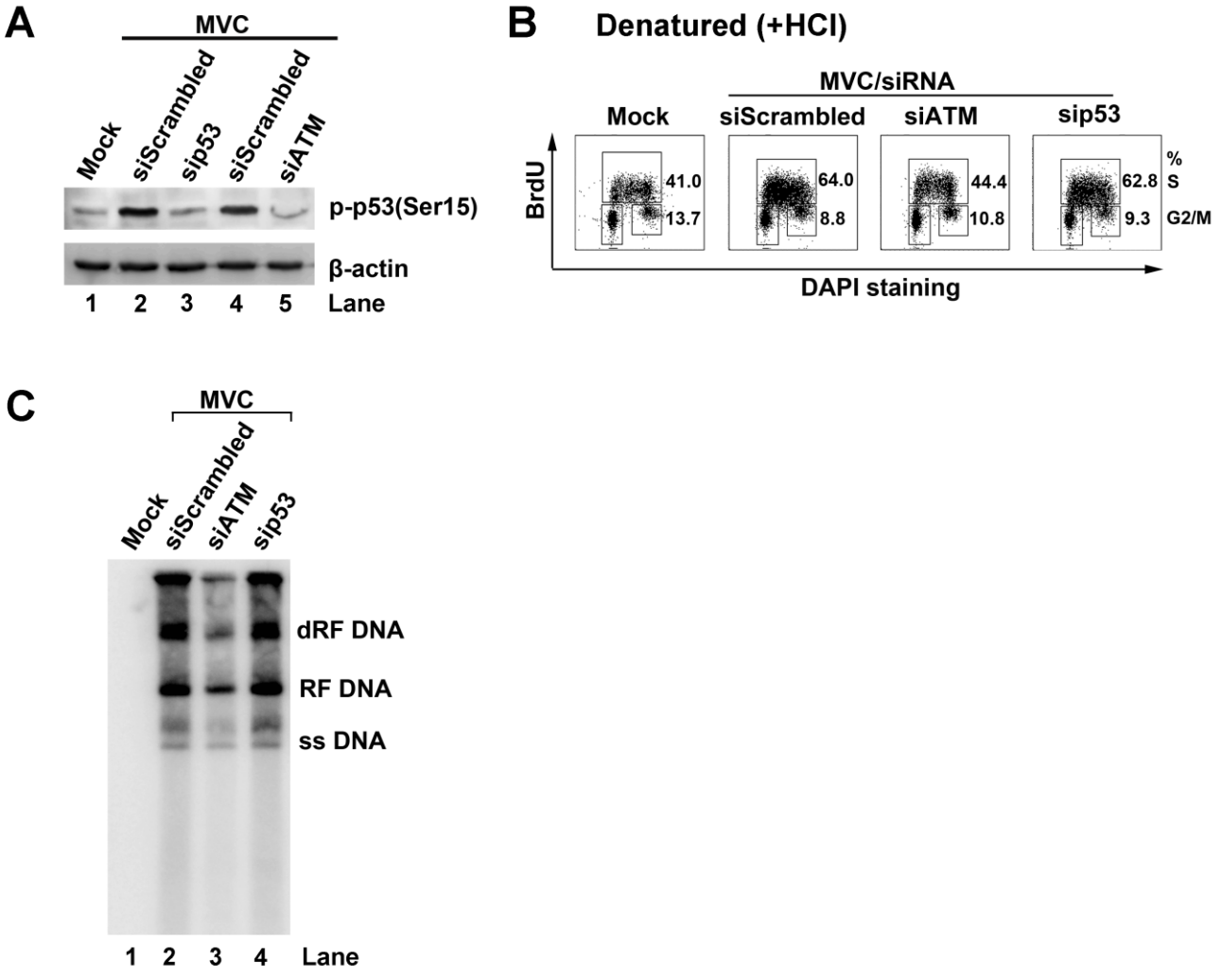
A
MVC
Mock
siScrambled
sip53
siScrambled
siATM
p-p53(Ser15)
β-actin
1 2 3 4 5
Lane
B
Denatured (+HCl)
MVC/siRNA
Mock
siScrambled
siATM
sip53
BrdU
41.0
13.7
64.0
8.8
44.4
10.8
62.8
9.3
%
S
G2/M
DAPI staining
C
MVC
Mock
siScrambled
siATM
sip53
dRF DNA
RF DNA
ss DNA
1 2 3 4
Lane

Figure 6. p53 is dispensable for MVC infection-induced S phase arrest.

WRD cells were transfected with scrambled siRNA (siScrambled) control, ATM siRNA (siATM), and p53 siRNA (sip53), and then infected with MVC. (A) Western blot analysis of phosphorylated p53. At 18h p.i., mock- and MVC-infected cells were collected and analyzed by Western blot for p53 phosphorylated at serine 15, p-p53(Ser15). The same membrane was reprobed with β-actin. (B) Flow cytometry analysis of the cell cycle. At 18h p.i., mock- or MVC-infected cells were incubated with BrdU for 1h. Labeled cells were treated with HCl and co-stained with an anti-BrdU antibody and DAPI, and then analyzed by flow cytometry. Numbers show percentages of cells in S phase and G2/M phase in each histogram. (C) Southern blot analysis of viral DNA repletion. At 18h p.i., mock- or MVC-infected cells were collected at the indicated times p.i., and Hirt DNA was extracted for Southern blot analysis.

SMC1 plays a key role in MVC infection-induced intra-S phase arrest.

As a well-established intra-S phase checkpoint protein, SMC1 is a downstream effector of the ATM signaling pathway sensed by the MRN complex [163]. We have shown previously that the MRN complex was recruited to the viral replication compartments, and that SMC1 was phosphorylated at serine 957 during MVC infection [30]. Therefore, we decided to assess the role of SMC1 in the MVC-induced intra-S phase arrest.

We observed that SMC1 was phosphorylated during early infection (Fig. 7A). Next, we next knocked down approximately 60% of the endogenous SMC1 (Fig. 7B), at which level the regular cell cycle pattern was not altered (Fig. 7C, Mock). Notably, knockdown of SMC1 caused a 14, 16, and 20% decrease in the cell population in S phase at 12h, 18h and 24h p.i., respectively (Fig. 7C). The cell cycle patterns of SMC1 siRNA (siSMC1)-treated groups at 12h and 18h p.i. were close to those of the mock groups. In addition, the reduction in the intra-S phase arrest caused by SMC1 knockdown significantly blocked MVC DNA replication (Fig. 7D).

Collectively, these results strongly suggest that SMC1 plays a key role in inducing the intra-S phase arrest during MVC infection, and that repression of viral DNA replication by SMC1 knockdown is likely the direct outcome of the abrogation of the intra-S phase checkpoint function of SMC1.

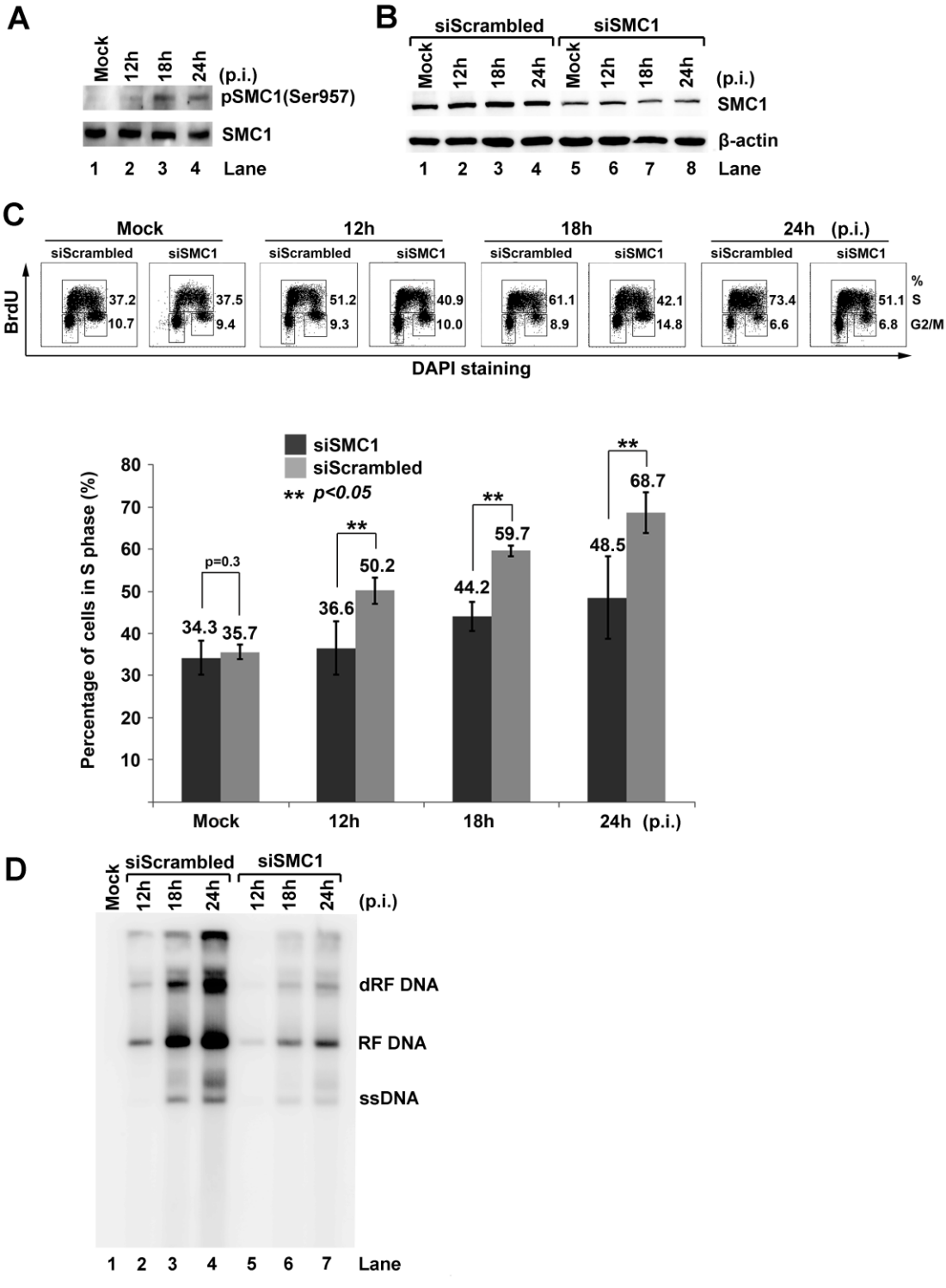
A
Mock
12h
18h
24h
(p.i.)
pSMC1(Ser957)
SMC1
1 2 3 4 Lane
B
siScrambled
siSMC1
Mock
12h
18h
24h
Mock
12h
18h
24h
(p.i.)
SMC1
β-actin
1 2 3 4 5 6 7 8 Lane
C
Mock
12h
18h
24h (p.i.)
siScrambled
siSMC1
BrdU
37.2
10.7
37.5
9.4
51.2
9.3
40.9
10.0
61.1
8.9
42.1
14.8
73.4
6.6
51.1
6.8
%
S
G2/M
DAPI staining
siSMC1
siScrambled
** p<0.05
Percentage of cells in S phase (%)
p=0.3
34.3
35.7
**
36.6
50.2
**
44.2
59.7
**
48.5
68.7
Mock
12h
18h
24h (p.i.)
D
Mock
siScrambled
siSMC1
12h
18h
24h
12h
18h
24h
(p.i.)
dRF DNA
RF DNA
ssDNA
1 2 3 4 5 6 7 Lane

Figure 7. Knockdown of SMC1 blocks MVC infection-induced intra-S phase arrest.

(A) Western blot analysis of SMC1 expression. WRD cells were infected with MVC. At the indicated times pi, the cells were collected and analyzed for expression of SMC1 and phosphorylated SMC1 at serine 957, p-SMC1(Ser957). Mock-infected cells were used as a control. (B-D) Knockdown of SMC1 reduced cell population in S phase and viral DNA replication. WRD cells were transfected with siRNA control (siScrambled) or SMC1 siRNA (siSMC1). At 2 days post-transfection, the cells were mock- or MVC-infected. At the indicated times p.i., cells were analyzed as follows. (B) One third of the cells were collected and analyzed for SMC1 by Western blotting. (C) One third of the cells were incubated with BrdU for 1h, denatured by HCl, and co-stained with an anti-BrdU antibody and DAPI for flow cytometry analysis. Numbers show percentages of the cell population in S phase and G2/M phase, respectively. The statistical analysis of the percentage of cells in S phase from three independent experiments is shown. Data are shown as mean ± standard deviation. *P* values were determined using Student's t-test. (D) One third of the cells were collected for Hirt DNA extraction and Southern blot analysis.

Phosphorylation of SMC1 at serines 957 and 966 is essential for the intra-S phase arrest induced during MVC infection.

Since phosphorylation of SMC1 at serines 957 and 966 is important for the checkpoint function of SMC1 [250], we assessed their role in the intra-S phase arrest induced during MVC infection. We observed that phosphorylated SMC1 co-localized with MVC NS1 during early infection (Fig. 8A). To test whether SMC1 phosphorylation at serines 957 and 966 is required for the intra-S phase arrest, endogenous SMC1 was replaced by ectopic expression of a wild-type human SMC1 ($hSMC1^{wt}$) or hSMC1 mutated at serines 957 and 966. Canine SMC1 mRNA (XM_538049.3) and human SMC1 (NM_006306.2) encode an identical SMC1 protein sequence [250]. The majority of endogenous SMC1 was complemented by $hSMC^{wt}$ (Fig. 8B, $hSMC1^{wt}$), which nearly fully restored the function of SMC1 in inducing the intra-S phase arrest (Fig. 8C, $hSMC1^{wt}$). A SMC1 protein band, shown by an arrow in Fig. 8B, at a position lower than the size of the endogenous SMC1 in transfected cells, is likely an isoform of the transfected human SMC1-encoding gene. Notably, while a dominant-negative form of SMC1 [250], termed $hSMC1^{(S957A/S966A)}$, was used to complement the lack of endogenous SMC1 in SMC1-knockdown cells, it was able to block approximately 17% of the cell population in S phase (Fig. 8C), indicating that the intra-S phase arrest is blocked by this dominant-negative mutant. Thus, these results suggest that the phosphorylation of SMC1 at serines 957 and 966 is necessary for the full function of SMC1 as an intra-S phase checkpoint during MVC infection.

Taken together, our results provide evidence that replication of MVC triggers SMC1 phosphorylation, which functions as a checkpoint protein to induce the intra-S phase arrest of the host cells.

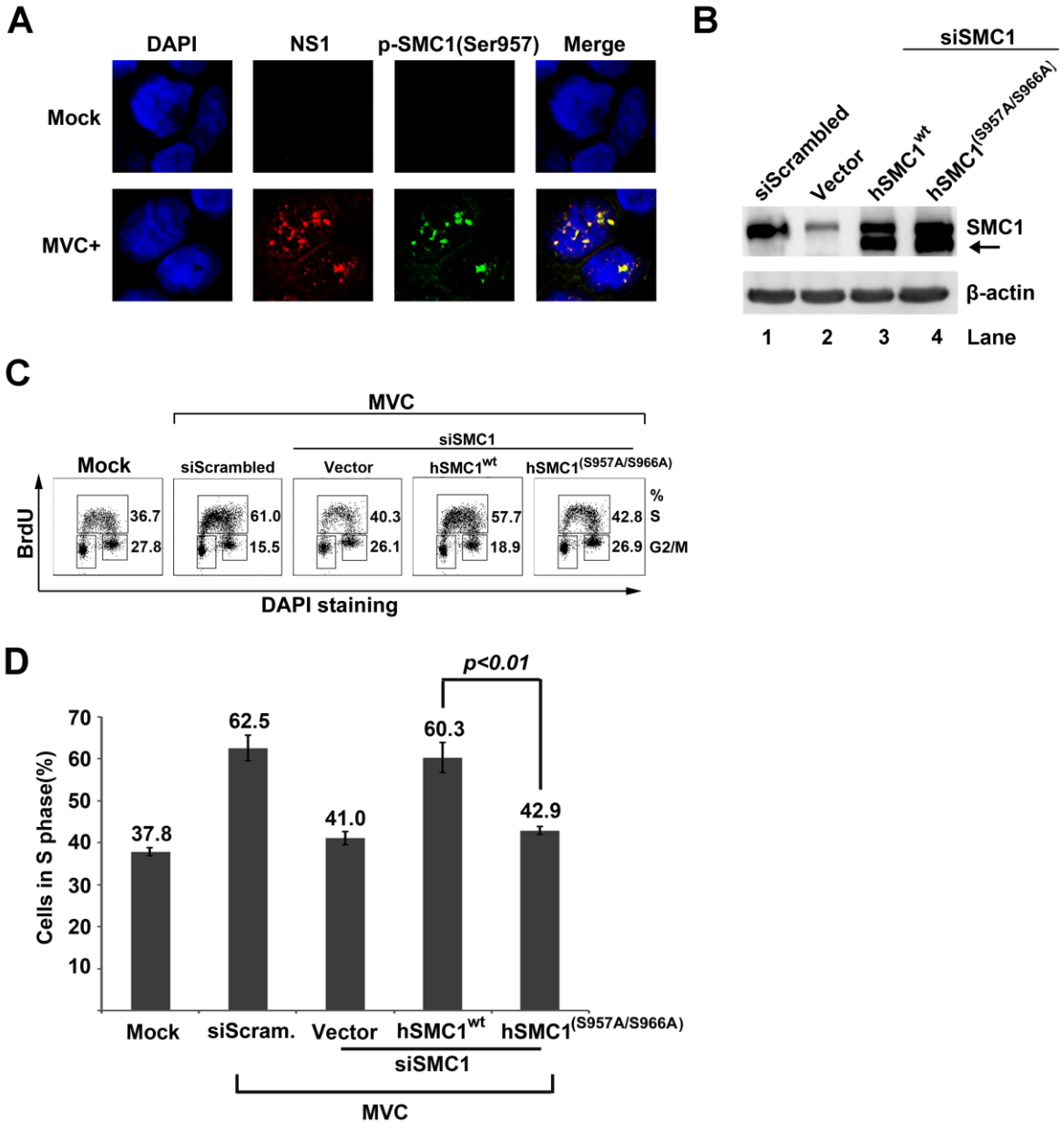
A
DAPI
NS1
p-SMC1(Ser957)
Merge
Mock
MVC+
B
siSMC1
siScrambled
Vector
hSMC1wt
hSMC1(S957A/S966A)
SMC1
β-actin
1
2
3
4
Lane
C
MVC
siSMC1
Mock
siScrambled
Vector
hSMC1wt
hSMC1(S957A/S966A)
BrdU
36.7
27.8
61.0
15.5
40.3
26.1
57.7
18.9
42.8
26.9
%
S
G2/M
DAPI staining
D
p<0.01
Cells in S phase(%)
70
60
50
40
30
20
10
37.8
62.5
41.0
60.3
42.9
Mock
siScram.
Vector
hSMC1wt
hSMC1(S957A/S966A)
siSMC1
MVC

Figure 8. Complementation of endogenous SMC1 with an SMC1 dominant-negative mutant (hSMC1$^{(S957A/966A)}$) rescues MVC infection-induced intra-S phase arrest.

(A) Immunofluorescence analysis of SMC1 phosphorylation. WRD cells were seeded on chamber slides 24h prior to MVC infection. At 18h p.i., cells were fixed and co-stained with an anti-MVC NS1 antibody, an anti-p-SMC1(Ser957) antibody and DAPI. Confocal images were taken at a magnification of ×100. Mock-infected cells were used as a negative control. (B-D) Analysis of SMC1 complementation with hSMC1$^{(S957A/S966A)}$ on the cell cycle. WRD cells were transfected twice with siScrambled or siSMC1 siRNA, and subsequently transfected with an empty vector, a plasmid expressing wild-type human SMC1A (hSMC1^{wt}) or dominant-negative mutant hSMC1$^{(S975A/S966A)}$. (B) At 24h post-transfection, cells were collected and analyzed by Western blotting using an anti-SMC1 antibody. The same membrane was reprobed for β-actin. Arrow shows a potential isoform of human SMC1. (C) At 24h post-transfection, cells were infected with MVC or mock-infected. Infected cells were incubated with BrdU for 1h at 18h p.i. Then cells were collected, treated with HCl, and co-stained with an anti-BrdU antibody and DAPI for cell cycle analysis by flow cytometry. Numbers shown in each histogram are percentages of the cell population in S phase and G2/M phase, respectively, as indicated. (D) The statistical analysis of the percentage of cells in S phase, performed from three independent experiments, is shown. Data are shown as mean ± standard deviation. *P* values were determined using Student's t-test.

Replicating viral genome, but not damaged cellular DNA, induces intra-S phase arrest during MVC infection.

Previous studies of DDR induced by autonomous parvoviruses, MVC, MVM, and B19V have demonstrated that viral DNA replication, but not individual viral protein, triggers a DDR [29,30,101]. To further examine the cause of MVC infection-induced DDR, we asked whether virus infection is able to cause cellular DNA damage. To this end, we performed a Comet assay, which is commonly used for the detection of both DSBs and SSBs of chromosome DNA [265–268]. H_2O_2 treatment, as a control, was able to cause severe damage to cellular DNA as shown by the fact that nearly all the cells were Comet-positive (DNA-damaged); however, neither mock- nor MVC-infected cells contained Comet-positive cells (Fig. 9A). These results suggest that the DDR signaling induced during MVC infection comes from viral DNA or its replicative intermediate molecules, rather than from cellular DNA.

To determine whether viral DNA replication is required for the intra-S phase arrest induced during early infection, we transfected cells with a wild-type infectious clone of MVC (pIMVC) and its derivative mutants, pMVC(NSCap), or pIMVC(NP-) and pIMVC(VP1/2-), which do not have the terminal hairpins or express NP1 and capsid proteins, respectively [118,119]. pMVC(NSCap) does not replicate but expresses all viral proteins, pIMVC(NP-) replicates very poorly (approximately 50-fold decrease compared with the wild-type), and pIMVC(VP1/2-) replicates at an intermediate level without production of ssDNA [30,118]. In addition, NS1 and NP1 (Flag-tagged) were expressed individually. Transfected cells were selected by either NS1 or Flag-tag and analyzed for the cell cycle pattern. Most of the cells transfected with pIMVC and pIMVC(VP1/2-), which replicate viral DNA, were accumulated in S phase, while cells transfected with other plasmids that were replication-incompetent or inefficient [118], failed to arrest cells in S

phase, though viral proteins were expressed (Fig. 9B). These results indicate that the replicating viral genome, but not viral proteins, was the cause of the intra-S phase arrest.

The MRN complex is not only the sensor of DDR, but also the initiator of the ATM-SMC1 signaling-induced intra-S phase arrest [36,163,250]. We hypothesized that the replicating viral DNA is likely sensed by the MRN complex as damaged DNA, which activates the DDR signaling and thereafter the intra-S phase arrest. To prove this, we checked the localization of the MRN complex in the nuclei of MVC-infected cells. At 18h p.i., a time point at which MVC DNA actively replicates, Mre11, Rad50 and phosphorylated NBS1 (p-Nbs1) all co-localized within the viral DNA replication centers as shown with anti-BrdU staining (Fig. 9C). Furthermore, we performed a BrdU-IP assay to determine whether the newly synthesized viral ssDNA/intermediates was associated with the MRN complex. Notably, we were able to precipitate Mre11, the DNA binding component of the MRN complex [269], from BrdU-incorporated MVC-infected cells but not from mock-infected cells (Fig. 9D, lane 4).

Collectively, we have provided evidence that cellular DNA is not damaged in MVC-infected cells, and that the viral DNA replication process is critical for the intra-S phase arrest induced during MVC infection. More importantly, the replicating viral DNA is able to mimic damaged cellular DNA, perhaps due to aberrant DNA structures, to recruit the MRN complex, which in turn activates ATM signaling and initiates the intra-S phase arrest.

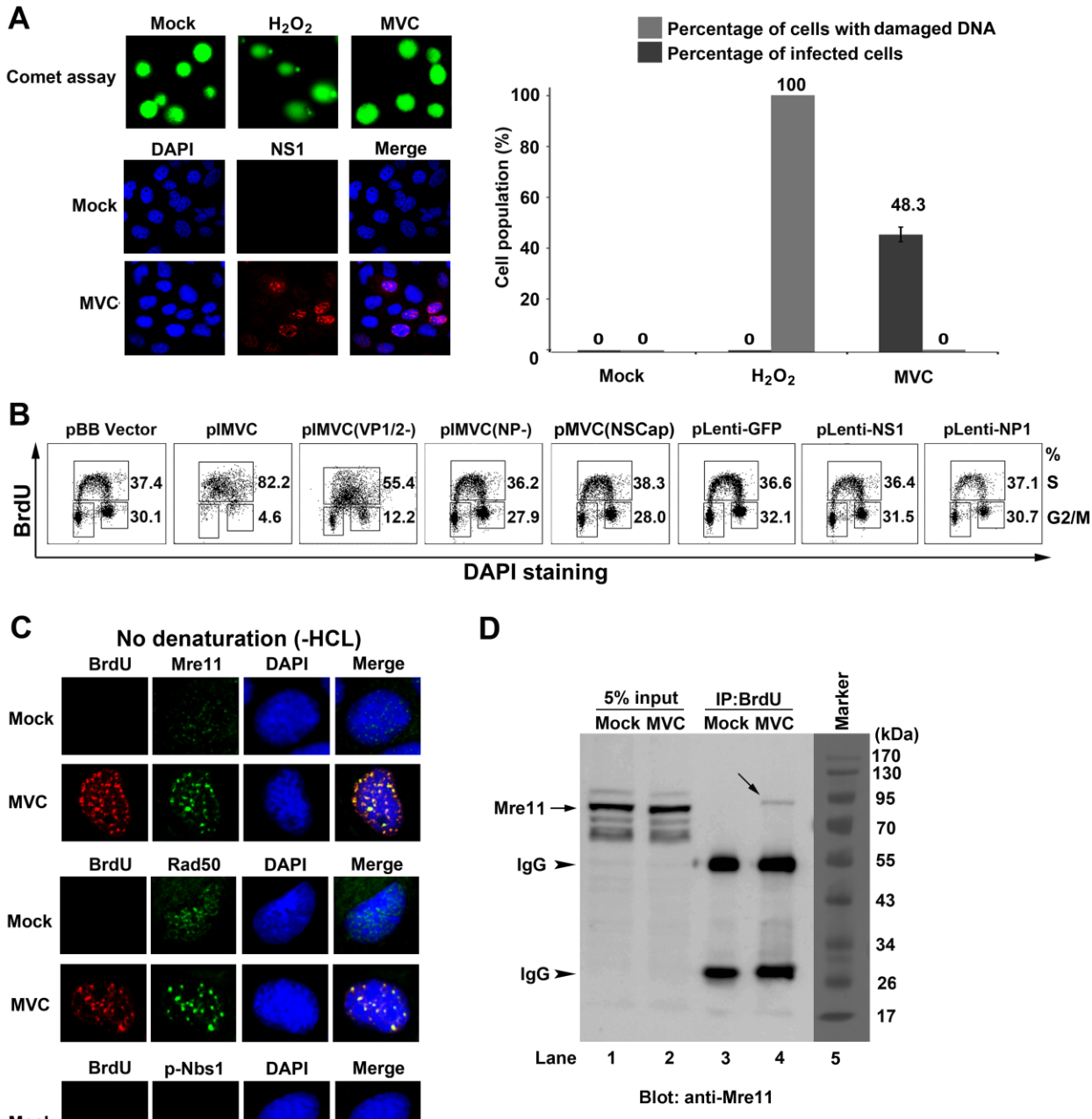
A
Mock
H2O2
MVC
Comet assay
DAPI
NS1
Merge
Mock
MVC
Percentage of cells with damaged DNA
Percentage of infected cells
Cell population (%)
100
48.3
0
Mock
H2O2
MVC
B
pBB Vector
pIMVC
pIMVC(VP1/2-)
pIMVC(NP-)
pMVC(NSCap)
pLenti-GFP
pLenti-NS1
pLenti-NP1
BrdU
37.4
30.1
82.2
4.6
55.4
12.2
36.2
27.9
38.3
28.0
36.6
32.1
36.4
31.5
37.1
30.7
%
S
G2/M
DAPI staining
C
No denaturation (-HCL)
BrdU
Mre11
DAPI
Merge
Mock
MVC
BrdU
Rad50
DAPI
Merge
Mock
MVC
BrdU
p-Nbs1
DAPI
Merge
Mock
MVC
D
5% input
IP:BrdU
Mock MVC
Mock MVC
Marker
(kDa)
170
130
95
70
55
43
34
26
17
Mre11
IgG
IgG
Lane 1 2 3 4 5
Blot: anti-Mre11

Figure 9. MVC infection-induced DDR and intra-S phase arrest are dependent on replicating viral DNA.

(A) Comet assay analysis. WRD cells were mock- or MVC-infected. At 18h p.i., half of the cells were collected and analyzed by Comet assay; the other half of the cells were fixed and co-stained with an anti-NS1 antibody and DAPI to quantify the percentage of infected (NS1+) cells by immunofluorescence analysis. Confocal images were taken at a magnification of ×40. A statistical analysis of the percentage of cells with damaged DNA was performed from three independent Comet assays. Data are shown as mean ± standard deviation. (B) Flow cytometry analysis of the cell cycle in transfected cells. WRD cells were transfected with the indicated plasmids for 18h, and then were incubated with BrdU for 1h. The cells were collected, treated with HCl and co-stained with DAPI, anti-BrdU and anti-NS1 antibodies (for pIMVC and mutant derivatives) or an anti-Flag antibody (for pLenti-based plasmids) for flow cytometry analysis. (C&D) The MRN complex is associated with replicating viral DNA. Mock- or MVC-infected cells were incubated with BrdU for 1h at 18h p.i. (C) Immunofluorescence analysis of the MRN complex. The cells were fixed and co-stained with the indicated antibodies and DAPI. Confocal images were taken at a magnification of ×100. (D) Co-immunoprecipitation with an anti-BrdU antibody. The BrdU-labeled cells were lysed and centrifuged. The supernatant containing BrdU-labeled viral genome was immunoprecipitated with an anti-BrdU antibody. Immunoprecipitated samples were blotted with an anti-Mre11 antibody. An amount of lysate equal to 5% was used as an input control for each sample. Arrows show Mre11 bands, whereas arrowheads show the immunoprecipitated light and heavy chains of the IgG antibody.

Discussion

This study demonstrated that autonomous parvovirus infection induces the intra-S phase arrest to delay S phase progression and to hijack cellular DNA replication factors for viral DNA replication. The intra-S phase arrest is mediated by ATM signaling through phosphorylation of SMC1. The study also provided evidence that the autonomous parvovirus infection-induced DDR is elicited by replicating viral DNA, which is sensed by the MRN complex. Thus, our study provides, for the first time, a novel DNA replication model for autonomous parvovirus (Figure 10).

In this model, MVC DNA replication triggers intra-S phase arrest through the MRN-ATM-SMC1 pathway. The replicating viral DNA mimics damaged DNA that is sensed by the MRN complex. The intra-S phase arrest blocks cellular DNA synthesis and therefore prolongs S phase in infected cells, presumably through degradation or transcriptional regulation of DNA replication factors. By contrast, the MRN complex may coordinate DNA replication and repair factors through SMC1 activation to facilitate viral DNA synthesis. The feedback loop between viral DNA replication and the intra-S phase arrest plays an essential role in modulation of the cellular environment by MVC to make it conducive to viral DNA replication.

One of the important findings of our study is that S phase is required but not sufficient for autonomous parvovirus replication. It has been reported that DNA replication of MVM is strictly dependent on cellular factors expressed during S phase [9,11,111]. The basic replication machinery components, such as PCNA, RPA, pol α, pol δ, and cyclin A, all co-localized within the autonomous parvovirus-associated replication (APAR) bodies [111,263]. In vitro studies indicated that the cyclin A level directly affects MVM DNA replication efficiency [13] and that PCNA, RPA, and pol δ are essential for MVM DNA replication [171,270]; however, like many other DNA viruses, autonomous parvovirus infection blocks cellular DNA synthesis [8,16,17,113,271], which was thought to be due to competition for access to the cellular

replication machinery by viral DNA replication [8,271]. Hence, the S phase is essential for autonomous parvovirus DNA. Here we show that MVC DNA replicates poorly in ATM-specific inhibitor-treated cells which have normal S phase progression (Figure 4). Thus, we provide evidence that S phase is not sufficient for autonomous parvovirus DNA replication. We conclude that, in addition to the requirement that infected cells be in S phase, which supplies DNA replication factors, the intra-S phase arrest is necessary for autonomous parvovirus to compete with cellular DNA synthesis for its own DNA replication. We hypothesize that it is likely that the intra-S phase arrest facilitates the recruitment of replication factors through a DNA repair pathway, since intra-S phase coordinates DNA repair following DDR induced by damaged cellular DNA [143,145] as well as restarts DNA replication forks [242].

Inhibition of cellular DNA replication is a common strategy for DNA viruses to modulate the host cellular environment to make it conducive to viral DNA replication. The inhibition processes are often regulated by viral proteins that target the cellular DNA replication machinery. For instance, via viral protein pUL117, human cytomegalovirus (HCMV) blocks host DNA synthesis by delaying the accumulation of the mini-chromosome maintenance (MCM) complex proteins onto chromatin [255]. Human papillomavirus (HPV) inhibits host DNA replication by viral early protein E4-mediated suppression of cellular replication origin licensing [254]; however, polyomaviruses take advantage of DDR signaling to block cellular DNA synthesis. SV40 infection uses the ATR-Δp53-p21 pathway to down-regulate cyclin A-CDK2/1 activity, which forces the host to remain in S phase [272]; whereas polyomavirus strain RA has been shown to utilize ATM-SMC1 signaling to override cell cycle regulation and prolong S phase [186]. As a result, viral infection-triggered intra-S phase arrest slowed down cellular DNA synthesis; however, the intra-S phase arrest induced by polyomaviruses is largely regulated by the viral large T antigen [186,199,234,273]. In contrast, none of the MVC-encoded proteins are involved in cell cycle

regulation [121] (Figure 8). Therefore, we have identified, for the first time, a viral DNA replication-dependent intra-S phase arrest that is ATM-mediated.

The ATM-SMC1 pathway is intimately involved in slowing down the cellular DNA replication rate in response to DSBs [145]; however, how phosphorylated SMC1 interferes with cellular DNA replication remains unclear. At least in MVC infection-induced intra-S phase arrest, RFC1, which is a key component of the RFC complex that loads PCNA to replicating DNA [274,275], is a major target for down-regulation (Figure 3). Notably, during the very early phase of infection, RFC1 co-localized within the viral replication centers, and later disappeared from the centers when viral DNA was actively replicating. This led to hypothesize that RFC1 is required for the conversion of viral ssDNA to the double-stranded replicative form (RF DNA) (Figure 9, Step 1) upon virus infection. Nevertheless, the down-regulation of RFC1 during the intra-S phase arrest provides a candidate for linking SMC1 activation with down-regulation of cellular DNA replication. The function of RFC1 in MVC DNA replication and in SMC1-mediated intra-S phase arrest warrants further investigation.

Studies on virus infection-induced DDR have uncovered novel mechanisms underlying viral-host interaction [49,81]. Although early studies indicated that infection of most DNA viruses was able to create lesions on cellular DNA involving viral proteins [113,199,276–279], whether this is common and the major cause of the activation of DDR signaling is not clear. Our study has shown that MVC infection did not cause obvious damage to cellular DNA (Figure 8), hence the DNA damage signaling induced during MVC infection must come from viral DNA. We and others previously have shown that replication of autonomous parvovirus is required for triggering a DDR [29,30,101]. Here, we provide evidence, for the first time, that replicating viral genomes (or intermediates), mimic damaged cellular DNA (likely DSBs), which, in the case of autonomous parvovirus, likely involves the unique hairpin structures, thereby recruiting the MRN complex and

DDR proteins. However, due to the difficulty to isolate such intermediate DNA, we are not able to provide direct evidence to show that such DNA structures can directly induce DDR signaling. Nevertheless, in addition to the fact that the DNA damage sensor, the MRN complex, is directly associated with the replicating viral DNA, Nbs1 was phosphorylated in the viral replication centers (Figure 8), strongly suggesting that a DNA repair pathway followed by intra-S phase arrest is involved in MVC DNA replication. Interestingly, accumulating evidence has shown that DNA repair factors are localized in the replication compartments of many DNA viruses, for instance the homologous recombinational repair (HRR) factors are recruited into the replication centers of EBV, SV40, and HPV [173,199,235]. It was suggested that HRR factors might be recruited to repair DSBs on the viral genome in the viral replication compartments, but not for viral DNA replication. It is understandable that the DSB-initiated repair pathways of homologous recombination of nonhomologous end joining (NHEJ) are involved in the replication of DNA viruses whose genome is dsDNA since their replication often involves a step of circularization; however, DNA replication of autonomous parvoviruses, whose genome is ssDNA, follows a rolling-hairpin strategy of DNA replication which does not involve circularization of any replication intermediates [114]. The fact that SMC1, a cohesion protein of chromosome DNA, plays a key role in MVC DNA replication may also suggest that it maintains proper alignment of the parvoviral minichromosome [280,281] for terminal resolution of RF DNA [114], in addition to its role in the intra-S phase arrest. How these DNA repair factors accumulated in the viral replication centers facilitate viral DNA replication, in particular during autonomous parvovirus infection, remains unknown and is a central question in parvovirus DNA replication.

In summary, MVC infection triggers a MRN-ATM-SMC1-mediated intra-S phase arrest to create an S phase environment and to recruit the cellular DNA replication machinery, and perhaps the DNA repair machinery, to facilitate MVC DNA replication. Such a strategy may

represent a common feature of the DDR induced by many small DNA viruses, which are dependent on S phase for replication in host cells.

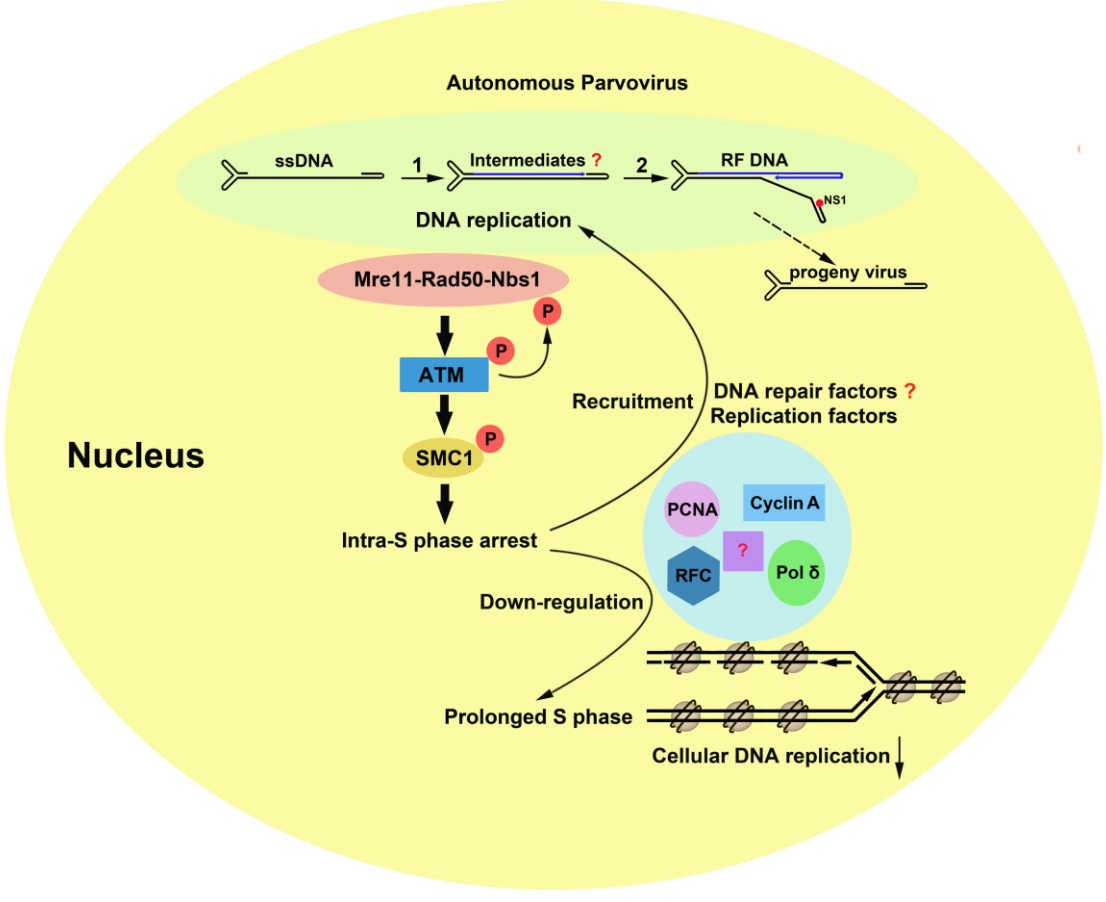
Autonomous Parvovirus
ssDNA
1
Intermediates ?
2
RF DNA
NS1
DNA replication
progeny virus
Mre11-Rad50-Nbs1
P
ATM
P
P
SMC1
Recruitment
DNA repair factors ?
Replication factors
Nucleus
PCNA
Cyclin A
?
RFC
Pol δ
Intra-S phase arrest
Down-regulation
Prolonged S phase
Cellular DNA replication

Figure 10. A proposed model for autonomous parvovirus DNA replication in the context of the intra-S phase arrest.

The proposed pathways utilized by autonomous parvovirus during replication are described in detail in the Discussion section. The question mark indicates steps not well understood.

Chapter 5

Conclusions and Discussion

Parvoviruses are widespread in different species and induce highly contagious diseases [1,2]. Human parvovirus B19V and HBoV1 are pathogens of life-threatening human diseases [124,230,231]. Unfortunately, there is currently no treatment for parvovirus infection-induced human diseases. Study of parvovirus infection-induced DDR has not only greatly improved our understanding of the basic replication mechanism of parvovirus, but has also revealed potential targets for the treatment of parvovirus-caused diseases. Moreover, parvovirus is the only virus type to introduce linear ssDNA into the host cell nucleus, therefore it is a unique *in vivo* model system to probe the mechanism of exogenous ssDNA-induced DDR.

Different parvovirus infection triggers different DDR signaling pathways. Both MVM and MVC activate the ATM signaling during their early and late stages of infection [29,30,112]. By contrast, B19V infection elicits a robust DDR with all the three PI3KKs phosphorylated [28]. The difference is likely due to their different genome structures and their host cells. Both MVM and MVC have asymmetric terminal repeats, which are different from those of B19V. The ITRs of B19V are similar to that of AAV2, which also triggers ATR activation when it is inactivated by UV [78,79]. Coinfection of AAV2 and HSV-1 also induces phosphorylation of all the three PI3KKs, although it is difficult to differentiate which pathway is activated by replication of AAV2 alone [69], since HSV-1 also interplays with the DDR machinery [71–73]. Moreover, the cell cycle pattern of B19V-infected cells differs from that of MVM- or MVC-infected cells. During early infection, MVM and MVC create a prolonged S phase environment to facilitate viral DNA replication [11,12,17,111,114]. By contrast, following B19V infection, infected cells quickly accumulated at the phase that had a 4N DNA content [15,18,100,101,282], which could be due to an arrest at

late S phase or G2/M phase. Such a difference in arresting the host cell cycle may result in activation of different DDR pathways [47].

Our study of MVC infection-induced DDR has revealed a novel model for parvovirus DNA replication. Early in *vivo* and *in vitro* studies of MVM DNA replication has indicated that S phase is required for parvovirus DNA replication [8–14], while some studies also noticed that the cellular replication rate is significantly reduced during parvovirus infection [16,17,113], indicating that a strategy is required for parvovirus to compete with host cellular DNA replication. Indeed, we observed that S phase is required but not sufficient for MVC DNA replication [30]. Treatment of an ATM-specific inhibitor did not perturb regular S phase progression, but significantly blocked viral DNA replication, suggesting that an ATM-dependent mechanism is essential to create a favorable microenvironment for MVC genome amplification. Further study demonstrates that MVC infection triggers an intra-S phase arrest that is dependent upon the ATM-SMC1 signaling pathway. The intra-S phase arrest not only blocks cellular DNA replication, but also delays S phase progression. Therefore, in the context of the intra-S phase arrest, MVC represses cellular DNA replication and continuously hijacks cellular DNA replication machinery. These findings have revealed the beneficial effects of the ATM activation on autonomous parvovirus DNA replication, and suggest a novel model for parvovirus DNA replication. Since the MVC genome shares 50-60% identity with HBoV1 [119], our study may also shed light on the HBoV1 replication mechanism as well as viral pathogenesis.

The parvovirus genome has the intrinsic ability to induce a DDR. Unlike many large DNA viruses which encode multiple viral proteins to interact with host cells, parvovirus only encodes 2-3 nonstructural proteins. The largest non-structural proteins of parvoviruses are conserved and essential for viral DNA replication. Although in some studies, the largest non-structural proteins have been shown to cause non-specific nicking of cellular DNA [10,65,113] , this is neither the

major cause of the DDR activation nor the driving force of S phase arrest, since the majority of the largest non-structural proteins colocalize with the viral DNA genome during active viral replication. In concert, expression of the MVC non-structural proteins failed to perturb the cell cycle pattern and induce a DDR [30,121]. As exogenous DNA, parvoviral genomes are aberrant from any cellular DNA structure. Our study indicates that the replicating MVC genome is associated with the MRN complex, which is not only the sensor for the activation of the ATM signaling, but also the initiator for the recruitment of many DNA repair factors [36,163,250]. It is likely that the MRN complex initially functions as an anti-virus device, as evidenced during coinfection of AAV with helper adenovirus [57]. However, this device is either destroyed by AAV through its helper virus [57], or hijacked for viral DNA replication during MVM and MVC infection [29,30]. The intra-S phase arrest also has a potential role to recruit DNA repair factors into the viral replication centers, resulting in a repair-dependent replication of parvovirial DNA [145,242,248]. Whether any downstream DNA repair factors of the MRN complex are recruited in the parvovirus DNA replication centers awaits further investigation.

Parvovirus infection-induced DDR contributes to viral infection-induced apoptosis. Parvovirus infection-induced cell death is directly associated with viral pathogenesis, e.g., hemolytic anemia caused by apoptosis of erythroid-lineage cells upon B19V infection [283,284]. Although several studies have revealed that non-structural proteins of parvoviruses, such as NS1 and 11-kDa proteins of B19V are able to trigger apoptosis [19,95,96], ectopical expression of individual non-structural proteins of MVC did not induce obvious cytopathic effects [121]. The role of DDR in apoptosis has been widely documented [39,227]. p53 plays a central role in coordinating DDR-induced cell cycle arrest, gene transcription and apoptosis [285]. Driven by the ATM kinase, p53 is phosphorylated at serine15 and 46, protecting p53 from the degradation by its negative regulator MDM2 [286,287]. The p53 protein regulates apoptosis through competition with DNA repair proteins for binding to exposed single-stranded regions of damaged DNA, and

transactivation of proapoptotic genes [288]. During infection of MVM, MVC and B19V, phosphorylation of p53 at serine 15 was observed [29,30,101]. However, p53 does not have a direct role in inducing cell cycle arrest during infection of these three viruses. Instead, knockdown of phosphorylated p53 during the late stage of MVC infection significantly blocked MVC infection-induced cell death [30]. Since our previous study has confirmed that MVC infection triggers a mitochondrion-mediated apoptosis [121], we conclude that MVC infection-induced cell death is regulated by the ATM-p53 mediated apoptosis. This observation has revealed a new strategy of parvovirus-induced cell death, which is critical for viral pathogenesis. Further studies are warranted to discern whether phosphorylation of p53 affects MVM and B19V infection-induced cell death.

Study of B19V infection-induced DDR has advanced our understanding of the B19V DNA replication mechanism as well as B19V infection-induced cell cycle arrest. As it is difficult to study B19V in human primary erythroid progenitor cells, very few cellular factors have been found to be involved in B19V DNA replication. We have identified that all three PI3KKs, along with many downstream effectors, co-localized to with the B19V replication centers [28]. More importantly, the ATR and DNA-PKcs signaling pathways contribute to B19V DNA replication through unclear mechanisms. The ATR signaling phosphorylates a number of proteins such as MCM (mini-chromosome maintenance proteins), RPA, PCNA and several DNA polymerases, to resume the replication of stalled replication forks [217]. Whether those downstream substrates of the ATR signaling are recruited to the B19V replication centers has not been studied. Surprisingly, although two checkpoint kinases, Chk1 and Chk2, were phosphorylated and co-localized with B19V replication centers, inhibition of them did not affect B19V infection-induced G2/M arrest [28]. By contrast, G2/M arrest turns out to be a direct outcome of B19V NS1 protein expression, which deregulates the E2F family of transcription factors [100]. The function of G2/M arrest during B19V infection is a mystery, since many other parvoviruses

take advantage of S phase arrest for productive virus infection [8–14]. It would be valuable to know whether the DDR signaling contributes to S phase (late S phase with a 4N DNA content) arrest during B19V infection.

Taken together, by using parvovirus as a model organism, we have probed the basic mechanism of the DDR induced by aberrant ssDNA. Our findings have greatly facilitated the understanding of the mechanism of parvovirus DNA replication, and have revealed new strategies by which parvovirus induces host cell cycle arrest and apoptosis. Our study also sheds light on the mechanisms by which other small DNA viruses induce a DDR. More importantly, our study will facilitate the identification of efficient anti-viral targets for the treatment of parvovirus-caused diseases.

Reference List

1. Bloom ME, Young N (2001) Parvoviruses. In: Knipe DM, editors. Fields Virology. Philadelphia: Lippincott Williams and Wilkins. pp. 2361-2379.

2. Bern KI, Parrish CR (2007) Parvoviruses. In: Knipe DM, Howley PM, Griffin DE, Lamb RA, Martin MA, editors. Fields Virology. Philadelphia: Lippincott Williams & Wilkins. pp. 2437-2477.

3. Tijssen P, Agbandje-McKenna M, Almendral JM, Bergoin M, Flegel TW, et al. (2011) Parvoviridae. In: King MQ, Adams MJ, Carstens E, Lefkowitz EJ, editors. Virus taxonomy: classification and nomenclature of viruses: Ninth Report of the International Committee on Taxonomy of Viruses. San Diego: Elsevier.

4. Ward P (2006) Replication of adeno-associated virus DNA. In: Kerr J, Cotmore SF, Bloom ME, Linden ME, Parrish CR, editors. The parvoviruses. London: Hodder Arnold. pp. 189-211.

5. Cotmore SF, Tattersall P (1987) The autonomously replicating parvoviruses of vertebrates. Adv Virus Res 33:91-174.: 91-174.

6. Hirt B (2000) Molecular biology of autonomous parvoviruses. Contrib Microbiol 4:163-77.: 163-177.

7. Qiu J, Yoto Y, Tullis GE, Pintel D (2006) Parvovirus RNA processing strategies. In: Kerr JR, Cotmore SF, Bloom ME, Linden ME, Parish CR, editors. Parvoviruses. London, UK: Hodder Arnold. pp. 253-274.

8. Oleksiewicz MB, Alexandersen S (1997) S-phase-dependent cell cycle disturbances caused by Aleutian mink disease parvovirus. J Virol 71: 1386-1396.

9. Deleu L, Pujol A, Faisst S, Rommelaere J (1999) Activation of promoter P4 of the autonomous parvovirus minute virus of mice at early S phase is required for productive infection. J Virol 73: 3877-3885.

10. Berthet C, Raj K, Saudan P, Beard P (2005) How adeno-associated virus Rep78 protein arrests cells completely in S phase. Proc Natl Acad Sci U S A 102: 13634-13639.

11. Wolter S, Richards R, Armentrout RW (1980) Cell cycle-dependent replication of the DNA of minute virus of mice, a parvovirus. Biochim Biophys Acta 607: 420-431.

12. Berns KI (1990) Parvovirus replication. Microbiol Rev 54: 316-329.

13. Bashir T, Horlein R, Rommelaere J, Willwand K (2000) Cyclin A activates the DNA polymerase delta -dependent elongation machinery in vitro: A parvovirus DNA replication model. Proc Natl Acad Sci U S A 97: 5522-5527.

14. Winocour E, Callaham MF, Huberman E (1988) Perturbation of the cell cycle by adeno-associated virus. Virology 167: 393-399.

15. Morita E, Tada K, Chisaka H, Asao H, Sato H, Yaegashi N, Sugamura K (2001) Human parvovirus B19 induces cell cycle arrest at G(2) phase with accumulation of mitotic cyclins. J Virol 75: 7555-7563.

16. Op De BA, Anouja F, Mousset S, Rommelaere J, Caillet-Fauquet P (1995) The nonstructural proteins of the autonomous parvovirus minute virus of mice interfere with the cell cycle, inducing accumulation in G2. Cell Growth Differ 6: 781-787.

17. Op De BA, Sobczak-Thepot J, Sirma H, Bourgain F, Brechot C, Caillet-Fauquet P (2001) NS1- and minute virus of mice-induced cell cycle arrest: involvement of p53 and p21(cip1). J Virol 75: 11071-11078.

18. Morita E, Sugamura K (2002) Human parvovirus B19-induced cell cycle arrest and apoptosis. Springer Semin Immunopathol 24: 187-199.

19. Moffatt S, Yaegashi N, Tada K, Tanaka N, Sugamura K (1998) Human parvovirus B19 nonstructural (NS1) protein induces apoptosis in erythroid lineage cells. J Virol 72: 3018-3028.

20. Zhou C, Trempe JP (1999) Induction of apoptosis by cadmium and the adeno-associated virus Rep proteins. Virology 261: 280-287.

21. Sol N, Le JJ, Vassias I, Freyssinier JM, Thomas A, Prigent AF, Rudkin BB, Fichelson S, Morinet F (1999) Possible interactions between the NS-1 protein and tumor necrosis factor alpha pathways in erythroid cell apoptosis induced by human parvovirus B19. J Virol 73: 8762-8770.

22. Ran Z, Rayet B, Rommelaere J, Faisst S (1999) Parvovirus H-1-induced cell death: influence of intracellular NAD consumption on the regulation of necrosis and apoptosis. Virus Res 65: 161-174.

23. Hristov G, Kramer M, Li J, El-Andaloussi N, Mora R, Daeffler L, Zentgraf H, Rommelaere J, Marchini A (2010) Through its nonstructural protein NS1, parvovirus H-1 induces apoptosis via accumulation of reactive oxygen species. J Virol 84: 5909-5922.

24. Nakashima A, Tanaka N, Tamai K, Kyuuma M, Ishikawa Y, Sato H, Yoshimori T, Saito S, Sugamura K (2006) Survival of parvovirus B19-infected cells by cellular autophagy. Virology 349: 254-263.

25. Fu Y, Ishii KK, Munakata Y, Saitoh T, Kaku M, Sasaki T (2002) Regulation of tumor necrosis factor alpha promoter by human parvovirus B19 NS1 through activation of AP-1 and AP-2. J Virol 76: 5395-5403.

26. Zipris D, Lien E, Nair A, Xie JX, Greiner DL, Mordes JP, Rossini AA (2007) TLR9-signaling pathways are involved in Kilham rat virus-induced autoimmune diabetes in the biobreeding diabetes-resistant rat. J Immunol 178: 693-701.

27. Chen AY, Qiu J (2010) Parvovirus infetcion-induced cell detah and cell cycle arrest. Future Virology 5: 731-741.

28. Luo Y, Lou S, Deng X, Liu Z, Li Y, Kleiboeker S, Qiu J (2011) Parvovirus B19 infection of human primary erythroid progenitor cells triggers ATR-Chk1 signaling, which promotes B19 virus replication. J Virol 85: 8046-8055.

29. Adeyemi RO, Landry S, Davis ME, Weitzman MD, Pintel DJ (2010) Parvovirus minute virus of mice induces a DNA damage response that facilitates viral replication. PLoS Pathog 6: e1001141.

30. Luo Y, Chen AY, Qiu J (2011) Bocavirus infection induces a DNA damage response that facilitates viral DNA replication and mediates cell death. J Virol 85: 133-145.

31. Harper JW, Elledge SJ (2007) The DNA damage response: ten years after. Mol Cell 28: 739-745.

32. Ciccia A, Elledge SJ (2010) The DNA damage response: making it safe to play with knives. Mol Cell 40: 179-204.

33. Nussenzweig A (2007) Causes and consequences of the DNA damage response. Cell Cycle 6: 2339-2340.

34. Yang J, Yu Y, Hamrick HE, Duerksen-Hughes PJ (2003) ATM, ATR and DNA-PK: initiators of the cellular genotoxic stress responses. Carcinogenesis 24: 1571-1580.

35. Durocher D, Jackson SP (2001) DNA-PK, ATM and ATR as sensors of DNA damage: variations on a theme? Curr Opin Cell Biol 13: 225-231.

36. Paull TT, Lee JH (2005) The Mre11/Rad50/Nbs1 complex and its role as a DNA double-strand break sensor for ATM. Cell Cycle 4: 737-740.

37. Lavin MF, Kozlov S (2007) ATM activation and DNA damage response. Cell Cycle 6: 931-942.

38. Lee JH, Paull TT (2007) Activation and regulation of ATM kinase activity in response to DNA double-strand breaks. Oncogene 26: 7741-7748.

39. Schmitt E, Paquet C, Beauchemin M, Bertrand R (2007) DNA-damage response network at the crossroads of cell-cycle checkpoints, cellular senescence and apoptosis. J Zhejiang Univ Sci B 8: 377-397.

40. Zhou BB, Elledge SJ (2000) The DNA damage response: putting checkpoints in perspective. Nature 408: 433-439.

41. Mari PO, Florea BI, Persengiev SP, Verkaik NS, Bruggenwirth HT, Modesti M, Giglia-Mari G, Bezstarosti K, Demmers JA, Luider TM, Houtsmuller AB, van Gent DC (2006) Dynamic assembly of end-joining complexes requires interaction between Ku70/80 and XRCC4. Proc Natl Acad Sci U S A 103: 18597-18602.

42. Zou L, Elledge SJ (2003) Sensing DNA damage through ATRIP recognition of RPA-ssDNA complexes. Science 300: 1542-1548.

43. Shiotani B, Zou L (2009) Single-stranded DNA orchestrates an ATM-to-ATR switch at DNA breaks. Mol Cell 33: 547-558.

44. Yang XH, Zou L (2006) Recruitment of ATR-ATRIP, Rad17, and 9-1-1 complexes to DNA damage. Methods Enzymol 409:118-31.: 118-131.

45. Flynn RL, Zou L (2011) ATR: a master conductor of cellular responses to DNA replication stress. Trends Biochem Sci 36: 133-140.

46. Liu S, Shiotani B, Lahiri M, Marechal A, Tse A, Leung CC, Glover JN, Yang XH, Zou L (2011) ATR autophosphorylation as a molecular switch for checkpoint activation. Mol Cell 43: 192-202.

47. Jazayeri A, Falck J, Lukas C, Bartek J, Smith GC, Lukas J, Jackson SP (2006) ATM- and cell cycle-dependent regulation of ATR in response to DNA double-strand breaks. Nat Cell Biol 8: 37-45.

48. Weitzman MD, Carson CT, Schwartz RA, Lilley CE (2004) Interactions of viruses with the cellular DNA repair machinery. DNA Repair (Amst) 3: 1165-1173.

49. Lilley CE, Schwartz RA, Weitzman MD (2007) Using or abusing: viruses and the cellular DNA damage response. Trends Microbiol 15: 119-126.

50. Chaurushiya MS, Weitzman MD (2009) Viral manipulation of DNA repair and cell cycle checkpoints. DNA Repair (Amst) 8: 1166-1176.

51. Turnell AS, Grand RJ (2012) DNA viruses and the cellular DNA-damage response. J Gen Virol .

52. Geoffroy MC, Salvetti A (2005) Helper functions required for wild type and recombinant adeno-associated virus growth. Curr Gene Ther 5: 265-271.

53. Kotin RM, Siniscalco M, Samulski RJ, Zhu XD, Hunter L, Laughlin CA, McLaughlin S, Muzyczka N, Rocchi M, Berns KI (1990) Site-specific integration by adeno-associated virus. Proc Natl Acad Sci U S A 87: 2211-2215.

54. Mueller C, Flotte TR (2008) Clinical gene therapy using recombinant adeno-associated virus vectors. Gene Ther 15: 858-863.

55. Nonnenmacher M, Weber T (2012) Intracellular transport of recombinant adeno-associated virus vectors. Gene Ther 19: 649-658.

56. Weitzman MD, Linden RM (2011) Adeno-associated virus biology. Methods Mol Biol 807:1-23.: 1-23.

57. Schwartz RA, Palacios JA, Cassell GD, Adam S, Giacca M, Weitzman MD (2007) The Mre11/Rad50/Nbs1 complex limits adeno-associated virus transduction and replication. J Virol 81: 12936-12945.

58. Myers MW, Laughlin CA, Jay FT, Carter BJ (1980) Adenovirus helper function for growth of adeno-associated virus: effect of temperature-sensitive mutations in adenovirus early gene region 2. J Virol 35: 65-75.

59. Matsushita T, Elliger S, Elliger C, Podsakoff G, Villarreal L, Kurtzman GJ, Iwaki Y, Colosi P (1998) Adeno-associated virus vectors can be efficiently produced without helper virus. Gene Ther 5: 938-945.

60. Blanchette P, Kindsmuller K, Groitl P, Dallaire F, Speiseder T, Branton PE, Dobner T (2008) Control of mRNA export by adenovirus E4orf6 and E1B55K proteins during productive infection requires E4orf6 ubiquitin ligase activity. J Virol 82: 2642-2651.

61. Woo JL, Berk AJ (2007) Adenovirus ubiquitin-protein ligase stimulates viral late mRNA nuclear export. J Virol 81: 575-587.

62. Stracker TH, Carson CT, Weitzman MD (2002) Adenovirus oncoproteins inactivate the Mre11-Rad50-NBS1 DNA repair complex. Nature 418: 348-352.

63. Cervelli T, Palacios JA, Zentilin L, Mano M, Schwartz RA, Weitzman MD, Giacca M (2008) Processing of recombinant AAV genomes occurs in specific nuclear structures that overlap with foci of DNA-damage-response proteins. J Cell Sci 121: 349-357.

64. Collaco RF, Bevington JM, Bhrigu V, Kalman-Maltese V, Trempe JP (2009) Adeno-associated virus and adenovirus coinfection induces a cellular DNA damage and repair response via redundant phosphatidylinositol 3-like kinase pathways. Virology 392: 24-33.

65. Schwartz RA, Carson CT, Schuberth C, Weitzman MD (2009) Adeno-associated virus replication induces a DNA damage response coordinated by DNA-dependent protein kinase. J Virol 83: 6269-6278.

66. Choi YK, Nash K, Byrne BJ, Muzyczka N, Song S (2010) The effect of DNA-dependent protein kinase on adeno-associated virus replication. PLoS ONE 5: e15073.

67. Song S, Laipis PJ, Berns KI, Flotte TR (2001) Effect of DNA-dependent protein kinase on the molecular fate of the rAAV2 genome in skeletal muscle. Proc Natl Acad Sci U S A 98: 4084-4088.

68. Choi VW, McCarty DM, Samulski RJ (2006) Host cell DNA repair pathways in adeno-associated viral genome processing. J Virol 80: 10346-10356.

69. Vogel R, Seyffert M, Strasser R, de Oliveira AP, Dresch C, Glauser DL, Jolinon N, Salvetti A, Weitzman MD, Ackermann M, Fraefel C (2012) Adeno-Associated Virus Type 2 Modulates the Host DNA Damage Response Induced by Herpes Simplex Virus 1 during Coinfection. J Virol 86: 143-155.

70. Weindler FW, Heilbronn R (1991) A subset of herpes simplex virus replication genes provides helper functions for productive adeno-associated virus replication. J Virol 65: 2476-2483.

71. Shirata N, Kudoh A, Daikoku T, Tatsumi Y, Fujita M, Kiyono T, Sugaya Y, Isomura H, Ishizaki K, Tsurumi T (2005) Activation of ataxia telangiectasia-mutated DNA damage checkpoint signal transduction elicited by herpes simplex virus infection. J Biol Chem 280: 30336-30341.

72. Wilkinson DE, Weller SK (2006) Herpes simplex virus type I disrupts the ATR-dependent DNA-damage response during lytic infection. J Cell Sci 119: 2695-2703.

73. Parkinson J, Lees-Miller SP, Everett RD (1999) Herpes simplex virus type 1 immediate-early protein vmw110 induces the proteasome-dependent degradation of the catalytic subunit of DNA-dependent protein kinase. J Virol 73: 650-657.

74. Namiki Y, Zou L (2006) ATRIP associates with replication protein A-coated ssDNA through multiple interactions. Proc Natl Acad Sci U S A 103: 580-585.

75. Raj K, Ogston P, Beard P (2001) Virus-mediated killing of cells that lack p53 activity. Nature 412: 914-917.

76. Jurvansuu J, Raj K, Stasiak A, Beard P (2005) Viral transport of DNA damage that mimics a stalled replication fork. J Virol 79: 569-580.

77. Jurvansuu J, Fragkos M, Ingemarsdotter C, Beard P (2007) Chk1 instability is coupled to mitotic cell death of p53-deficient cells in response to virus-induced DNA damage signaling. J Mol Biol 372: 397-406.

78. Ingemarsdotter C, Keller D, Beard P (2010) The DNA damage response to non-replicating adeno-associated virus: Centriole overduplication and mitotic catastrophe independent of the spindle checkpoint. Virology 400: 271-286.

79. Garner E, Martinon F, Tschopp J, Beard P, Raj K (2007) Cells with defective p53-p21-pRb pathway are susceptible to apoptosis induced by p84N5 via caspase-6. Cancer Res 67: 7631-7637.

80. Yakobson B, Hrynko TA, Peak MJ, Winocour E (1989) Replication of adeno-associated virus in cells irradiated with UV light at 254 nm. J Virol 63: 1023-1030.

81. Weitzman MD, Lilley CE, Chaurushiya MS (2010) Genomes in conflict: maintaining genome integrity during virus infection. Annu Rev Microbiol 64:61-81.: 61-81.

82. Ozawa K, Kurtzman G, Young N (1986) Replication of the B19 parvovirus in human bone marrow cell cultures. Science 233: 883-886.

83. Srivastava A, Lu L (1988) Replication of B19 parvovirus in highly enriched hematopoietic progenitor cells from normal human bone marrow. J Virol 62: 3059-3063.

84. Yaegashi N, Niinuma T, Chisaka H, Uehara S, Moffatt S, Tada K, Iwabuchi M, Matsunaga Y, Nakayama M, Yutani C, Osamura Y, Hirayama E, Okamura K, Sugamura K, Yajima A (1999) Parvovirus B19 infection induces apoptosis of erythroid cells in vitro and in vivo. J Infect 39: 68-76.

85. Morey AL, Fleming KA (1992) Immunophenotyping of fetal haemopoietic cells permissive for human parvovirus B19 replication in vitro. Br J Haematol 82: 302-309.

86. Anderson MJ, Khousam MN, Maxwell DJ, Gould SJ, Happerfield LC, Smith WJ (1988) Human parvovirus B19 and hydrops fetalis. Lancet 1: 535.

87. Weir E (2005) Parvovirus B19 infection: fifth disease and more. CMAJ 172: 743.

88. Lamont R, Sobel J, Vaisbuch E, Kusanovic J, Mazaki-Tovi S, Kim S, Uldbjerg N, Romero R (2011) Parvovirus B19 infection in human pregnancy. BJOG 118: 175-186.

89. Mrzljak A, Kardum-Skelin I, Cvrlje VC, Kanizaj TF, Sustercic D, Gustin D, Kocman B (2010) Parvovirus B 19 (PVB19) induced pure red cell aplasia (PRCA) in immunocompromised patient after liver transplantation. Coll Antropol 34: 271-274.

90. Koduri PR, Kumapley R, Khokha ND, Patel AR (1997) Red cell aplasia caused by parvovirus B19 in AIDS: use of i.v. immunoglobulin. Ann Hematol 75: 67-68.

91. Mouthon L, Guillevin L, Tellier Z (2005) Intravenous immunoglobulins in autoimmune- or parvovirus B19-mediated pure red-cell aplasia. Autoimmun Rev 4: 264-269.

92. Rechavi G, Vonsover A, Manor Y, Mileguir F, Shpilberg O, Kende G, Brok-Simoni F, Mandel M, Gotlieb-Stematski T, Ben-Bassat I, . (1989) Aplastic crisis due to human B19 parvovirus infection in red cell pyrimidine-5'-nucleotidase deficiency. Acta Haematol 82: 46-49.

93. Young NS, Brown KE (2004) Mechanism of disease:Parvovirus B19. N Engl J Med 350: 586-597.

94. Gareus R, Gigler A, Hemauer A, Leruez-Ville M, Morinet F, Wolf H, Modrow S (1998) Characterization of cis-acting and NS1 protein-responsive elements in the p6 promoter of parvovirus B19. J Virol 72: 609-616.

95. Hsu TC, Wu WJ, Chen MC, Tsay GJ (2004) Human parvovirus B19 non-structural protein (NS1) induces apoptosis through mitochondria cell death pathway in COS-7 cells. Scand J Infect Dis 36: 570-577.

96. Chen AY, Zhang EY, Guan W, Cheng F, Kleiboeker S, Yankee TM, Qiu J (2010) The small 11kDa non-structural protein of human parvovirus B19 plays a key role in inducing apoptosis during B19 virus infection of primary erythroid progenitor cells. Blood 115: 1070-1080.

97. Wong S, Zhi N, Filippone C, Keyvanfar K, Kajigaya S, Brown KE, Young NS (2008) Ex vivo-generated CD36+ erythroid progenitors are highly permissive to human parvovirus B19 replication. J Virol 82: 2470-2476.

98. Pillet S, Le GN, Hofer T, NguyenKhac F, Koken M, Aubin JT, Fichelson S, Gassmann M, Morinet F (2004) Hypoxia enhances human B19 erythrovirus gene expression in primary erythroid cells. Virology 327: 1-7.

99. Chen AY, Kleiboeker S, Qiu J (2011) Productive Parvovirus B19 Infection of Primary Human Erythroid Progenitor Cells at Hypoxia is Regulated by STAT5A and MEK Signaling but not HIF alpha. PLoS Pathog 7: e1002088.

100. Wan Z, Zhi N, Wong S, Keyvanfar K, Liu D, Raghavachari N, Munson PJ, Su S, Malide D, Kajigaya S, Young NS (2010) Human parvovirus B19 causes cell cycle arrest of human erythroid progenitors via deregulation of the E2F family of transcription factors. J Clin Invest 120: 3530-3544.

101. Lou S, Luo Y, Cheng F, Huang Q, Shen W, Kleiboeker S, Tisdale JF, Liu Z, Qiu J (2012) Human Parvovirus B19 DNA Replication Induces a DNA Damage Response That is Dispensable for Cell Cycle Arrest at G2/M Phase. J Virol Jul 25.: [Epub ahead of print]-PMID: 22837195.

102. Darzynkiewicz Z, Juan G (2001) Analysis of DNA content and BrdU incorporation. Curr Protoc Cytom Chapter 7:Unit 7.7.: Unit.

103. Hang H, Fox MH (2004) Analysis of the mammalian cell cycle by flow cytometry. Methods Mol Biol 241:23-35.: 23-35.

104. Poole BD, Kivovich V, Gilbert L, Naides SJ (2011) Parvovirus B19 nonstructural protein-induced damage of cellular DNA and resultant apoptosis. Int J Med Sci 8: 88-96.

105. Liu Q, Guntuku S, Cui XS, Matsuoka S, Cortez D, Tamai K, Luo G, Carattini-Rivera S, DeMayo F, Bradley A, Donehower LA, Elledge SJ (2000) Chk1 is an essential kinase that is regulated by Atr and required for the G(2)/M DNA damage checkpoint. Genes Dev 14: 1448-1459.

106. Bartek J, Lukas J (2003) Chk1 and Chk2 kinases in checkpoint control and cancer. Cancer Cell 3: 421-429.

107. Smith J, Tho LM, Xu N, Gillespie DA (2010) The ATM-Chk2 and ATR-Chk1 pathways in DNA damage signaling and cancer. Adv Cancer Res 108:73-112.: 73-112.

108. Tattersall P, Ward DC (1976) Rolling hairpin model for replication of parvovirus and linear chromosomal DNA. Nature 263: 106-109.

109. Astell CR, Thomson M, Chow MB, Ward DC (1983) Structure and replication of minute virus of mice DNA. Cold Spring Harb Symp Quant Biol 47 Pt 2:751-62.: 751-762.

110. Rommelaere J, Geletneky K, Angelova AL, Daeffler L, Dinsart C, Kiprianova I, Schlehofer JR, Raykov Z (2010) Oncolytic parvoviruses as cancer therapeutics. Cytokine Growth Factor Rev 21: 185-195.

111. Bashir T, Rommelaere J, Cziepluch C (2001) In vivo accumulation of cyclin A and cellular replication factors in autonomous parvovirus minute virus of mice-associated replication bodies. J Virol 75: 4394-4398.

112. Ruiz Z, Mihaylov IS, Cotmore SF, Tattersall P (2011) Recruitment of DNA replication and damage response proteins to viral replication centers during infection with NS2 mutants of Minute Virus of Mice (MVM). Virology 410: 375-384.

113. Op De BA, Caillet-Fauquet P (1997) The NS1 protein of the autonomous parvovirus minute virus of mice blocks cellular DNA replication: a consequence of lesions to the chromatin? J Virol 71: 5323-5329.

114. Cotmore SF, Tattersall P (2005) A rolling-haipin strategy: basic mechanisms of DNA replication in the parvoviruses. In: Kerr J, Cotmore SF, Bloom ME, Linden RM, Parrish CR, editors. Parvoviruses. London: Hoddler Arond. pp. 171-181.

115. Simon HU, Haj-Yehia A, Levi-Schaffer F (2000) Role of reactive oxygen species (ROS) in apoptosis induction. Apoptosis 5: 415-418.

116. Barzilai A, Yamamoto K (2004) DNA damage responses to oxidative stress. DNA Repair (Amst) 3: 1109-1115.

117. Schwartz D, Green B, Carmichael LE, Parrish CR (2002) The canine minute virus (minute virus of canines) is a distinct parvovirus that is most similar to bovine parvovirus. Virology 302: 219-223.

118. Sun Y, Chen AY, Cheng F, Guan W, Johnson FB, Qiu J (2009) Molecular characterization of infectious clones of the minute virus of canines reveals unique features of bocaviruses. J Virol 83: 3956-3967.

119. Chen AY, Cheng F, Lou S, Luo Y, Liu Z, Delwart E, Pintel D, Qiu J (2010) Characterization of the gene expression profile of human bocavirus. Virology 403: 145-154.

120. Binn LN, Lazar EC, Eddy GA, Kajima M (1970) Recovery and Characterization of a Minute Virus of Canines. Infect Immun 1: 503-508.

121. Chen AY, Luo Y, Cheng F, Sun Y, Qiu J (2010) Bocavirus infection induces a mitochondrion-mediated apoptosis and cell cycle arrest at G2/M-phase. J Virol 84: 5615-5626.

122. Roos WP, Kaina B (2006) DNA damage-induced cell death by apoptosis. Trends Mol Med 12: 440-450.

123. Banin S, Moyal L, Shieh S, Taya Y, Anderson CW, Chessa L, Smorodinsky NI, Prives C, Reiss Y, Shiloh Y, Ziv Y (1998) Enhanced phosphorylation of p53 by ATM in response to DNA damage. Science 281: 1674-1677.

124. Allander T, Jartti T, Gupta S, Niesters HG, Lehtinen P, Osterback R, Vuorinen T, Waris M, Bjerkner A, Tiveljung-Lindell A, van den Hoogen BG, Hyypia T, Ruuskanen O (2007) Human bocavirus and acute wheezing in children. Clin Infect Dis 44: 904-910.

125. Kahn J (2008) Human bocavirus: clinical significance and implications. Curr Opin Pediatr 20: 62-66.

126. Schildgen O, Muller A, Allander T, Mackay IM, Volz S, Kupfer B, Simon A (2008) Human bocavirus: passenger or pathogen in acute respiratory tract infections? Clin Microbiol Rev 21: 291-304.

127. Lee JI, Chung JY, Han TH, Song MO, Hwang ES (2007) Detection of human bocavirus in children hospitalized because of acute gastroenteritis. J Infect Dis 196: 994-997.

128. Arnold JC, Singh KK, Spector SA, Sawyer MH (2006) Human bocavirus: prevalence and clinical spectrum at a children's hospital. Clin Infect Dis 43: 283-288.

129. Lau SK, Yip CC, Que TL, Lee RA, Au-Yeung RK, Zhou B, So LY, Lau YL, Chan KH, Woo PC, Yuen KY (2007) Clinical and molecular epidemiology of human bocavirus in respiratory and fecal samples from children in Hong Kong. J Infect Dis 196: 986-993.

130. Vicente D, Cilla G, Montes M, Perez-Yarza EG, Perez-Trallero E (2007) Human bocavirus, a respiratory and enteric virus. Emerg Infect Dis 13: 636-637.

131. Albuquerque MC, Rocha LN, Benati FJ, Soares CC, Maranhao AG, Ramirez ML, Erdman D, Santos N (2007) Human bocavirus infection in children with gastroenteritis, Brazil. Emerg Infect Dis 13: 1756-1758.

132. Carmichael LE, Schlafer DH, Hashimoto A (1991) Pathogenicity of minute virus of canines (MVC) for the canine fetus. Cornell Vet 81: 151-171.

133. Jarplid B, Johansson H, Carmichael LE (1996) A fatal case of pup infection with minute virus of canines (MVC). J Vet Diagn Invest 8: 484-487.

134. Pratelli A, Buonavoglia D, Tempesta M, Guarda F, Carmichael L, Buonavoglia C (1999) Fatal canine parvovirus type-1 infection in pups from Italy. J Vet Diagn Invest 11: 365-367.

135. Binn LN, Marchwicki RH, Eckermann EH, Fritz TE (1981) Viral antibody studies of laboratory dogs with diarrheal disease. Am J Vet Res 42: 1665-1667.

136. Mochizuki M, Hashimoto M, Hajima T, Takiguchi M, Hashimoto A, Une Y, Roerink F, Ohshima T, Parrish CR, Carmichael LE (2002) Virologic and serologic identification of minute virus of canines (canine parvovirus type 1) from dogs in Japan. J Clin Microbiol 40: 3993-3998.

137. Spahn GJ, Mohanty SB, Hetrick FM (1966) Experimental infection of calves with hemadsorbing enteric (HADEN) virus. Cornell Vet 56: 377-386.

138. Dijkman R, Koekkoek SM, Molenkamp R, Schildgen O, van der Hoek L (2009) Human bocavirus can be cultured in differentiated human airway epithelial cells. J Virol 83: 7739-7748.

139. Shiloh Y (2003) ATM and related protein kinases: safeguarding genome integrity. Nat Rev Cancer 3: 155-168.

140. Jackson SP (2009) The DNA-damage response: new molecular insights and new approaches to cancer therapy. Biochem Soc Trans 37: 483-494.

141. Li J, Stern DF (2005) Regulation of CHK2 by DNA-dependent protein kinase. J Biol Chem 280: 12041-12050.

142. Pommier Y, Weinstein JN, Aladjem MI, Kohn KW (2006) Chk2 molecular interaction map and rationale for Chk2 inhibitors. Clin Cancer Res 12: 2657-2661.

143. Branzei D, Foiani M (2008) Regulation of DNA repair throughout the cell cycle. Nat Rev Mol Cell Biol 9: 297-308.

144. Kastan MB, Bartek J (2004) Cell-cycle checkpoints and cancer. Nature 432: 316-323.

145. Bartek J, Lukas C, Lukas J (2004) Checking on DNA damage in S phase. Nat Rev Mol Cell Biol 5: 792-804.

146. Cotmore SF, Tattersall P (2005) Structure and Organization of the Viral Genome. In: Kerr J, Cotmore SF, Bloom ME, Linden RM, Parrish CR, editors. Parvoviruses. London: Hodder Arnold. pp. 73-94.

147. Fragkos M, Breuleux M, Clement N, Beard P (2008) Recombinant adeno-associated viral vectors are deficient in provoking a DNA damage response. J Virol 82: 7379-7387.

148. Cuconati A, Mukherjee C, Perez D, White E (2003) DNA damage response and MCL-1 destruction initiate apoptosis in adenovirus-infected cells. Genes Dev 17: 2922-2932.

149. Balajee AS, Geard CR (2004) Replication protein A and gamma-H2AX foci assembly is triggered by cellular response to DNA double-strand breaks. Exp Cell Res 300: 320-334.

150. Ward IM, Chen J (2001) Histone H2AX is phosphorylated in an ATR-dependent manner in response to replicational stress. J Biol Chem 276: 47759-47762.

151. Hickson I, Zhao Y, Richardson CJ, Green SJ, Martin NM, Orr AI, Reaper PM, Jackson SP, Curtin NJ, Smith GC (2004) Identification and characterization of a novel and specific inhibitor of the ataxia-telangiectasia mutated kinase ATM. Cancer Res 64: 9152-9159.

152. Won J, Kim M, Kim N, Ahn JH, Lee WG, Kim SS, Chang KY, Yi YW, Kim TK (2006) Small molecule-based reversible reprogramming of cellular lifespan. Nat Chem Biol 2: 369-374.

153. Bhattacharya S, Ray RM, Johnson LR (2009) Role of polyamines in p53-dependent apoptosis of intestinal epithelial cells. Cell Signal 21: 509-522.

154. Cruet-Hennequart S, Glynn MT, Murillo LS, Coyne S, Carty MP (2008) Enhanced DNA-PK-mediated RPA2 hyperphosphorylation in DNA polymerase eta-deficient human cells treated with cisplatin and oxaliplatin. DNA Repair (Amst) 7: 582-596.

155. Goldstein M, Roos WP, Kaina B (2008) Apoptotic death induced by the cyclophosphamide analogue mafosfamide in human lymphoblastoid cells: contribution of DNA replication, transcription inhibition and Chk/p53 signaling. Toxicol Appl Pharmacol 229: 20-32.

156. Yang XH, Shiotani B, Classon M, Zou L (2008) Chk1 and Claspin potentiate PCNA ubiquitination. Genes Dev 22: 1147-1152.

157. Alao JP, Sunnerhagen P (2009) The ATM and ATR inhibitors CGK733 and caffeine suppress cyclin D1 levels and inhibit cell proliferation. Radiat Oncol 4: 51.

158. Leahy JJ, Golding BT, Griffin RJ, Hardcastle IR, Richardson C, Rigoreau L, Smith GC (2004) Identification of a highly potent and selective DNA-dependent protein kinase (DNA-PK) inhibitor (NU7441) by screening of chromenone libraries. Bioorg Med Chem Lett 14: 6083-6087.

159. Nakanishi S, Kakita S, Takahashi I, Kawahara K, Tsukuda E, Sano T, Yamada K, Yoshida M, Kase H, Matsuda Y, . (1992) Wortmannin, a microbial product inhibitor of myosin light chain kinase. J Biol Chem 267: 2157-2163.

160. Uziel T, Lerenthal Y, Moyal L, Andegeko Y, Mittelman L, Shiloh Y (2003) Requirement of the MRN complex for ATM activation by DNA damage. EMBO J 22: 5612-5621.

161. Lee JH, Paull TT (2005) ATM activation by DNA double-strand breaks through the Mre11-Rad50-Nbs1 complex. Science 308: 551-554.

162. Yazdi PT, Wang Y, Zhao S, Patel N, Lee EY, Qin J (2002) SMC1 is a downstream effector in the ATM/NBS1 branch of the human S-phase checkpoint. Genes Dev 16: 571-582.

163. Kitagawa R, Bakkenist CJ, McKinnon PJ, Kastan MB (2004) Phosphorylation of SMC1 is a critical downstream event in the ATM-NBS1-BRCA1 pathway. Genes Dev 18: 1423-1438.

164. Schar P, Fasi M, Jessberger R (2004) SMC1 coordinates DNA double-strand break repair pathways. Nucleic Acids Res 32: 3921-3929.

165. Difilippantonio S, Nussenzweig A (2007) The NBS1-ATM connection revisited. Cell Cycle 6: 2366-2370.

166. Burma S, Chen BP, Murphy M, Kurimasa A, Chen DJ (2001) ATM phosphorylates histone H2AX in response to DNA double-strand breaks. J Biol Chem 276: 42462-42467.

167. Mukherjee B, Kessinger C, Kobayashi J, Chen BP, Chen DJ, Chatterjee A, Burma S (2006) DNA-PK phosphorylates histone H2AX during apoptotic DNA fragmentation in mammalian cells. DNA Repair (Amst) 5: 575-590.

168. Furuta T, Takemura H, Liao ZY, Aune GJ, Redon C, Sedelnikova OA, Pilch DR, Rogakou EP, Celeste A, Chen HT, Nussenzweig A, Aladjem MI, Bonner WM, Pommier Y (2003) Phosphorylation of histone H2AX and activation of Mre11, Rad50, and Nbs1 in response to replication-dependent DNA double-strand breaks induced by mammalian DNA topoisomerase I cleavage complexes. J Biol Chem 278: 20303-20312.

169. Rao VA, Fan AM, Meng L, Doe CF, North PS, Hickson ID, Pommier Y (2005) Phosphorylation of BLM, dissociation from topoisomerase IIIalpha, and colocalization with gamma-H2AX after topoisomerase I-induced replication damage. Mol Cell Biol 25: 8925-8937.

170. Wu X, Shell SM, Zou Y (2005) Interaction and colocalization of Rad9/Rad1/Hus1 checkpoint complex with replication protein A in human cells. Oncogene 24: 4728-4735.

171. Christensen J, Tattersall P (2002) Parvovirus initiator protein NS1 and RPA coordinate replication fork progression in a reconstituted DNA replication system. J Virol 76: 6518-6531.

172. Ni TH, McDonald WF, Zolotukhin I, Melendy T, Waga S, Stillman B, Muzyczka N (1998) Cellular proteins required for adeno-associated virus DNA replication in the absence of adenovirus coinfection. J Virol 72: 2777-2787.

173. Kudoh A, Iwahori S, Sato Y, Nakayama S, Isomura H, Murata T, Tsurumi T (2009) Homologous recombinational repair factors are recruited and loaded onto the viral DNA genome in Epstein-Barr virus replication compartments. J Virol 83: 6641-6651.

174. Vassin VM, Wold MS, Borowiec JA (2004) Replication protein A (RPA) phosphorylation prevents RPA association with replication centers. Mol Cell Biol 24: 1930-1943.

175. Hein J, Boichuk S, Wu J, Cheng Y, Freire R, Jat PS, Roberts TM, Gjoerup OV (2009) Simian virus 40 large T antigen disrupts genome integrity and activates a DNA damage response via Bub1 binding. J Virol 83: 117-127.

176. Digweed M, Demuth I, Rothe S, Scholz R, Jordan A, Grotzinger C, Schindler D, Grompe M, Sperling K (2002) SV40 large T-antigen disturbs the formation of nuclear DNA-repair foci containing MRE11. Oncogene 21: 4873-4878.

177. Lanson NA, Jr., Egeland DB, Royals BA, Claycomb WC (2000) The MRE11-NBS1-RAD50 pathway is perturbed in SV40 large T antigen-immortalized AT-1, AT-2 and HL-1 cardiomyocytes. Nucleic Acids Res 28: 2882-2892.

178. Wu X, Avni D, Chiba T, Yan F, Zhao Q, Lin Y, Heng H, Livingston D (2004) SV40 T antigen interacts with Nbs1 to disrupt DNA replication control. Genes Dev 18: 1305-1316.

179. Moody CA, Laimins LA (2009) Human papillomaviruses activate the ATM DNA damage pathway for viral genome amplification upon differentiation. PLoS Pathog 5: e1000605.

180. Petrini JH, Stracker TH (2003) The cellular response to DNA double-strand breaks: defining the sensors and mediators. Trends Cell Biol 13: 458-462.

181. Valyi-Nagy T, Olson SJ, Valyi-Nagy K, Montine TJ, Dermody TS (2000) Herpes simplex virus type 1 latency in the murine nervous system is associated with oxidative damage to neurons. Virology 278: 309-321.

182. Milatovic D, Zhang Y, Olson SJ, Montine KS, Roberts LJ, Morrow JD, Montine TJ, Dermody TS, Valyi-Nagy T (2002) Herpes simplex virus type 1 encephalitis is associated with elevated levels of F2-isoprostanes and F4-neuroprostanes. J Neurovirol 8: 295-305.

183. Huang KJ, Zemelman BV, Lehman IR (2002) Endonuclease G, a candidate human enzyme for the initiation of genomic inversion in herpes simplex type 1 virus. J Biol Chem 277: 21071-21079.

184. Wohlrab F, Chatterjee S, Wells RD (1991) The herpes simplex virus 1 segment inversion site is specifically cleaved by a virus-induced nuclear endonuclease. Proc Natl Acad Sci U S A 88: 6432-6436.

185. Thompson SR, Sarnow P (2003) Enterovirus 71 contains a type I IRES element that functions when eukaryotic initiation factor eIF4G is cleaved. Virology 315: 259-266.

186. Dahl J, You J, Benjamin TL (2005) Induction and utilization of an ATM signaling pathway by polyomavirus. J Virol 79: 13007-13017.

187. Bartek J, Lukas J (2006) Cell biology. Balancing life-or-death decisions. Science 314: 261-262.

188. Kim H, Tu HC, Ren D, Takeuchi O, Jeffers JR, Zambetti GP, Hsieh JJ, Cheng EH (2009) Stepwise activation of BAX and BAK by tBID, BIM, and PUMA initiates mitochondrial apoptosis. Mol Cell 36: 487-499.

189. van den Bosch M, Bree RT, Lowndes NF (2003) The MRN complex: coordinating and mediating the response to broken chromosomes. EMBO Rep 4: 844-849.

190. D'Amours D, Jackson SP (2002) The Mre11 complex: at the crossroads of dna repair and checkpoint signalling. Nat Rev Mol Cell Biol 3: 317-327.

191. Stracker TH, Theunissen JW, Morales M, Petrini JH (2004) The Mre11 complex and the metabolism of chromosome breaks: the importance of communicating and holding things together. DNA Repair (Amst) 3: 845-854.

192. Lilley CE, Carson CT, Muotri AR, Gage FH, Weitzman MD (2005) DNA repair proteins affect the lifecycle of herpes simplex virus 1. Proc Natl Acad Sci U S A 102: 5844-5849.

193. Carson CT, Schwartz RA, Stracker TH, Lilley CE, Lee DV, Weitzman MD (2003) The Mre11 complex is required for ATM activation and the G2/M checkpoint. EMBO J 22: 6610-6620.

194. Zhao X, Madden-Fuentes RJ, Lou BX, Pipas JM, Gerhardt J, Rigell CJ, Fanning E (2008) Ataxia telangiectasia-mutated damage-signaling kinase- and proteasome-dependent destruction of Mre11-Rad50-Nbs1 subunits in Simian virus 40-infected primate cells. J Virol 82: 5316-5328.

195. Gregory DA, Bachenheimer SL (2008) Characterization of mre11 loss following HSV-1 infection. Virology 373: 124-136.

196. Taylor TJ, Knipe DM (2004) Proteomics of herpes simplex virus replication compartments: association of cellular DNA replication, repair, recombination, and chromatin remodeling proteins with ICP8. J Virol 78: 5856-5866.

197. Wilkinson DE, Weller SK (2004) Recruitment of cellular recombination and repair proteins to sites of herpes simplex virus type 1 DNA replication is dependent on the composition of viral proteins within prereplicative sites and correlates with the induction of the DNA damage response. J Virol 78: 4783-4796.

198. Sancar A, Lindsey-Boltz LA, Unsal-Kacmaz K, Linn S (2004) Molecular mechanisms of mammalian DNA repair and the DNA damage checkpoints. Annu Rev Biochem 73:39-85.: 39-85.

199. Boichuk S, Hu L, Hein J, Gjoerup OV (2010) Multiple DNA damage signaling and repair pathways deregulated by simian virus 40 large T antigen. J Virol 84: 8007-8020.

200. Fauquet, C. M., Mayo, M. A., Desselberger, U., and Ball, L. A. (2005) Virus Taxonomy: VIIIth report of the International Committee on Taxonomy of Viruses. Academic Press.

201. Young NS, Brown KE (2004) Parvovirus B19. N Engl J Med 350: 586-597.

202. Zhi N, Zadori Z, Brown KE, Tijssen P (2004) Construction and sequencing of an infectious clone of the human parvovirus B19. Virology 318: 142-152.

203. Ozawa K, Kurtzman G, Young N (1987) Productive infection by B19 parvovirus of human erythroid bone marrow cells in vitro. Blood 70: 384-391.

204. Chen AY, Guan W, Lou S, Liu Z, Kleiboeker S, Qiu J (2010) Role of Erythropoietin Receptor Signaling in Parvovirus B19 Replication in Human Erythroid Progenitor Cells. J Virol 84: 12385-12396.

205. Andegeko Y, Moyal L, Mittelman L, Tsarfaty I, Shiloh Y, Rotman G (2001) Nuclear retention of ATM at sites of DNA double strand breaks. J Biol Chem 276: 38224-38230.

206. Petermann E, Caldecott KW (2006) Evidence that the ATR/Chk1 pathway maintains normal replication fork progression during unperturbed S phase. Cell Cycle 5: 2203-2209.

207. Ball HL, Myers JS, Cortez D (2005) ATRIP binding to replication protein A-single-stranded DNA promotes ATR-ATRIP localization but is dispensable for Chk1 phosphorylation. Mol Biol Cell 16: 2372-2381.

208. Kasten U, Plottner N, Johansen J, Overgaard J, Dikomey E (1999) Ku70/80 gene expression and DNA-dependent protein kinase (DNA-PK) activity do not correlate with double-strand break (dsb) repair capacity and cellular radiosensitivity in normal human fibroblasts. Br J Cancer 79: 1037-1041.

209. Houtgraaf JH, Versmissen J, van der Giessen WJ (2006) A concise review of DNA damage checkpoints and repair in mammalian cells. Cardiovasc Revasc Med 7: 165-172.

210. Lehmann HW, von LP, Modrow S (2003) Parvovirus B19 infection and autoimmune disease. Autoimmun Rev 2: 218-223.

211. Wong S, Brown KE (2006) Development of an improved method of detection of infectious parvovirus B19. J Clin Virol 35: 407-413.

212. Guan W, Wong S, Zhi N, Qiu J (2009) The genome of human parvovirus B19 virus can replicate in non-permissive cells with the help of adenovirus genes and produces infectious virus. J Virol 83: 9541-9553.

213. Rhode SL, III, Paradiso PR (1989) Parvovirus replication in normal and transformed human cells correlates with the nuclear translocation of the early protein NS1. J Virol 63: 349-355.

214. Block WD, Yu Y, Lees-Miller SP (2004) Phosphatidyl inositol 3-kinase-like serine/threonine protein kinases (PIKKs) are required for DNA damage-induced phosphorylation of the 32 kDa subunit of replication protein A at threonine 21. Nucleic Acids Res 32: 997-1005.

215. Mah LJ, El-Osta A, Karagiannis TC (2010) gammaH2AX: a sensitive molecular marker of DNA damage and repair. Leukemia 24: 679-686.

216. Stucki M, Jackson SP (2006) gammaH2AX and MDC1: anchoring the DNA-damage-response machinery to broken chromosomes. DNA Repair (Amst) 5: 534-543.

217. Cimprich KA, Cortez D (2008) ATR: an essential regulator of genome integrity. Nat Rev Mol Cell Biol 9: 616-627.

218. Sarkaria JN, Busby EC, Tibbetts RS, Roos P, Taya Y, Karnitz LM, Abraham RT (1999) Inhibition of ATM and ATR kinase activities by the radiosensitizing agent, caffeine. Cancer Res 59: 4375-4382.

219. Chaturvedi P, Eng WK, Zhu Y, Mattern MR, Mishra R, Hurle MR, Zhang X, Annan RS, Lu Q, Faucette LF, Scott GF, Li X, Carr SA, Johnson RK, Winkler JD, Zhou BB (1999) Mammalian Chk2 is a downstream effector of the ATM-dependent DNA damage checkpoint pathway. Oncogene 18: 4047-4054.

220. Zhao H, Piwnica-Worms H (2001) ATR-mediated checkpoint pathways regulate phosphorylation and activation of human Chk1. Mol Cell Biol 21: 4129-4139.

221. Griffith AJ, Blier PR, Mimori T, Hardin JA (1992) Ku polypeptides synthesized in vitro assemble into complexes which recognize ends of double-stranded DNA. J Biol Chem 267: 331-338.

222. Ruis BL, Fattah KR, Hendrickson EA (2008) The catalytic subunit of DNA-dependent protein kinase regulates proliferation, telomere length, and genomic stability in human somatic cells. Mol Cell Biol 28: 6182-6195.

223. Nash K, Chen W, Salganik M, Muzyczka N (2009) Identification of cellular proteins that interact with the adeno-associated virus rep protein. J Virol 83: 454-469.

224. Nash K, Chen W, Muzyczka N (2008) Complete in vitro reconstitution of adeno-associated virus DNA replication requires the minichromosome maintenance complex proteins. J Virol 82: 1458-1464.

225. Nash K, Chen W, McDonald WF, Zhou X, Muzyczka N (2007) Purification of host cell enzymes involved in adeno-associated virus DNA replication. J Virol 81: 5777-5787.

226. Chen C, Shimizu S, Tsujimoto Y, Motoyama N (2005) Chk2 regulates transcription-independent p53-mediated apoptosis in response to DNA damage. Biochem Biophys Res Commun 333: 427-431.

227. Plesca D, Mazumder S, Almasan A (2008) DNA damage response and apoptosis. Methods Enzymol 446:107-22.: 107-122.

228. Ljungman M (2010) The DNA damage response--repair or despair? Environ Mol Mutagen 51: 879-889.

229. Allander T, Tammi MT, Eriksson M, Bjerkner A, Tiveljung-Lindell A, Andersson B (2005) Cloning of a human parvovirus by molecular screening of respiratory tract samples. Proc Natl Acad Sci U S A 102: 12891-12896.

230. Meriluoto M, Hedman L, Tanner L, Simell V, Makinen M, Simell S, Mykkanen J, Korpelainen J, Ruuskanen O, Ilonen J, Knip M, Simell O, Hedman K, Soderlund-Venermo M (2012) Association of Human Bocavirus 1 Infection with Respiratory Disease in Childhood Follow-up Study, Finland. Emerg Infect Dis 18: 264-271.

231. Edner N, Castillo-Rodas P, Falk L, Hedman K, Soderlund-Venermo M, Allander T (2011) Life-threatening respiratory tract disease with human bocavirus-1 infection in a four-year-old child. J Clin Microbiol 50: 531-532.

232. Ursic T, Jevsnik M, Zigon N, Krivec U, Beden AB, Praprotnik M, Petrovec M (2012) Human bocavirus and other respiratory viral infections in a 2-year cohort of hospitalized children. J Med Virol 84: 99-108.

233. Jartti T, Hedman K, Jartti L, Ruuskanen O, Allander T, Soderlund-Venermo M (2011) Human bocavirus-the first 5 years. Rev Med Virol 22: 46-64.

234. Nikitin PA, Luftig MA (2011) At a crossroads:Human DNA tumor viruses and the host DNA damage response. Future Virology 6: 813-830.

235. Gillespie KA, Mehta KP, Laimins LA, Moody CA (2012) Human Papillomaviruses Recruit Cellular DNA Repair and Homologous Recombination Factors to Viral Replication Centers. J Virol .

236. Xie A, Scully R (2007) Hijacking the DNA damage response to enhance viral replication: gamma-herpesvirus 68 orf36 phosphorylates histone H2AX. Mol Cell %20;27: 178-179.

237. Tarakanova VL, Leung-Pineda V, Hwang S, Yang CW, Matatall K, Basson M, Sun R, Piwnica-Worms H, Sleckman BP, Virgin HW (2007) Gamma-herpesvirus kinase actively initiates a DNA damage response by inducing phosphorylation of H2AX to foster viral replication. Cell Host Microbe 1: 275-286.

238. E X, Pickering MT, Debatis M, Castillo J, Lagadinos A, Wang S, Lu S, Kowalik TF (2011) An E2F1-mediated DNA damage response contributes to the replication of human cytomegalovirus. PLoS Pathog 7: e1001342.

239. Kudoh A, Fujita M, Zhang L, Shirata N, Daikoku T, Sugaya Y, Isomura H, Nishiyama Y, Tsurumi T (2005) Epstein-Barr virus lytic replication elicits ATM checkpoint signal transduction while providing an S-phase-like cellular environment. J Biol Chem 280: 8156-8163.

240. Gottifredi V, Prives C (2005) The S phase checkpoint: when the crowd meets at the fork. Semin Cell Dev Biol 16: 355-368.

241. Grallert B, Boye E (2008) The multiple facets of the intra-S checkpoint. Cell Cycle 7: 2315-2320.

242. Hu J, Sun L, Shen F, Chen Y, Hua Y, Liu Y, Zhang M, Hu Y, Wang Q, Xu W, Sun F, Ji J, Murray JM, Carr AM, Kong D (2012) The intra-s phase checkpoint targets dna2 to prevent stalled replication forks from reversing. Cell 149: 1221-1232.

243. Busino L, Donzelli M, Chiesa M, Guardavaccaro D, Ganoth D, Dorrello NV, Hershko A, Pagano M, Draetta GF (2003) Degradation of Cdc25A by beta-TrCP during S phase and in response to DNA damage. Nature 426: 87-91.

244. Demidova AR, Aau MY, Zhuang L, Yu Q (2009) Dual regulation of Cdc25A by Chk1 and p53-ATF3 in DNA replication checkpoint control. J Biol Chem 284: 4132-4139.

245. Karnani N, Dutta A (2011) The effect of the intra-S-phase checkpoint on origins of replication in human cells. Genes Dev 25: 621-633.

246. Mailand N, Falck J, Lukas C, Syljuasen RG, Welcker M, Bartek J, Lukas J (2000) Rapid destruction of human Cdc25A in response to DNA damage. Science 288: 1425-1429.

247. Falck J, Petrini JH, Williams BR, Lukas J, Bartek J (2002) The DNA damage-dependent intra-S phase checkpoint is regulated by parallel pathways. Nat Genet 30: 290-294.

248. Errico A, Costanzo V (2012) Mechanisms of replication fork protection: a safeguard for genome stability. Crit Rev Biochem Mol Biol 47: 222-235.

249. Strunnikov AV, Jessberger R (1999) Structural maintenance of chromosomes (SMC) proteins: conserved molecular properties for multiple biological functions. Eur J Biochem 263: 6-13.

250. Kim ST, Xu B, Kastan MB (2002) Involvement of the cohesin protein, Smc1, in Atm-dependent and independent responses to DNA damage. Genes Dev 16: 560-570.

251. Lehmann AR (2005) The role of SMC proteins in the responses to DNA damage. DNA Repair (Amst) 4: 309-314.

252. Wakeman TP, Kim WJ, Callens S, Chiu A, Brown KD, Xu B (2004) The ATM-SMC1 pathway is essential for activation of the chromium[VI]-induced S-phase checkpoint. Mutat Res 554: 241-251.

253. Antoccia A, Sakamoto S, Matsuura S, Tauchi H, Komatsu K (2008) NBS1 prevents chromatid-type aberrations through ATM-dependent interactions with SMC1. Radiat Res 170: 345-352.

254. Roberts S, Kingsbury SR, Stoeber K, Knight GL, Gallimore PH, Williams GH (2008) Identification of an arginine-rich motif in human papillomavirus type 1 E1;E4 protein necessary for E4-mediated inhibition of cellular DNA synthesis in vitro and in cells. J Virol 82: 9056-9064.

255. Qian Z, Leung-Pineda V, Xuan B, Piwnica-Worms H, Yu D (2010) Human cytomegalovirus protein pUL117 targets the mini-chromosome maintenance complex and suppresses cellular DNA synthesis. PLoS Pathog 6: e1000814.

256. Hermanns J, Schulze A, Jansen D, Kleinschmidt JA, Schmidt R, zur HH (1997) Infection of primary cells by adeno-associated virus type 2 results in a modulation of cell cycle-regulating proteins. J Virol 71: 6020-6027.

257. Hirt B (1967) Selective extraction of polyoma DNA from infected mouse cell cultures. J Mol Biol 26: 365-369.

258. Guan W, Cheng F, Yoto Y, Kleiboeker S, Wong S, Zhi N, Pintel DJ, Qiu J (2008) Block to the production of full-length B19 virus transcripts by internal polyadenylation is overcome by replication of the viral genome. J Virol 82: 9951-9963.

259. Gratzner HG (1982) Monoclonal antibody to 5-bromo- and 5-iododeoxyuridine: A new reagent for detection of DNA replication. Science 218: 474-475.

260. Lachmann S, Rommeleare J, Nuesch JP (2003) Novel PKCeta is required to activate replicative functions of the major nonstructural protein NS1 of minute virus of mice. J Virol 77: 8048-8060.

261. Ueda J, Saito H, Watanabe H, Evers BM (2005) Novel and quantitative DNA dot-blotting method for assessment of in vivo proliferation. Am J Physiol Gastrointest Liver Physiol 288: G842-G847.

262. Moran R, Darzynkiewicz Z, Staiano-Coico L, Melamed MR (1985) Detection of 5-bromodeoxyuridine (BrdUrd) incorporation by monoclonal antibodies: role of the DNA denaturation step. J Histochem Cytochem 33: 821-827.

263. Cziepluch C, Lampel S, Grewenig A, Grund C, Lichter P, Rommelaere J (2000) H-1 parvovirus-associated replication bodies: a distinct virus-induced nuclear structure. J Virol 74: 4807-4815.

264. Delia D, Fontanella E, Ferrario C, Chessa L, Mizutani S (2003) DNA damage-induced cell-cycle phase regulation of p53 and p21waf1 in normal and ATM-defective cells. Oncogene 22: 7866-7869.

265. Ostling O, Johanson KJ (1984) Microelectrophoretic study of radiation-induced DNA damages in individual mammalian cells. Biochem Biophys Res Commun 123: 291-298.

266. Singh NP, McCoy MT, Tice RR, Schneider EL (1988) A simple technique for quantitation of low levels of DNA damage in individual cells. Exp Cell Res 175: 184-191.

267. Olive PL (2002) The comet assay. An overview of techniques. Methods Mol Biol 203:179-94.: 179-194.

268. Shaposhnikov SA, Salenko VB, Brunborg G, Nygren J, Collins AR (2008) Single-cell gel electrophoresis (the comet assay): loops or fragments? Electrophoresis 29: 3005-3012.

269. Stracker TH, Petrini JH (2011) The MRE11 complex: starting from the ends. Nat Rev Mol Cell Biol 12: 90-103.

270. Christensen J, Cotmore SF, Tattersall P (1997) A novel cellular site-specific DNA-binding protein cooperates with the viral NS1 polypeptide to initiate parvovirus DNA replication. J Virol 71: 1405-1416.

271. Hardt N, Dinsart C, Spadari S, Pedrali-Noy G, Rommelaere J (1983) Interrelation between viral and cellular DNA synthesis in mouse cells infected with the parvovirus minute virus of mice. J Gen Virol 64: 1991-1998.

272. Rohaly G, Korf K, Dehde S, Dornreiter I (2010) Simian virus 40 activates ATR-Delta p53 signaling to override cell cycle and DNA replication control. J Virol 84: 10727-10747.

273. Shi Y, Dodson GE, Shaikh S, Rundell K, Tibbetts RS (2005) Ataxia-telangiectasia-mutated (ATM) is a T-antigen kinase that controls SV40 viral replication in vivo. J Biol Chem 280: 40195-40200.

274. Zhang G, Gibbs E, Kelman Z, O'Donnell M, Hurwitz J (1999) Studies on the interactions between human replication factor C and human proliferating cell nuclear antigen. Proc Natl Acad Sci U S A 96: 1869-1874.

275. Bowman GD, O'Donnell M, Kuriyan J (2004) Structural analysis of a eukaryotic sliding DNA clamp-clamp loader complex. Nature 429: 724-730.

276. Nichols WW, Bradt CI, Toji LH, Godley M, Segawa M (1978) Induction of sister chromatid exchanges by transformation with simian virus 40. Cancer Res 38: 960-964.

277. Fortunato EA, Spector DH (2003) Viral induction of site-specific chromosome damage. Rev Med Virol 13: 21-37.

278. Zur HH (1967) Induction of specific chromosomal aberrations by adenovirus type 12 in human embryonic kidney cells. J Virol 1: 1174-1185.

279. Chenet-Monte C, Mohammad F, Celluzzi CM, Schaffer PA, Farber FE (1986) Herpes simplex virus gene products involved in the induction of chromosomal aberrations. Virus Res 6: 245-260.

280. Ben-Asher E, Bratosin S, Aloni Y (1982) Intracellular DNA of the parvovirus minute virus of mice is organized in a minichromosome structure. J Virol 41: 1044-1054.

281. Doerig C, McMaster G, Sogo J, Bruggmann H, Beard P (1986) Nucleoprotein complexes of minute virus of mice have a distinct structure different from that of chromatin. J Virol 58: 817-824.

282. Morita E, Nakashima A, Asao H, Sato H, Sugamura K (2003) Human parvovirus B19 nonstructural protein (NS1) induces cell cycle arrest at G(1) phase. J Virol 77: 2915-2921.

283. Smith MA, Shah NS, Lobel JS (1989) Parvovirus B19 infection associated with reticulocytopenia and chronic autoimmune hemolytic anemia. Am J Pediatr Hematol Oncol 11: 167-169.

284. Chisaka H, Morita E, Yaegashi N, Sugamura K (2003) Parvovirus B19 and the pathogenesis of anaemia. Rev Med Virol 13: 347-359.

285. Meek DW (2009) Tumour suppression by p53: a role for the DNA damage response? Nat Rev Cancer 9: 714-723.

286. Kodama M, Otsubo C, Hirota T, Yokota J, Enari M, Taya Y (2010) Requirement of ATM for rapid p53 phosphorylation at Ser46 without Ser/Thr-Gln sequences. Mol Cell Biol 30: 1620-1633.

287. Shieh SY, Ikeda M, Taya Y, Prives C (1997) DNA damage-induced phosphorylation of p53 alleviates inhibition by MDM2. Cell 91: 325-334.

288. Liu Y, Kulesz-Martin M (2001) p53 protein at the hub of cellular DNA damage response pathways through sequence-specific and non-sequence-specific DNA binding. Carcinogenesis 22: 851-860.